Phase field simulation of solidification in binary Al-Cu alloys

By

Karanastasis Christos-Konstantinos C.

A Thesis submitted in partial fulfillment of the requirement for the degree of

Diploma in Mechanical Engineering

At the

UNIVERSITY OF THESSALY

DEPARTMENT OF MECHANICAL ENGINEERING

Thesis Advisor : Dr. Anna Zervaki

July 2014

Volos

ABSTRACT

The present work focuses on the prediction of the solidification microstructures of selected binary Al:Cu alloys by employing the phase filed method which was implemented in the MICRESS software installed recently at the Laboratory of Materials. The motivation behind this thesis arises from the necessity of understanding and modeling the solidification process in bimetallic Al:Cu joints currently used for the construction of modern solar absorber systems.

Four binary Al:Cu alloys were selected for the simulations included in this work i.e. Al-3%Cu wt., Al-30%Cu, Al-33%Cu (eutectic) and Al-45%Cu. The input parameters were adjusted according to references retrieved from the open literature, as well as, from ThermoCalc calculations. The goal was to achieve a reliable representation of the microstructural evolution in shape and time, as well as, to acquire information on the alloying element distribution in the calculation domain, which was selected to be in the micro-scale.

The results demonstrate the ability of MICRESS to describe reliably the formation of microstructure in the alloys studied, and to provide useful information on the phase fractions formed, as well as on their composition as a function of time and space. The results of the simulations contribute further to the understanding of solidification procedure and can be further exploited in the case of industrial processes such as casting and welding.

ACKNOWLEDGEMENTS

I would like to express my great gratitude to my advisor Dr. Anna Zervaki and to Director of the Laboratory of Materials Dr. G. N. Haidemenopoulos. Thanks for giving me the opportunity to be part of the Laboratory of Materials and special thanks for their time, patience, and understanding. It was honor for me to be student of these people. Through their advices and the knowledge I gained from their lectures I found new interests in the field of engineering.

TABLE OF CONTENTS

LIST OF FIGURES

LIST OF TABLES

1. INTRODUCTION

The present work focuses on the prediction of the solidification microstructures of selected binary Al:Cu alloys by employing the phase filed method which was implemented in the MICRESS software installed recently at the Laboratory of Materials [1]. The motivation behind this thesis arises from the necessity of understanding and modeling the solidification process in bimetallic Al:Cu joints currently used for the construction of modern solar absorber systems[2].

Understanding the mechanism of formation of microstructural patterns and shapes during solidification is of great importance in materials science because the resulting microstructures determine the properties of the material. Depending on the applied processing parameters and the alloy physical properties a variety of solidified microstructures caused by instability of the solid–liquid interface are observed in various kinds of solidification processes. Crucial theoretical and computational achievements gained in recent decades have provided the research community with a fundamental understanding of the dynamics of microstructure growth in the solidification process and at the same time, with reliable tools to design and improve further several industrial products. Numerical simulation offers a convenient way to visualize the evolution process during microstructure formation and provides quantitative predictions of detailed features in the morphologies it is a helpful tool for a deeper understanding of the mechanisms of microstructure formation, towards optimization and exploitation of existing processes or developing novel materials.

The phase-field approach is considered as one of the numerical simulation methods to model complex microstructure evolution during solidification and has emerged as a powerful method to simulate the pattern formation during solidification by making phase boundaries diffusive, which circumvents explicit tracking of the solid–liquid interface. The Phase-field models were developed mainly for studying solidification of pure materials, being then extended to the solidification of binary and ternary alloys. A number of phase-field simulations have been performed by researchers worldwide to simulate dendritic growth, not only from single equiaxed crystal growth [2–17] to polycrystalline growth [18–20] but also from primary phase solidification to multi-phase solidification [21,22].

The areas of application though initially limited to solidification have spread to many metallurgical phenomena, involving solid-state diffusion, deformation behavior, heat treatment, re-crystallization, grain boundary pre-melting, grain coarsening etc. The popularity of the phase-field method is due to the approach with which it treats moving boundary problems that can also be solved by the sharp interface methods. The interface representing the boundary between two moving phases is replaced with a smoothly varying function called a *phase-field*, whose change represents phase evolution. This approach obviates the necessity to

track the interface and hence allows large scale simulations of microstructure evolution involving complicated geometrical changes computationally tractable.

The application of the phase-field method starts with the creation of the functional which includes the material properties involving both the surface properties of the interfaces in the system and the thermodynamic energy of the bulk phases in the system. A variational derivative of this functional with respect to any of the changing phase-field variables, provides the driving force for the transformation. Depending on whether a pure component or multi-component system is treated, this driving force is a function of just the temperature or includes the compositions of the different components in the system also as variables. The source of thermodynamics of the bulk phases, can be derived either from linearized phase diagrams or through the direct coupling of ThermoCalc and DICTRA databases [23,24,25].

Although the motivation of this work came from welding, the simulations carried out was devoted mainly in understanding on how MICRESS software treats the solidification of binary Al:Cu alloys under low cooling rates in small simulation domains. It is worth mentioning that this work is the first one trying to employ MICRESS in addressing solidification problems. MICRESS has already been used for the simulation of recrystallization and grain growth [26] in LoM.

1.2 Aim

Since a variety of alloys were formed during the welding of the solar absorber systems, four binary Al:Cu alloys were selected for the simulations within the frame of the current work i.e.

- Al-3%Cu
- Al-30%Cu
- Al-33%Cu (Eutectic) and
- Al-45%Cu.

The results allow the visualization of the microstructure evolution in space and time and provide useful information on phase morphology, phase fractions as well as profiles of solute concentration. The results are in reliable agreement with those referred in the literature and can be further exploited for the weld case by adjusting proper boundary conditions.

The thesis is structured in the following chapters:

2. Literature Review on Solidification, phase filed method and basic features of MICRESS

3. Methodology

4. Results and Discussion

5. Conclusions

6. Future Work

2. LITERATURE REVIEW

2.1 Solidification

The processes of cooling and melting were present at the beginnings of the Earth and continue to affect the natural and industrial worlds. The solidification of a liquid or the melting of a solid involves a complex interplay of many physical effects.

The solidification of a liquid or the melting of a solid involves a complex interplay of many physical effects. The solid-liquid interface is an active free boundary, from which latent heat is liberated during phase transformation. This heat is conducted away from the interface through the solid and the liquid, resulting in the presence of thermal boundary layers near the interface. Across the interface, the density changes from ρ^L to ρ^S. Thus, if $\rho^L < \rho^S$, so that the material shrinks upon solidification. If the liquid is not pure but contains solute, preferential rejection or incorporation of solute occurs at the interface. This rejected material will be diffused away from the interface through the solid, the liquid, or both, resulting in the presence of concentration boundary layers near the interface. The thermal and concentration boundary layer structures determine, in large part, whether morphological instabilities of the interface exist and what the ultimate microstructure of the solid becomes.

Cooling can create solids whose microstructures are determined by the process parameters and the intrinsic instabilities of the solid-liquid front result in amorphous microstructure. However under certain conditions the moving solidification front can be susceptible to traveling-wave instabilities, giving structural patterns that can be made understandable. When a eutectic alloy is cooled, the solid can take the form of a lamellar structure, alternate plates of two alloys spatially periodic perpendicular to the freezing direction. Under certain conditions this mode of growth is stable, giving rise to the more complex modes of growth. Under conditions of rapid solidification, the microstructure can take on metastable states and patterns inconsistent with equilibrium thermodynamics. If the solidification process occurs in a gravitational field, the thermal and solutal gradients may induce buoyancy-driven convection, which is known to affect the interfacial patterns greatly and, hence, the solidification microstructures present in the solidified material.

The coupling of fluid flow in the melt with phase transformation at the interface can result in changes of microstructure scale and pattern due to alterations of frontal instabilities and the creation of new ones. When an alloy is cooled at moderate speeds and dendritic arrays are formed, interesting dynamics occur in the dendrite liquid mixture, which called the mushy zone. The solutal convection creates channels parallel to the freezing direction. The channels frozen into the solid are called freckles, and their presence can significantly weaken the structure of the solid. Given that the solid has crystalline structure, intrinsic symmetries in the

material properties help define the continuum material. The surface energy and the kinetic coefficient on the interface as well as the bulk transport properties inherit the directional properties of the crystal, and thus anisotropies are often significant in determining the cellular or dendritic patterns that emerge. If the anisotropy is strong enough, the front can exhibit facets and corners.

When a binary liquid is cooled, it usually rejects some or all of its solute because that solute is more soluble in the liquid than in the crystalline solid. The degree of rejection can be obtained from the phase diagram for systems in thermodynamical equilibrium. The rejected solute in the liquid is subject to diffusion, and thus, a major difference between the dynamics of pure material and that of alloys is the need to track both the temperature and concentration fields.

System scale

Consider a directional solidification setup. Thermal flux balance at the solidification interface leads to the relation:

$$K_s G_s - K_L G_L = \rho_s L R \tag{2.1.1}$$

Here, K_s and K_L are thermal conductivities at W/mK, G_s and G_L, thermal gradients in solid and liquid at K/m, and ρ_s, L and R are density of the solid at Kg/m^3, latent heat at J/kg and solidification rate at m/s respectively. Neglecting the situation of a highly undercooled melt, when $G_L \to 0$, the highest directional solidification rate achievable for a given system size is limited by the conduction mode heat removal by the solidified metal alone and is given by,

$$R_{max} = \frac{K_s G_s}{\rho_s L} \tag{2.1.2}$$

Equation (2.1.2) assumes no resistance to heat transfer. For a casting process, heat transfer through the surrounding mould is a limiting factor. In this case, (2.1.2) needs to be modified by incorporating resistance to heat transfer by the mould. In this case, solidified thickness or the modulus of solidification (V/A) is related to the solidification time by,

$$\frac{V}{A} = \frac{T_M - T_0}{\rho_s L}\left(\frac{2}{\pi^{1/2}}(K_M \rho_M C_M)^{1/2}(t_f)^{1/2} + n\frac{K_M t_f}{2r}\right) \tag{2.1.3}$$

Here the subscript M represents mould, V and A represent volume and area of the mould, r the radius of curvature of the mould, and n is a geometric constant. The time for completion of solidification is t_f and T_0 is the initial liquid temperature. Apparently, the equation consists of terms outside the bracket that are controlled essentially by the material properties. The first term in the bracket reflects the properties of the mould while the second term reflects the

geometry. The term n takes different values depending on the geometry of the casting, and thus influences the solidification process. For example, a spherical mould (n = 2) solidifies faster than a cylindrical mould (n = 1). For a conducting mould, the main resistance to heat transfer occurs at the mould–metal interface. In such a case (for example, chill casting), the solidification thickness (S) is limited by the heat transfer coefficient h across the metal–mould interface. A simple heat transfer analysis allows us to obtain the following governing equation for this case,

$$S = h\frac{T_m - T_o}{\rho_s L}t_f \tag{2.1.4}$$

Thus the rate of solidification becomes a function of the thermal parameters of the process and the materials properties. However, it should be noted that in processes such as the Bridgeman technique growth rate and temperature gradient can be controlled independently. This enables study of these two important parameters on solidification microstructure and properties [27].

Segregation

Equilibrium solidification assumes that the solid-liquid interface moves at an infinitesimally slow pace such that the thermal and the solutal fields redistribute to adjust to the temperature and the composition values given by the equilibrium phase diagram. However, as can be gathered from the previous section, the solidification speed R is finite. The scale of the system for this to happen is given by,

$$D_s \gg L_X R \tag{2.1.5}$$

Here, L_X is the system length scale in one dimension and D_S is the solute diffusivity in solid. Thermal and solutal diffusivities are finite and usually very small. This imposes a limit on the system scale to qualify for equilibrium solidification. Substituting typical diffusivities (thermal: 10–4 cm^2/s, solutal: 10–6 cm^2/s), for a system size of 1 cm, the solidification rate should be below 10–6 cm/s, a very small value. Most of the solidification processes in reality are at rates of about three orders of magnitude larger. As a result, the solutal field equilibration is not achieved and microsegregation patterns will result. The composition of the liquid C_L left over after a fraction f_L has solidified from a liquid of initial composition C_0 is now no longer be given by the equilibrium lever rule. This problem has been resolved by [28]. The formulation assumes no solid diffusivity and infinite liquid diffusivity. The concentration of the liquid in this case is given by,

$$C_L = C_0 f_L^{(k-1)} \tag{2.1.6}$$

Here, k is the solute partition coefficient (C_S/C_L) which depends on the nature of the phase diagram. This is popularly known as Scheil's equation or non-equilibrium lever rule.

For large system scales, the solute field in the liquid itself might not be uniform due to convection and the solute content of the solid formed at various locations in the system might be non-uniform, resulting in macrosegregation [27].

Microstructure evolution

In the previous sections we have discussed about the rate of solidification and composition profiles that come about at the system scale. However, as the solidification proceeds, the solid–liquid interface could undergo perturbations and develop instabilities that lead to the final microstructure of the solid.

Cellular pattern

For a pure metal, a positive thermal gradient in the liquid leads to a stable plane front solidification and a negative thermal gradient in the liquid leads to instability of plane front giving rise to 'thermal dendrites' that are not distinguishable by microstructural analysis. Consider a thermal gradient situation, as in Figure 2.1.1, for an alloy. A small perturbation on the interface for the stable interface (Figure 2.1.1.c) will 'see' temperature higher than the liquidus temperature and hence will melt back. Thus the stability of the flat interface will be maintained. But for the unstable interface (Figure 2.1.1.d), interface across a small perturbation 'sees' more undercooling at its location and grows further, leading to a breakdown of the planar front. The critical thermal gradient in the liquid at which such breakdown can take place is given by,

$$G_L/R \geq M_L C_0(1-k)/kD_L \tag{2.1.7}$$

The microstructural patterns that form in this manner are termed 'cellular'.

Effect of surface tension on plane front solidification

Although Figure 2.1.1 is highly successful in predicting the onset of the interface breakdown during growth, this is not valid at high growth. At high growth velocity, the perturbation wavelengths become smaller. When the perturbations are small, surface tension plays an important role, comparable in magnitude to that of the solute field and can stabilize the plane front. [29] assumed interface equilibrium, isotropic surface energy and no convection to obtain a thermal condition at which the plane front is stabilized by the surface tension.

Dendritic pattern

Anisotropy of surface tension and instabilities at the growing tip of the cell can lead to side branching. A cell with side branches resembles a tree and so is termed 'dendrite'. While the growth direction of cells is determined by the maximum thermal gradient, the growth direction

of dendrites deviates from it. It is a compromise between the direction of maximum thermal gradient and of the crystallographic easy

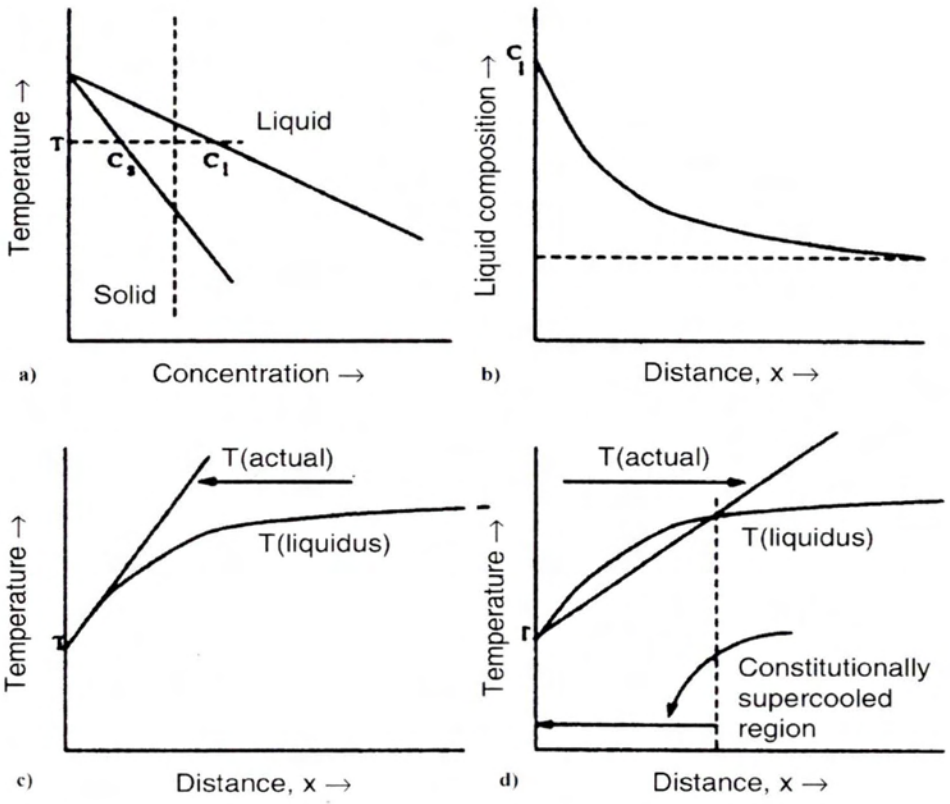

Figure 2.1.2: Schematic drawing indicating constitutional supercooling. a) Phase diagram, b) Solute enriched-layer in front of solid–liquid interface, c) Stable interface, d) Unstable interface

growth, which is $\langle 100 \rangle$ for FCC and BCC and $\langle 10\bar{1}0 \rangle$ for HCP. Dendrite tip temperature (T_D), modified by the presence of nonequilibrium compositions at the interface and the curvature, is given as

$$T_D = T_M + m_R C_L - \Delta C_L \tag{2.1.8}$$

Here, m_R is the liquidus slope modified for the solidification velocity R, C_L is the liquid composition and ΔC_L is the curvature undercooling.

The curvature at the tip of a dendrite can be seen as due to a pressure field and the resultant decrease in the freezing temperature is given by the Gibbs–Thomson relation.

$$\Delta T_c = \gamma k / \Delta S \tag{2.1.9}$$

Here, γ is surface tension, k is curvature of interface and ΔS is entropy of fusion per unit volume. [30] have modelled the dendritic growth assuming that the dendrite tip is a hemisphere with radius equal to the wavelength of the critical instability of the solid–liquid interface. By minimizing the undercooling with respect to the radius of curvature of the tip, they have obtained steady-state growth velocity as given by,

$$R = \frac{2D(Gr^2 + 4\pi^2\Gamma)}{r^3\rho G - 2(1-k)C_0 m + 4\pi^2 r(1-k)} \tag{2.1.10}$$

Here, r is the radius of the dendrite tip, and Γ is the surface tension. In the limiting cases, we observe the following behavior.

At small R :

$$R = \frac{2DG}{r(1-k)G - 2(1-k)C_0 m} \tag{2.1.11}$$

$$r = \frac{2D}{R(1-k)} + \frac{2mC_0}{G} \tag{2.1.12}$$

At large R:

$$R = \frac{4\pi^2 D\Gamma}{r^2(1-k)C_0 m} \tag{2.1.13}$$

$$r = 2\pi(D\Gamma/Rk\Delta T_0)^{1/2} \tag{2.1.14}$$

$$\Delta T_0 = -mC_0\,(1-k)/k \tag{2.1.15}$$

i.e., at small growth rates, the radius declines rapidly with increasing growth rate and at large growth rates, the radius falls parabolically with increasing growth rates.

Eutectic growth

In the discussion above, we have considered one solid phase growing in to liquid under various thermal conditions. However, in eutectic alloy systems two solid phases grow in to a liquid simultaneously. The microstructure exhibited by the eutectic solids is also varied. They can be classified as regular eutectic with lamellar or rod morphology and irregular eutectic showing no regularity of distribution of the two phases. Regular eutectic growth is modelled by [31] who solved the solute diffusion equation for a steady state growth at minimum undercooling. The resultant equation gives a relation between the undercooling, growth rate and eutectic spacing [31].

$$\Delta T/m = R\lambda + (A/\lambda) \tag{2.1.16}$$

$$Q = P(1+\varsigma)^2 C_0/\varsigma D \tag{2.1.17}$$

$$A = 2(1+\varsigma)\,(\alpha_\alpha^L/m_a)/(\alpha_\beta^L/m_\beta) \tag{2.1.18}$$

$$\varsigma = S_\alpha/S_\beta \tag{2.1.19}$$

where, λ is a function of the thermal gradient *G*, *m* is the harmonic mean of the liquidus slopes for *a* and *b* phases, *P* is a function of the volume fraction, S_a and S_b are the half-spacings of the lamellae/rods and α_α^L and α_β^L , the Gibbs–Thompson coefficients of *a* and *b* phases respectively.

Assuming that the solid grows at the maximum growth rate for a given undercooling, the eutectic spacing, velocity and undercooling are related as:

$$\lambda^2 R = A/Q, \tag{2.1.20}$$

$$\Delta T^2/R = 4m^2 AQ, \tag{2.1.21}$$

$$\Delta T\lambda = 2mA, \tag{2.1.22}$$

The above analysis is successful in predicting the lamellar or rod spacings under different growth conditions as well as the shape of the solid–liquid interface. This also explains the transformation of the lamellar eutectic to rod eutectic at low volume fraction. The analysis of the other eutectic morphologies is more complex.

Effect of convection

Most of the models in the solidification literature have been developed under the assumption that the liquid is static, in real systems convection cannot be ignored. Convection enhances transport of heat and species, thereby introducing a correction to thermal and solutal diffusivity. Enhanced diffusion helps in the coarsening of microstructures and the final pattern spacing falls into a band of values rather than a single selected value. Convection also influences morphological instability and interface structure. There have been observations on massive transparent specimens revealing that convection results in a gradient of microstructure along the interface from smooth interface to dendrites [32,33] .

2.2 Phase field model

The phase field method has proved to be extremely powerful in the visualization of the development of microstructure without having to track the evolution of individual interfaces, as is the case with sharp interface models. The method, within the framework of irreversible thermodynamics, also allows many physical phenomena to be treated simultaneously. Phase field equations are quite elegant in their form and clear for all to appreciate, but the details,

approximations and limitations which lead to the mathematical form are perhaps not as transparent to those whose primary interest is in the application of the method.

Imagine the growth of a precipitate which is isolated from the matrix by an interface. There are three distinct entities to consider: the precipitate, matrix and interface. The interface can be described as an evolving surface whose motion is controlled according to the boundary conditions consistent with the mechanism of transformation. The interface in this mathematical description is simply a two-dimensional surface; it is said to be a sharp interface which is associated with an interfacial energy σ per unit area.

In the phase field method, the state of the entire microstructure is represented continuously by a single variable known as the order parameter φ. For example, $\varphi=1$, $\varphi=0$ and $0<\varphi<1$ represent the precipitate, matrix and interface respectively. The latter is therefore located by the region over which φ changes from its precipitate value to its matrix value (Figure 2.1.2). The range over which it changes is the width of the interface. The set of values of the order parameter over the whole volume is the phase field. The total free energy G of the volume is then described in terms of the order parameter and its gradients, and the rate at which the structure evolves with time is set in the context of irreversible thermodynamics, and depends on how G varies with φ. It is the gradients in thermodynamic variables that drive the evolution of structure.

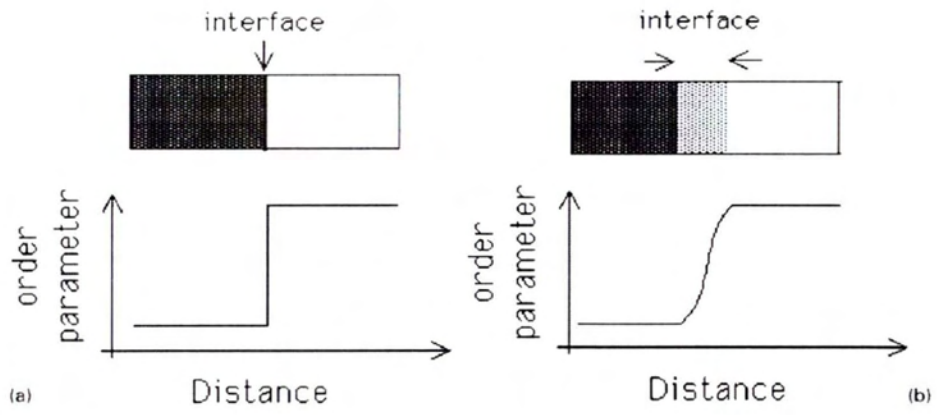

Figure 2.1.2: **a) Sharp interphase, b) Diffuse interphase**

The number of equations to be solved increases with the number of domains separated by interfaces and the location of each interface must be tracked during transformation. This may make the computational task prohibitive. The phase field method clearly has an advantage in this respect, with a single functional to describe the evolution of the phase field, coupled with equations for mass and heat conduction, i.e. three equations in total, irrespective of the number of particles in the system. The interface illustrated in Figure 2.2.3 simply becomes a region over which the order parameter varies between the values specified for the phases on

either side. The locations of the interfaces no longer need to be tracked but can be inferred from the field parameters during the calculation.

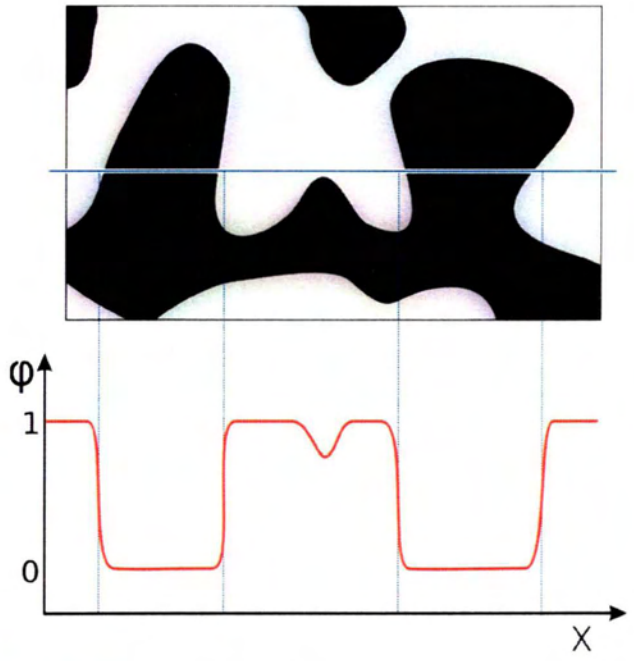

Figure 2.2.3: **A two phase mictostructure and the order parameter φ profile is depicted on a line across the domain. Gradual change of order parameter from one phase to another illustriates diffuse nature of the interphase.**

Order parameter

The order parameters in phase field models may or may not have macroscopic physical interpretations. For two-phase materials, φ is typically set to 0 and 1 for the individual phases, and the interface is the domain where $0<\varphi<1$. For the general case of N phases present in a matrix, there will be a corresponding number of phase field order parameters φ_i with i=1 to N. $\varphi_i = 1$ then represents the domain where phase i exists, $\varphi_i = 0$ where it is absent and $0< \varphi_i <1$ its bounding interfaces. Suppose that the matrix is represented by φ_0 then it is necessary that at any location.

$$\sum_{i=0}^{N} \varphi i = 1 \qquad (2.2.1)$$

It follows that the interface between phases 1 and 2, where $0 <\varphi_1 <1$ and $0 <\varphi_2 <1$ is given by $\varphi_1+\varphi_1=1$; similarly, for a triple junction between three phases where $0< \varphi_i <1$ for i=1,2,3, the junction is the domain where $\varphi_1+ \varphi_2+ \varphi_3=1$.

The evolution of the microstructure with time is assumed to be proportional to the variation of the free energy functional with respect to the order parameter:

$$\frac{\partial \varphi}{\partial t} = M \frac{\partial g}{\partial \varphi} \tag{2.2.2}$$

where M is a mobility. A Taylor expansion for a single variable about X = 0 is given by:

$$J\{X\} = 1 + J'\{0\}\frac{x}{1!} + J''\{X\}\frac{x^2}{2!} + \cdots \tag{2.2.3}$$

A Taylor expansion like this can be generalized to more than one variable. Cahn assumed that the free energy due to heterogeneities in a solution can be expressed by a multivariable Taylor expansion:

$$g\{y, z, \ldots\} = g\{c_0\} + y\frac{\partial g}{\partial y} + z\frac{\partial g}{\partial z} + \cdots + \frac{1}{2}\left[y^2\frac{\partial^2 g}{\partial y^2} + z^2\frac{\partial^2 g}{\partial z^2} + 2yz\frac{\partial^2 g}{\partial y \partial z} \ldots\right] + \cdots \tag{2.2.4}$$

In which the variables, y, z, . . . in our context are the spatial composition derivatives (dc/dx, d^2c/dx^2, etc). For the free energy of a small volume element containing a one–dimensional composition variation (and neglecting third and high–order terms), this gives

$$g = g\{c_0\} + k_1\frac{dc}{dx} + k_2\frac{d^2c}{dx^2} + k_3\left(\frac{dc}{dx}\right)^2 \tag{2.2.5}$$

Where c_0 is the average composition. Also

$$k_1 = \frac{\partial g}{\partial\left(\frac{dc}{dx}\right)} \tag{2.2.6}$$

$$k_2 = \frac{\partial g}{\partial\left(\frac{d^2c}{dx^2}\right)} \tag{2.2.7}$$

$$k_3 = \frac{1}{2}\frac{\partial^2 g}{\partial\left(\frac{dc}{dx}\right)^2} \tag{2.2.8}$$

In this, k_1 is zero for a centrosymmetric crystal since the free energy must be invariant to a change in the sign of the coordinate x. The total free energy is obtained by integrating over the volume:

$$g_T = \int_V \left[g\{c_0\} + k_2 \frac{\partial^2 c}{\partial x^2} + k_3 \left(\frac{\partial c}{\partial x} \right)^2 \right] \tag{2.2.9}$$

On integrating the third term in this equation by parts:

$$\int k_2 \frac{d^2 c}{dx^2} = \int k_2 \frac{dc}{dx} - \int \frac{dk_2}{dc} \left(\frac{dc}{dx} \right)^2 dx \tag{2.2.10}$$

Similarly, the first term on the right is zero, so that an equation of the form below is obtained for the free energy of a heterogeneous system and g describes how the free energy varies as a function of the order parameter at constant T and P.

$$g = \int_V [g_0\{\varphi, T\} + \varepsilon(\nabla\varphi)^2] \tag{2.2.11}$$

Where V and T represent the volume and temperature respectively. The second term in this equation depends only on the gradient of and hence is non–zero only in the interfacial region; it is a description therefore of the interfacial energy. The first term is the sum of the free energies of the precipitate and matrix, and may also contain a term describing the activation barrier across the interface. For the case of solidification:

$$g_0 = hg^S + (1-h)g^L + Qf \tag{2.2.12}$$

where g^S and g^L refer to the free energies of the solid and liquid phases respectively, Q is the height of the activation barrier at the interface. If the temperature varies then the functional is expressed in terms of entropy rather than free energy

$$h = \varphi^2 + (3 - 2\varphi) \tag{2.2.13}$$

$$f = \varphi^2 + (1-\varphi)^2 \tag{2.2.14}$$

Notice that the term $hg^S + Qf$ vanishes when $\varphi = 0$ (i.e. only liquid is present), and similarly, $(1-h)g^L + Qf$ vanishes when $\varphi = 1$ (i.e. only solid present). As expected, it is only when both solid and liquid are present that Qf becomes non–zero. The time–dependence of the phase field then becomes:

$$\frac{\partial\varphi}{\partial t} = M[\varepsilon(\nabla\varphi)^2 + h'\{g^L - g^S\} - Qf'] \tag{2.2.15}$$

The parameters, M and ε have to be derived assuming some mechanism of transformation.

Advantages

1. Particularly suited for the visualization of microstructure development.
2. Straightforward numerical solution of a few equations.
3. The number of equations to be solved is far less than the number of particles in system.
4. Flexible method with phenomena such as morphology changes, particle coalescence or splitting and overlap of diffusion fields naturally handled. Possible to include routinely, a variety of physical effects such as the composition dependence of mobility, strain gradients, soft impingement, hard impingement, anisotropy etc.

Disadvantages

1. Very few quantitative comparisons with reality; most applications limited to the observation of shape.
2. Large domains computationally challenging.
3. Interface width is an adjustable parameter which may be set to physically unrealistic values. Indeed, in most simulations the thickness is set to values beyond those known for the system modeled. This may result in a loss of detail and unphysical interactions between different interfaces.
4. The point at which the assumptions of irreversible thermodynamics would fail is not clear.
5. The extent to which the Taylor expansions that lead to the popular form of the phase field equation remain valid is not clear.
6. The definition of the free energy density variation in the boundary is somewhat arbitrary and assumes the existence of systematic gradients within the interface. In many cases there is no physical justification for the assumed forms. A variety of adjustable parameters can therefore be used to fit an interface velocity to experimental data or other models.

Available software based on the phase field method

OpenPhase is the open source software project targeted at the phase field simulations of complex scientific problems involving microstructure formation in systems undergoing first order phase transformation. The core of the library is based on the multiphase field model. The project has the form of a library and is written in object oriented C++. It has a modular structure which allows easy extensions of the library and simplifies the development of user programs. The aim of the project is to enable interested scientists to quickly develop phase field simulation programs for a variety of problems involving solid-liquid and solid-solid first order phase transformations as well as the structural transformations, e. g. grain growth, recrystallization etc. The development of the library is done in the department of Prof. Dr. Ingo Steinbach at the Interdisciplinary Centre for Advanced Materials Simulation (ICAMS) at Ruhr-University Bochum.

PACE3D - Parallel Algorithms for Crystal Evolution in 3D is a parallelized phase-field simulation package including multi-phase multi-component transformations, large scale grain structures and coupling with fluid flow, elastic, plastic and magnetic interactions. It is developed at the Karlsruhe University of Applied Sciences and Karlsruhe Institute of Technology.

The Mesoscale Microstructure Simulation Project (MMSP) is a collection of C++ classes for grid-based microstructure simulation.

MOOSE massively parallel open source C++ multiphysics finite element framework with support for phase field simulations developed at Idaho National Laboratory.

The Microstructure Evolution Simulation Software (MICRESS) is a multi-phase field simulation package developed at RWTH-Aachen.

2.3 Micress Software

MICRESS software(Microstructure evolution simulation software), employed for the simulations performed in the current work, is developed for time- and space-resolved numerical simulations of solidification, grain growth, recrystallisation or solid state transformations in metallic alloys. MICRESS® covers phase evolution, solute and thermal diffusion and transformation strain in the solid state. It enables the calculation of microstructure formation in time and space by solving the free boundary problem of moving phase boundaries. Microstructure evolution is governed essentially by thermodynamic driving forces, diffusion and curvature. In case of multicomponent alloys, the required thermodynamic data can either be provided to MICRESS® in the form of locally linearised phase diagrams, or by direct coupling to thermodynamic data sets via a special TQ-interface, developed in collaboration with Thermo Calc™ AB, Stockholm.

MICRESS® is based on the multiphase-field method which defines a phase-field parameter for each phase involved. The phase-field parameter describes the fraction of each phase as a continuous function of space and time. Each single grain is mapped to a distinct phase-field parameter and is treated as an individual phase. A set of coupled partial differential equations is formed which describes the evolution of the phase-field parameter, together with concentration, temperature, stress and flow fields. The total set of equations is solved explicitly by the finite difference method on a cubic grid. Furthermore, 2D and 3D simulations are possible. The size of the simulation domain, the number of grains, phases and components is restricted mainly by the available memory size and CPU speed.

Binary and ternary phase diagrams being available in printed form in books or publications have provided the basis for the development of materials ever since. Increasing availability of computers has allowed for the continuous development of computational thermodynamics and respective databases in the last decades. Such software tools and databases are nowadays available for complex alloy systems comprising a number of alloy elements, e.g. (Thermo-Calc, Pandat, FactSage, JMatPro). Their databases are established using a well-defined assessment scheme (Calphad). They allow determining phase diagrams, calculating the sequence of phase transitions, the amount of phase fractions being stable at a given temperature and other thermodynamic properties, Figure 2.2.4. Even more important for describing the evolution of a microstructure is that such models also allow the calculation of the driving forces for the phase transformations.

Continuing from the knowledge about equilibrium phase fractions, which do not provide any information about how fast this equilibrium is reached, subsequent developments aimed at describing the kinetics of diffusion controlled phase transitions. One example for a software tool especially suitable for the description of multicomponent diffusion using respective databases is DICTRA [24,25]. The underlying approach here is based on 1-D systems like e.g. diffusion couples, concentric cylinders or concentric spheres. Under some specific assumptions phenomena like coarsening of a precipitate distribution can also be tackled.

Most interesting for metallurgists and materials engineers, however, is the microstructure and – even further–the properties of a material being based on its microstructure. The simulation of microstructures in technical alloy systems probably has its origin in the first dendrites being simulated using the phase-field method [28] and the subsequent extension of the phase-field method to multiple phase-fields [34] allowing early simulations of eutectic and peritectic systems. This multiphase-field model later has been coupled to thermodynamic and mobility databases, thus providing the basis for all the examples on simulations of technical alloy grades being depicted in this paper[36-38].

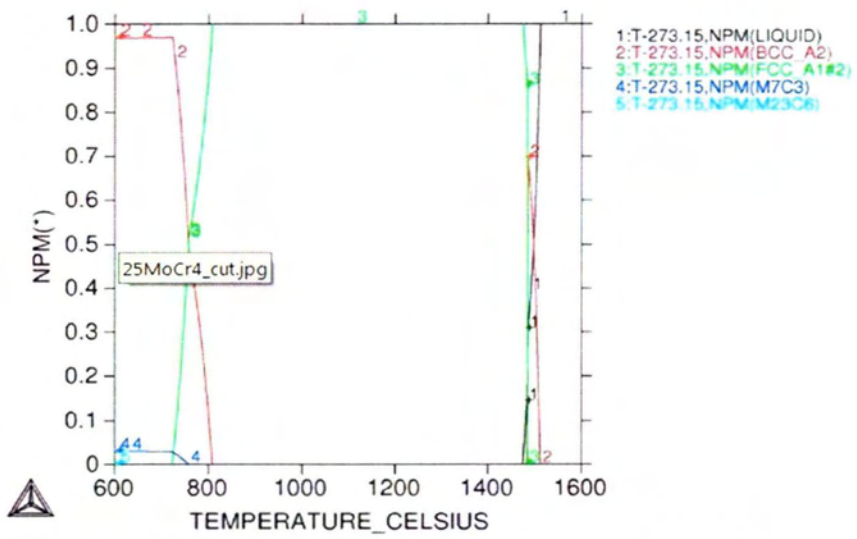

Figure 2.2.4: **Equilibrium phase fractions of different phases in a 25MoCr4 steel as a function of temperature (calculated using Thermo-Calc and the TCFe6 database)**

The phase-field method can be rigorously derived from thermodynamic principles and theories of phase transitions, and a lot of dedicated literature is available covering these fundamental and mathematical aspects [39,40]). In this paper we will give a phenomenological approach for a rather intuitive interpretation of the phase-field concept and equations.

The first step towards the simulation of the dynamics of microstructure evolution is the basic description of a static microstructure, Figure 2.2.5. A simple approach is to use a so called order parameter φ for simulations of microstructure evolution in a simple solid/liquid system. φ itself

is a function of space x and time t i.e. and may $\varphi(x,t)$ take values between 0 and 1. Metallurgists may relate $\varphi = \varphi(x,t)$ this order parameter to the fraction of a specific phase (e.g. φ corresponds to the fraction solid in fig. 2.2.5) to be present at a specific point of space x and at a specific time t.

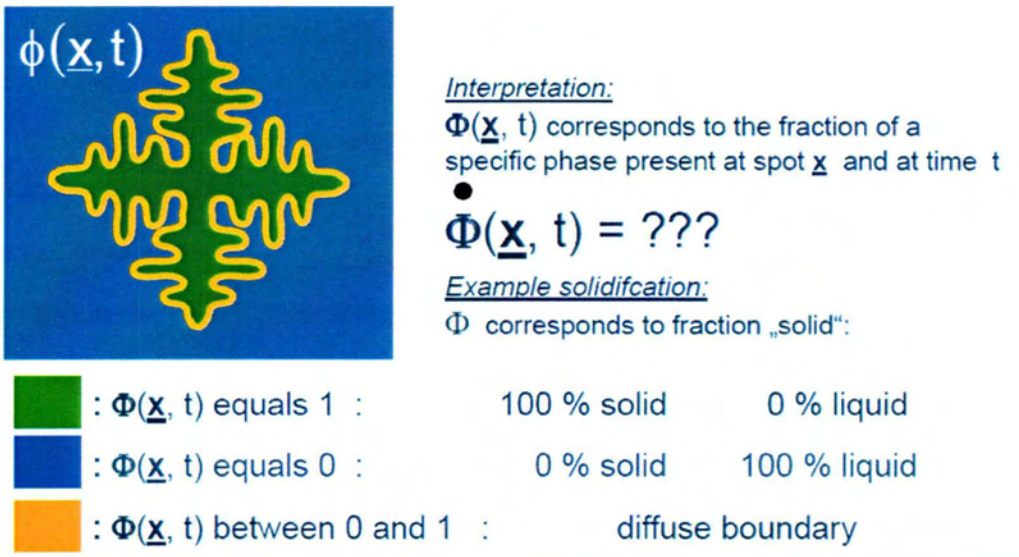

Figure 2.2.5: **Description of a solidifying microstructure by an order parameter at a given moment t.**

This method of describing microstructures has been extended to the description of multiple grains and multiple phases in the multiphase-field method, where multiple, i.e. "i" different phase fields $\varphi_i = \varphi(x,t)$ denote the individual phases or even all different grains. In short, any object which can be identified in the microstructure may have its own phase-field variable in respective multiphase-field models.

Before entering multiphase-field models it seems wise to understand or at least to get a feeling for a description of the evolution of the simple solidification situation depicted in Figure 2.2.4. Describing the evolution of the microstructure thus means to identify the time derivative of the $\varphi = \varphi(x,t)$.
A possible first step towards identification of a description of $\varphi'(x,t)$ is to start from a diffusion equation (Figure.2.2.6, blue contribution). A pure diffusion approach however would lead to a smear out of an initially sharp interface eventually ending up with a smooth and flat curve. In order to describe a stable, stationary interface an additional term thus is needed (Figure 2.2.6, green contribution), which stabilizes the interface. Note that this contribution is negative for $0 < \varphi < 0.5$ and positive for $0.5 < \varphi < 1$. This term thus balances the effect of the diffusion term (blue) leading to a stationary, stabilized interface profile. Depending on the actual choice of this term, different stationary interface profiles may result (e.g. a hyperbolic tangent profile for a double well potential or a sine–profile for a double obstacle potential). Eventually any deviation

from equilibrium (Figure 2.2.6, red contribution) will lead to a movement of the stationary interface profile. The deviation from equilibrium is characterized by Δg.Depending on the sign of Δg the motion will result either in growth or shrinkage of the respective phase. When equilibrium is reached ($\Delta g = 0$) the profile characterizing the interface position will become stationary and stable.

$$\dot{\phi}(\vec{x},t) = \mu \left[\sigma \left(\nabla^2 \phi - \frac{(1-\phi)(1-2\phi)\phi}{\eta^2} \right) + \frac{1}{\eta} \Delta G \, \phi (1-\phi) \right]$$

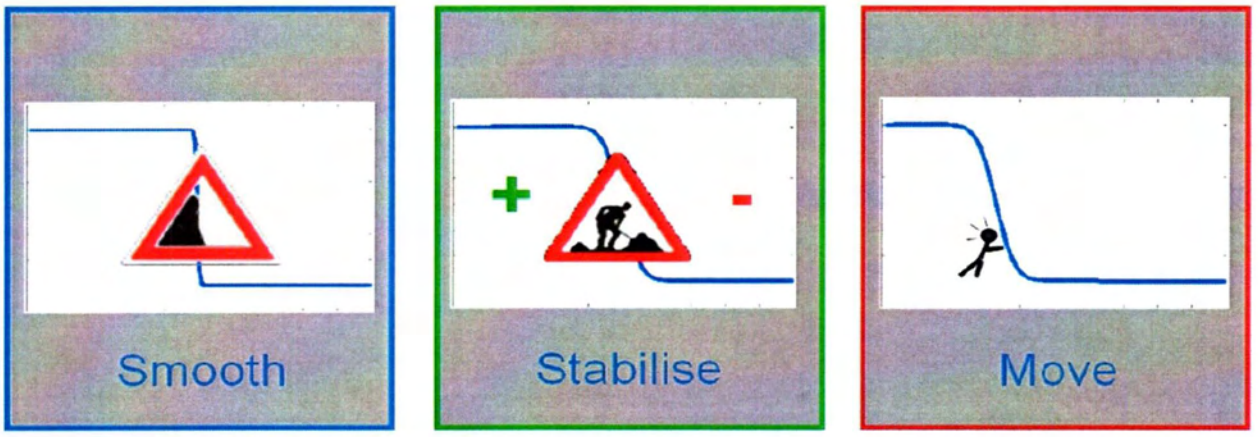

Figure 2.2.6: **The phase-field equation in a very simple analysis.**

Further variables in the respective equation denote the interfacial energy (σ), the interfacial thickness (η) and the interfacial mobility (μ).

Another engineering approach to the phase-field equation is based on the "Gibbs Thomson equation" giving a relation between interface velocity, thermal and solutal undercooling and interface curvature and being well known to metallurgists since decades [41], [42].

A closer look at the phase-field equation (equation in Figure 2.2.6) reveals a rotational symmetry as the diffusion equation (Figure 2.2.6 blue contribution) does not comprise any anisotropy. In order to include anisotropy into the model, both the interfacial energy σ and the interface mobility μ are assumed to be anisotropic. In 2 dimensions this can be accomplished by making these parameters dependant on the angle θ between the growth direction and the crystal orientation i.e. $\sigma = \sigma(\theta)$ and $\mu = \mu(\theta)$. For a simple cubic symmetry in 2D these functions could look like $\sigma = \sigma(1-\cos(4\theta))$ and $\mu = \mu(1-\cos(4\theta))$. For a hexagonal symmetry in 2 D functions like $\sigma = \sigma(1-\cos(6\theta))$ and $\mu = \mu(1-\cos(6\theta))$ would represent a first approach.

Please note that in case of spatially varying interfacial energies the Gibbs-Thomson coefficient Γ has to be modified by including the second derivative of the interfacial energy:

$$\Gamma = \frac{\sigma}{L_0 T_m} \quad turns\ to \quad \Gamma = \frac{\sigma - \sigma^{''}}{L_0 T_m}$$

In order to describe anisotropy in 3D configurations a more complicated description becomes necessary. The driving force ΔG depends on local conditions of external fields like temperature T or concentration c_i of the i different alloy elements (but also: stresses/strains, electric/magnetic fields, ...): $\Delta G = \Delta G(T, c_i)$. A non-vanishing ΔG will lead to a finite change in phase fraction i.e. a finite $\varphi'(x,t)$. This change in phase fraction in turn will affect the external fields, Figure 2.2.7. Thus there is a need of solving the coupled system of partial differential equations for the phase-field (in multiphase-field models: the multiple phase fields) and for all external fields affecting the phase *transition.*

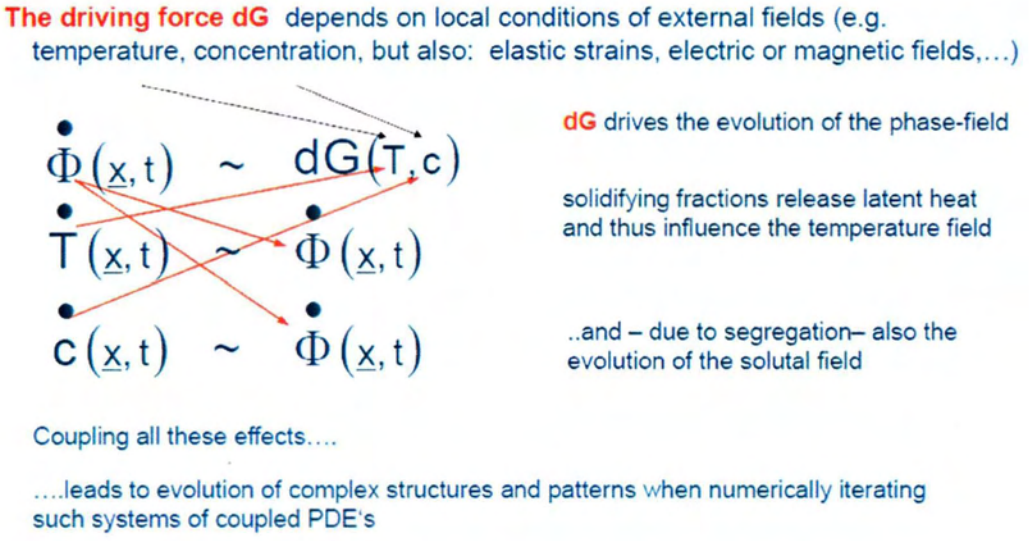

Figure2.2.7: **The driving force**

Technical alloys comprise multiple grains, multiple phases and multiple components. Their description in numerical models requires at least the introduction of multiple phase fields, the description of multicomponent diffusion and thermodynamic and kinetic data. The basic ideas of the multiphase-field approach [43] are:

- Definition of one phase field for each phase and for each grain of a phase
- Pairwise interaction for each pair of phases/grains like in standard phase-field
- Possibility of implementation of specific phase boundary/grain boundary properties

Basic model development

Starting from the initial idea of describing microstructure evolution in multiphase systems [34] a number of further developments was necessary to make the model applicable and useful for

technical alloy systems. The respective major topics are shortly outlined in the following and the reader is referred to respective articles for further reading. In detail – amongst others - the following topics have continuously been addressed since 1996:

- aspects of multiphase equilibria
- sharp interface asymptotics
- aspects of computational efficiency
- coarsening phenomena
- coupling to concentration fields including solute diffusion
- consideration of fluid flow
- coupling to thermodynamic databases
- incorporation of nucleation phenomena
- incorporation of elasticity/plasticity
- self-consistent coupling to macroscopic simulations

In the field of aluminium alloys, there is a high interest in microstructure simulation originating from automotive industry being caused by demands for lightweight alloys with optimized mechanical properties. Consequently, several approaches for the simulation of microstructure formation in technical aluminum alloys have been used by now, incorporating thermodynamic data on different levels [44-46]. The multiphase-field model [47] with direct coupling to thermodynamic data bases has been used for the calculation of microsegregation in the hypoeutectic alloy AA6061, the widely used A356 casting alloy, and eventually the slightly hypereutectic piston alloy KS1295 comprising up to 14 thermodynamic phases [48] (Figure 2.2.8).Recent work on Al-Alloys comprises effects of flow on dendritic growth [49], simulations on grain refinement [50], rheo-casting of Al alloys [51] and porosity formation during solidification of A356 [52]. Equiaxed solidification of the magnesium alloy AZ31 has been simulated using a two-dimensional hexagonal anisotropy and a seed density model for the description of nucleation of the primary dendrites [53]. Major objectives of further studies were the influence of alloy composition and process parameters on the grain size [54-56]. Phase-field simulations of solidification of Mg-alloys in three dimensions have been applied in order to investigate the role of the Mg-specific hexagonal dendrite morphology in the process of competitive grain growth and the resulting selection mechanisms [55, 57, 58]. Further work, e.g. addresses the castability of technical Mg-alloy grades [59].

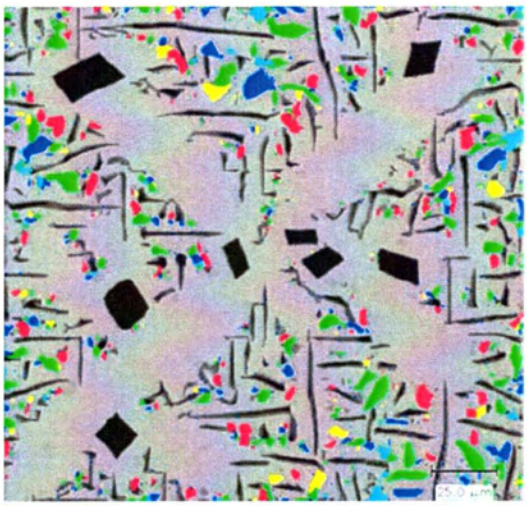

Figure 2.2.8: **Simulation of the solidification of a commercial Al alloy grade comprising seven alloy elements. Some of these alloy elements tend to form intermetallic phases, and a total of 14 different thermodynamic phases has been considered in this simulation [48]**

2.4 Fields of application-Alloy systems

The following sections will describe investigations and developments aiming at the description of microstructure evolution in technical alloy grades, which have been performed with the help of the software MICRESS. They will address steels, cast iron, superalloys, Al- and Mg-alloys, solders, intermetallic compounds and other alloys/systems. Along with the evolution of the underlying model basis, the phenomena being tackled have become increasingly sophisticated for each of these materials.

Steels

Already in ancient times the complex interplay between diffusion, precipitation, dissolution and re-precipitation as well as their control by well defined process scenarios has been exploited to develop sophisticated steel grades, like, e.g. the damascene steel revealing high-tech structures on the micro and even nano-scale. It is however worth noting that approximately 70% of the present 2500 different steel grades have been developed during the last 20 years. Steels provide a variety of different phenomena occurring both during solidification and during subsequent solid state transformations, the microstructure resulting from the preceding process step in most cases being of major importance for its further evolution during the subsequent steps. Probably for this reason, steels have been the first technological materials being investigated by multiphase-field methods.

Solidification of steels

First activities aimed at modeling the peritectic solidification in a binary Fe–C system [60]. Recent work describes modeling of the solidification of technical steel grades [61] and also addresses aspects like hot ductility during solidification of steel grades in continuous casting processes [62]. The phenomena considered in such simulations comprise, e.g. the formation of MnS precipitates, effects of cross-diffusion leading to inverse segregation of specific elements like P, the formation of segregation bands as consequence of discontinuous solidification conditions and many others.

Gamma-alpha transition

Next step for the microstructure evolution in technical steel grades are solid state transformations, especially the gamma-alpha transition. This phenomenon has first been modelled in 2D in 2001 [63] and be further extended and experimentally verified [64–66] and applied to model the heat affected zone during welding of low carbon steel [67]. Recent simulations of the gamma-alpha transition in 3D reveal the importance of different nucleation sites not occurring in 2D simulations like quadruple points or triple lines [68] and the effects of stresses affecting the transition [69]. Work on austenitization upon heating indicates this process not being the simple reverse of the ferrite formation [70]. Nucleation of austenite may start from ultrafine ferrite-carbide aggregates [71]. The successful use of a recently developed NPLE (non-partitioning, local equilibrium) model was demonstrated by simulation of austenite formation from an experimental ferrite plus pearlite microstructure and comparison to experimental results [72].

Pearlite formation

Pearlite transformation is a well-known eutectoid transformation, where a solid parent phase decomposes into two solid phases simultaneously. It is similar to eutectic solidification, where the phase state of the parent phase is the liquid. Both transformations can lead to a lamellar microstructure, and diffusion plays a major role for the spacing selection in this structure. First multiphase-field investigations on pearlite formation thus addressed the diffusion in both ferrite and austenite and aimed at describing the resulting spacing/growth rate. Respective results [73] already predicted a larger growth rate as compared to classical theoretical models [74, 75] but still could not close the discrepancies with experimental observations. Further investigations revealed that the transformation strain inhibits the cooperative growth mode of cementite and ferrite and provokes the salient growth of cementite needles ahead of the ferrite front. The predicted growth velocities are in the right order of magnitude as compared to the experiment and thus close the gap between predictions by classical models being based

on diffusion only and experimental observations [76]. While all above simulations locally resolve the distinct thermodynamic phases of the pearlite (i.e. ferrite and cementite), present model developments aim at describing pearlite as an "effective" phase without resolving the individual ferrite-cementite lamella [77]. For this purpose a combination of thermodynamic descriptions taken from databases and of linearized "phase-diagrams" for the pearlite pseudo phase has recently been implemented into a multi-phase-field code [1].

Grain growth

Phase-field models do not always require an explicit thermodynamic driving force to drive the evolution of a microstructure. Because the respective equations can be derived from the Gibbs–Thomson relation, they implicitly tend to minimize curvature and thus allow for the description of ripening and grain growth. Following models for ideal grain growth [78], effects of particle pinning on the mobility of the grain boundaries have been included [79]. Respective models now allow for the description of abnormal grain growth [80], e.g. during case hardening [81] or for the description of grain growth in microalloyed line-pipe steels [82] (Figure 2.2.9).

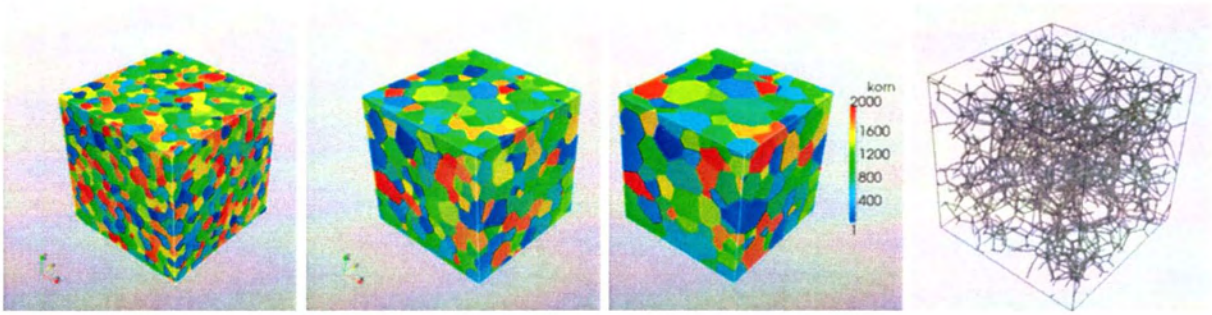

Figure 2.2.9: **3D grain growth simulation for different time steps starting from 2000 individual grains. Different gray values correspond to the individual grains (left). On the right representation of the triple lines of intersecting grain boundaries.**

Cast iron

Few simulations in the area of cast iron have by now addressed aspects of nucleation conditions for graphite in dependence on the segregation profile of different alloy elements. In a simulation study [83], nucleation of graphite on MnS particles, which form during solidification, has been identified as a possible scenario for formation of lamellar graphite in gray iron. Based on this scenario, especially the Ti composition turned out to be a decisive factor: Too high levels of Ti lead to suppression of nucleation and poor development of graphite lamellae. Respective simulations could be confirmed by experiments (Figure 2.2.10).

Figure 2.2.10: **Solidification simulation in cast iron. The formation and the growth of tiny MnS particles in the liquid influence the subsequent formation of graphite [83].**

Superalloys

Nickel-based superalloys find widespread use in high-temperature applications, e.g. in turbines for aero-engines, gas or steam turbines for power generation. Many of the respective components like turbine blades and/or vanes are produced using methods of investment casting and subsequent directional solidification. Solidification can then cause melt-related defects in these components. The morphological evolution of the dendritic structure and the subsequent solid-state decomposition upon cooling and homogenization heat treatment thus are important for applications. Multiphase-field models coupled to thermodynamic databases can account for the full compositional complexity of technically relevant superalloys [84]. Microsegregation, the phase fractions in the as-cast and directionally solidified [85] microstructures, formation of eutectic islands [86] the solidification-rate dependent dimensions of the mushy zone and the sequence of phase formation can be correctly predicted for phase transformations occurring during solidification effects of back-diffusion have been identified as being important. Extensions of the method which include homogenization of the as-cast microsegregation have been demonstrated [87]. Recent studies have addressed the long term behavior ([100,000 h) of precipitates in technical superalloy grades [62].

Mg-alloys

Mg-based alloys are gaining increasing technical importance due to the high demand for weight reduction, especially in transportation industry. A specific feature of magnesium solidification is the hexagonal anisotropy of the hcp lattice. Equiaxed solidification of the magnesium alloy AZ31 has been simulated using a two-dimensional hexagonal anisotropy and a seed density model for the description of nucleation of the primary dendrites [53]. Major objectives of further studies were the influence of alloy composition and process parameters on the grain

size [57]. Phase-field simulations of solidification of Mg-alloys in three dimensions have been applied in order to investigate the role of the Mg-specific hexagonal dendrite morphology in the process of competitive grain growth and the resulting selection mechanisms [54]. Further work, e.g. addresses the castability of technical Mg-alloy grades [58] (Figure 2.2.11).

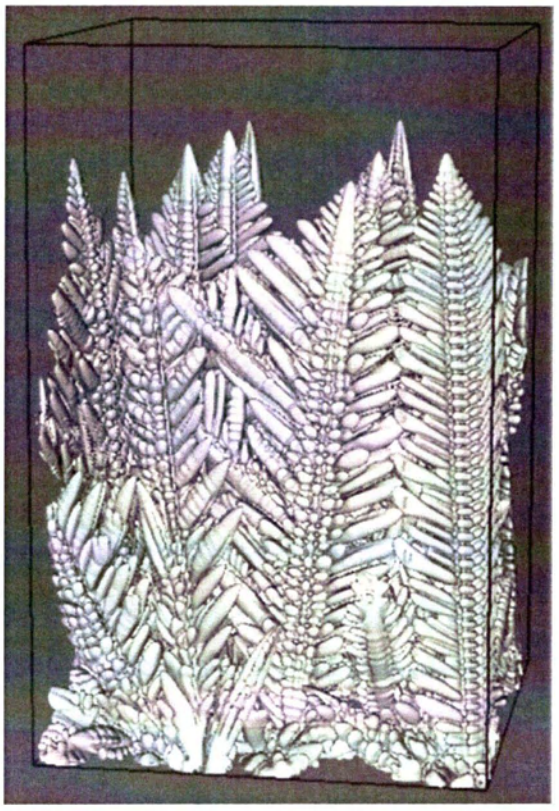

Figure 2.2.11: 3D-simulation of texture evolution in Mg-6% Al. Only few grains prevail after a short distance of directional solidification. The simulation has been started from 50 initial nuclei being randomly oriented [54, 55].

Solders

Failure of electronic components often occurs at solder joints and particularly at microstructural features, like, e.g. phase boundaries with intermetallics. Especially new solder alloys on the basis of ternary and higher alloyed solder systems like Sn–Ag–Cu are gaining importance and cannot be easily described by analytical approaches. Increasing integration density moreover leads to additional constituent elements originating from either boards and components or from their surface finish. These constituents have also to be considered for microstructure evolution. In addition to recent thermodynamic and kinetic modeling describing the range of possible stable phases, the phase-field approach allows describing their spatial distribution i.e. the microstructure. Such a simulated microstructure [88] may serve as a basis for future lifetime and reliability prediction of the respective solder joint. Special interest may originate from modeling electric current distributions in the microstructure and their influence

on inhomogeneous heating during operation of the joint or on electromigration of components affecting microstructure evolution.

Intermetallic compounds

The properties of modern TiAl-based intermetallic alloys critically depend on the solidified microstructure. Commonly, a rather coarse grain structure is obtained if a(Ti) forms via the peritectic reaction 'liquid + b(Ti) → a(Ti)'. A multiphase-field model has been applied to qualitatively simulate the interaction between nucleation and growth of the peritectic a(Ti) in TiAl alloys with Al content varying between 43 and 47 at.% Al. With increasing aluminum content, the fraction of the pro-peritectic b(Ti) phase being present at the peritectic temperature decreases. A higher Al-content additionally increases the grain refining effect due to growth restriction [89].

2.5 Phase-field studies in solidification

Main challenge is the correct treatment of solute redistribution and the calculation of the driving forces across diffuse interfaces revealing a numerically finite thickness. This has been first realized for a multiphase binary system [90,91]. Aspects of combined heat and solute diffusion during solidification of a binary alloy have been treated by Ramirez et.al. [92].

Besides diffusion, fluid flow is a major transport mechanism for species and heat. In general fluid flow however takes place on a larger length scale as compared to the evolution of the microstructure and thus may be considered by selecting suitable boundary conditions for a microstructure simulation. But also on the scale of the microstructure itself fluid-flow has significant influence on dendrite growth morphology [42, 93], and on dendrite spacing selection [49].

Nucleation is an area where a lot of studies have been made and in the near future will be a significant field of research as a principal factor of solidification. Moreover the description of nucleation in simulations on the scale of individual grains has to draw back on other nucleation models. A variety of models have been implemented to phase-field codes allowing, e.g. to assign different nucleation probabilities in the bulk volume of the phases as compared to nucleation at interfaces and triple or higher order junctions. [94].

2.6 Research groups

MICRESS® is currently installed worldwide (Table 2.7.1) both in Universities and Research Centers as well as in the industry.

Table 2.7.1: Research groups using Micress software

Institute	Research interest
Oak Ridge National Laboratory	solidification, solid state transformations
University Ghent Laboratory for Iron and Steel-making. Department of Metallurgical and Materials Science	solidification of Zn-Al-Mg coatings
RWTH Aachen University Department of Ferrous Metallurgy	solid-state phase transformations, e.g. austenite to ferrite transformation in carbon steels
Netherlands Institute for Metals Research NIMR	grain growth, recrystallisation and phase transformations during welding
University of Wollongong	peritectic phase transition in steel, solidification of metallic coatings
Forschungszentrum Karlsruhe GmbH Institut für Materialforschung I	Materials research and development
Ohio State University	Phase Transformations during non-equilibrium processing
ICAMS Ruhr-University Bochum	Materials Simulation on different length scales atomistic, mesoscopic, macroscopic
University of Erlangen-Nürnberg	Process and alloy development of superalloys
Central Mechanical Engineering Research Institute	Semi-solid processing of Al-alloys
Laboratory of Materials.Department of Mechanical Engineering.University of Thessaly	welding, casting
Computational Alloy Design Group, IMDEA Materials Institute	solidification microstructure of die-casting Mg alloys and microstructure of beta Ti alloys after thermo-mechanical treatment

3. METHODOLOGY

The numerical simulation of real processes such as microstructure evolution requires mathematical models that describe the existing physical ones. MICRESS solves the so-called Stefan problem with a modified Gibbs-Thomson relation to model microstructure evolution. The solution of the mathematical problem of e.g. solidification involves process and material parameters, description of initial conditions, nucleation criteria, definition of the calculation domain as well as the consideration of some numerical parameters for PDE solvers. The phase-field method is used by MICRESS® as a numerical approach to the Stefan problem.

By now, the phase-field method is the most appropriate numerical approach for bridging the length scales between the interface capillarity length of a few nanometres and the millimetre scale of diffusion. The main characteristic feature of the phase-field model is the diffusiveness of the interface between two phases. The interface is described by a steep but continuous transition of the phase-field variable $\varphi(x,t)$ between two states [38]. However, technical alloys consist of multiple grains, multiple phases and multiple components. Their description requires among others the introduction of multiple phase fields, description of multicomponent diffusion and coupling to thermodynamic databases. Some of the basic ideas of the multiphase-field approach (see Figure 3.2.) are:

- definition of one phase field for each phase and for each grain of this phase
- pairwise interaction for each pair of phases/grains similar to the standard phase field.
- possibility of implementation of specific phase/ grain boundary properties
- optional use of higher order interactions in triple or multiple junctions

Further concepts of the multiphase field approach are the coupling to thermodynamic databases and the coupling to mobility databases. In order to obtain reasonable simulation results, MICRESS® performs time loops among the nucleation model, the multiphase-field solver, multicomponent diffusion solver and the temperature solver. Coupling to thermodynamic database yields information about the nucleation undercooling, the driving force, the solute partitioning, the diffusion matrix, latent heat, etc. The obtained information is necessary for the different solvers in order to be able to perform the corresponding calculations for each time loop.

The input file/driving file

MICRESS® requests input data from the terminal by a read statement. This input contains all the necessary information to start a simulation. It can be read from a text file, the so called driving file, via a shell or directly from keyboard. The driving file has the extension "*.dri" or "*_dri.txt". The MICRESS® input data is given in a sequential form with the input file divided into several sections. Their function and meaning will be explained in the following lines. The end of the

chapter explains how to create an input file.

Language settings

You can choose English, German and French language options. When running the input file, all text outputs are generated in the language selected by the user.

```
...
# Language settings
# Please select a language:
# 'English', 'Deutsch' or 'Francais'
English
...
```

Geometry

The input begins with the dimension and the numerical resolution of the simulation domain, i.e. the user has to specify the number of numerical grid cells in each direction and the grid spacing. In this context, the user decides whether to perform a 1D, 2D or a 3D simulation. Here, the x, y and z direction are not completely equivalent: temperature gradients or profiles e.g. can only be defined in z-direction (except for temperature coupling, see below). Therefore, for 1D simulations, the number of cells in x and y direction ("AnzX" and "AnzY") should be set to 1. For 2D simulations, "AnzY" must be set to 1. The definition of a 2D calculation domain is shown in the driving file section below.

The grid spacing is specified in micrometers. It is one of the most important numerical parameters as it determines the numerical resolution. The grid resolution should be high enough to resolve the diffusion profiles, depending on the diffusion coefficients and the growth velocity of the interface, and the curvatures of the finest expected microstructures. The simulation itself is not affected by this parameter.

```
...
# Geometry
# --------
# Grid size?
# (for 2D calculations: AnzY=1, for 1D calculations: AnzX=1, AnzY=1)
# AnzX:
200
# AnzY:
1
# AnzZ:
200
# Cell dimension (grid spacing in micrometers):
# (optionally followed by rescaling factor for the output in the form of '3/4')
0.50000
```

...

Flags

Type of coupling

In the "Flags" section the type of coupling to be used for the numerical approach has to be specified. The option "phase" means that the pure phase-field model will be used with no coupling to other fields. The choice is best e.g. for grain growth simulations in pure, polycrystalline phases. If "concentration" is selected, concentration-field coupling will be performed. This option is the most common used for the analysis of alloys.

...
Flags
Type of coupling?
Options: phase concentration temperature temp_cyl_coord
#[stress] [stress_coupled] [flow] [dislocation]
Concentration
...

Type of potential

The user can select either "double_obstacle" or "multi_obstacle. .In the special case of a two phase systems, it exactly recovers the 'double_obstacle'functional. The option "multi_obstacle" especially comprises corrections for triple junction terms and is important for correct wetting characteristics.

...
Type of coupling?
Options: phase concentration temperature temp_cyl_coord
[stress] [stress_coupled] [flow] [dislocation]
concentration
Type of potential?
Options: double_obstacle multi_obstacle [fd_correction]
double_obstacle
Enable one dimensional far field approximation for diffusion?
Options: 1d_far_field no_1d_far_field
no_1d_far_field
Shall an additional 1D field be defined in z direction
for temperature coupling?
Options: no_1d_temp 1d_temp 1d_temp_cylinder 1d_temp_polar [kin. Coeff]
kin. Coeff: Kinetics of latent heat release (default is 0.01)
1d_temp
Number of cells?
500
cell width (micrometer):
100.000000000000
...

1D_temp

If concentration coupling is activated, an explicit 1D temperature field can optionally be defined in z-direction. This field can be used as an improved thermal boundary condition for the micro-simulation domain and thus replaces the normal definition of thermal boundary conditions. In the 1D temperature field, heat flow and release of latent heat is solved explicitly.

The use of the 1D_temp option requires further inputs for the field size (number of cells) and the field resolution (cell width in micrometer) as well as further input of thermal diffusivities (parameter for latent heat) and boundary conditions. The total size of the temperature field must be equal or larger than the height of the microstructure simulation domain (in z-direction). As temperature is solved explicitly in the 1D temperature field, the use of latent heat is mandatory.

Phase field data structure

In this section, the initial dimensions for the internal fields iFace and nTupel must be specified. During runtime, the size of these fields is determined automatically, so in most cases the given values are of minor importance.

The values have to be given relative to the size of the simulation domain, a value of 1.0 for iFace for example would assume that the whole calculation domain could be covered by (two-grain or two-phase) interfaces without exceeding the given initial list size. The same holds for nTupel and the coverage of the domain with triple or higher junctions. The actual usage for both fields can be found in the TabL output.

The arrays iFace and nTupel are fully dynamic, so the influence of the initial values is quite limited. In extreme cases, the specification of excessively high initial values can lead to a memory overflow during the program startup. Too low values can lead to an unnecessarily high number of reallocation steps which slow down the initialisation process e. g. in the case of grain growth simulation with a high number of initial grains. Initial values of 0.10 for both parameters are recommended and work in practically all cases.

```
...
# Phase field data structure
# ----------------------------------
# Coefficient for initial dimension of field iFace
# [minimum usage] [target usage]
0.10
# Coefficient for initial dimension of field nTupel
# [minimum usage] [target usage]
0.10
...
```

Restart options

MICRESS® allows the user either to start a new simulation ("new") or to restart from the last output of an old one ("restart"). The "restart" option thus gives the possibility to continue a stopped simulation or to start various simulations (e.g. for a parameter variation) from a common starting point defined by a previous simulation. Thus, calculation time and effort can be saved.

Even if the restart option is used, all input parameters have to be specified like for a new simulation run. Those parameters which represent initial conditions like initial composition and temperature are replaced automatically by the values from the restart file.

```
...
# Restart options
# ===============
# Restart using old results?
# Options:   new     restart [reset_time]
new
#
....
```

Selection of the outputs

In this section, the types of output files which shall be written by MICRESS® must be specified. These outputs are either binary files which can be viewed with DP_MICRESS (unless another format is specified explicitly in the "Name of output files"section), or text files which can be opened with standard text editors. Conservatively, each output type has to be activated or deactivated in an extra line in the driving file and in the requested order by using the corresponding positive or negative keyword, e.g. "out_restart" or "no_out_restart" for writing or not writing a restart file.

```
...
#
# Name of output files
# ====================
# Name of result files?
C:\Users\User\Desktop\Kar\Results_3%
# Overwrite files with the same name?
# Options:   overwrite    write_protected    append
#          [zipped|not_zipped|vtk]
#          [unix|windows|non_native]
Overwrite
#
...
```

Time input data

The times for user-defined intermediate outputs can be specified in this section. For convenience, the user should include an early output time in order to check whether the simulation has started correctly. Series of outputs with a constant interval or factor between the times can be easily defined with 'linear_step' or 'logarithmic_step' (for geometric series). In the example shown here, the user requests outputs for t = 00.25 s and 01.00 s, every 00.50 s until 10.00 s, and every 01.00 s until 25.00 s.

All these input elements can be combined and repeated in arbitrary way. This input section is to be finished with the keyword "end_of_simulation"'.

```
...
# Time input data
# ============
# Finish input of output times (in seconds) with 'end_of_simulation'
# 'regularly-spaced' outputs can be set with 'linear_step'
# or 'logarithmic_step' and then specifying the increment
# and end value
#  'first'              : additional output for first time-step
#  'end_at_temperature'    : additional output and end of simulation
# at given temperature
linear_step 0.01 0.8
end_of_simulation
...
```

Phase data

This section begins with an input of the number of solid phases which will be used in the simulation. Phase number 0 is the "background" or "matrix" phase which is implicitly defined and which is assumed to be isotropic (liquid). Then, for each phase specific properties have to be defined. First, the user has to specify whether a stored energy will be defined for this phase and whether recrystallisation will be included into the simulation.

Then, the type of anisotropy for each solid phase has to be specified as "isotropic", "anisotropic", „faceted" or "antifaceted". If the choice is not "isotropic", further information on the crystal symmetry is required. The different growth shapes of crystals are a consequence of their atomic lattice structure, which results in orientation-dependent interface energies and kinetics. The most common type of anisotropy is the cubic crystal symmetry. No grain categorisation is used and metallic anisotropy which in the 2D case is grain orientation is defined by 2d angles represented by a 4-fold cosine function.

Next, the user has to decide whether to use grain categorization. This option allows for sorting the grains of each phase in a user-defined number of orientation "categories". Using

categorization, simulations can be speed up, as some operations in MICRESS® are quadratic with respect to the number of grains (or categories). The "categorize" keyword here means that you want to assign grains with identical properties (including orientation) to the same grain number for a given phase. No additional parameter is required after the keyword "categorize".

```
...
# Phase data
# ==========
# Number of distinct solid phases?
2
#
# Data for phase 1:
# -----------------
# Simulation of recrystallisation in phase 1?
# Options: recrystall no_recrystall [verbose|no_verbose]
no_recrystall
# Is phase 1 anisotrop?
# Options: isotropic anisotropic faceted antifaceted
anisotropic
# Crystal symmetry of the phase?
# Options: none cubic hexagonal tetragonal orthorhombic
cubic
# Should grains of phase 1 be reduced to categories?
# Options: categorize no_categorize
no_categorize
#
# Data for phase 2:
# -----------------
# [identical phase number]
# Simulation of recrystallisation in phase 2?
# Options: recrystall no_recrystall [verbose|no_verbose]
no_recrystall
# Is phase 2 anisotrop?
# Options: isotropic anisotropic faceted antifaceted
isotropic
# Should grains of phase 2 be reduced to categories?
# Options: categorize no_categorize
categorize
#
...
```

Grain orientation

At next, the user has to decide in which way grain orientations shall be specified through the rest of the input file. As shown, following options are now available. One angle in 2D ("angle_2D") and in 3D, a definition via 3 Euler angles ("euler_zxz") or one rotation angle plus a corresponding axis in the 3D space ("angle_axis") or via Miller indices ("miller_indices") or directly defined as a quaternion ("quaternion"). In the program the different grain orientation definitions are transformed in a quaternion.

```
...
#
# Phase data
# =========
# Number of distinct solid phases?
1
# Data for phase 1:
# -------------------------
...
# Orientation
# -----------------
# How shall grain orientations be defined?
# Options: angle_2d euler_zxz angle_axis miller_indices quaternion
angle_2d
#
...
```

Grain input

In this section, the microstructure at the beginning of the simulation needs to be specified. The input begins with determining the type of grain positioning. The initial grain structure can either be specified explicitly grain by grain ("deterministic"), by stochastic means ("random") or by reading in a file which represents the initial geometry of the grains ("from_file").

A general rule during grain input is that grain numbers are chosen automatically in a consecutive manner. Grains with a higher number can erase those with lower number if they completely cover them. In case of a partial overlap, the overlapping region by default belongs to the grain with a higher number. Only if the "Voronoi" option is chosen, the overlapping region is distributed between the grains by use of the Voronoi construction. If a grain radius is defined which is smaller than the grid resolution $\Delta\xi$, a grain consisting of only one interface cell is created which has a grain fraction corresponding to the 3D volume specified by the radius. For those grains, no reasonable curvature can be evaluated using the normall phase-field equation. Therefore, an alternative curvature treatment has to be defined.

The "stabilisation" model neglects the curvature as long as the grain is still small. In the "analytical_curvature" model, curvature is calculated from the phase fraction, assuming a spherical morphology. In this case an extra critical radius has to be defined, which determines the maximum value of the curvature for this grain. If there are no grains to be present at the beginning of the simulation, the user should specify "deterministic" and define the number of grains at the beginning as 0. In this case, no additional input is necessary in this section.

deterministic

With this option, first the number of grains at the beginning has to be specified. For each grain, the geometry (round, rectangular or elliptic) and the grain positioning is defined by Cartesian coordinates with the origin at the bottom left-hand corner (in 2D simulations, only the x and z coordinate has to be given). Round grains are defined by their radius, rectangular and elliptic grains by the length along the x and the z-axis. If round grain geometry has been chosen, the curvature model which is to be used in case of small grains has to be specified. Furthermore, the user has to specify whether in case of overlapping grains the Voronoi construction is to be used and which phase number is associated with the grain. Depending on the properties of this phase, the recrystallisation energy and the orientation of the grain has further to be given.

Random

For random grain positioning, an integer for randomization is required as first input. Essentially, this "random seed" assures reproducibility of the initial grain structure when other parameters of the input file are changed. Afterwards, the number of different types of grains has to be specified. By the different types it is possible to e.g. define complex size distributions or to fill different zones of the simulation domain with grains of different size or geometry. For each grain type, the number of grains and the grain geometry must be specified. As in the case of deterministic grain positioning the user can define round, rectangular or elliptic grains. Furthermore, a minimum and a maximum value are required for each-space coordinate in order to define the region over which the grains of this type shall be randomly redistributed. Depending on the type of the geometry chosen, the user has to further specify a minimum and a maximum radius (round geometry) or a minimum and a maximum length size along each-axis (rectangular or elliptic geometry) in order to define the size distribution of the actual grain type. In the same way as for deterministic input, the curvature model which is to be used in case of small grains has to be specified (if a "round" geometry has been selected), the user has to specify whether the Voronoi construction is to be used, which phase number is associated with the grain of the actual type and, depending on the phase properties, the recrystallisation energy has further to be given. Additionally, a minimum distance betweenthe grains (in µm) is required. This parameter, besides the minimum and maximum radius, helps to avoid overlapping of grains. In Voronoi construction, this parameter is helpful to obtain equal size distributions.

from_file

In case of reading the initial grain structure from file, first its name (and path) needs to be specified. For defining the initial grain structure, an image file in ASCII format is required. The geometry of this file has to be given as AnzX and AnzZ (for 2D simulations). These dimensions have not necessarily to be the same as the dimensions of the simulation domain specified at the top of the input file.

The number of grains at the beginning can be either specified explicitly or read from the input file. If the grain properties for the defined number of grains are specified in an extra file, its name and path has to be given. Otherwise, the grain properties are read in directly from the command line. They can be set to "identical", i.e. all grains have the same properties, or they can be read as blocks. The latter would mean grain 1 to 3 and grain 4 to 6 if the number of grains was set to 6.

```
...
#
# Grain input
# ===========
# Type of grain positioning?
# Options: deterministic  random  from_file
deterministic
# NB: the origin of coordinate system is the bottom left-hand corner,
#    all points within the simulation domain having positive coordinates.
# Number of grains at the beginning?
0
#
...
```

Data for further nucleation

There are different nucleation models used by MICRESS® which refer to different types of phases or circumstances where nucleation is to occur. These are for example a specific interface, in the bulk or phase regions. Moreover, it is important to know whether a fixed critical undercooling or some other criteria based on the seeding particle properties, stored energies in recrystallisation, etc. shall be used as a nucleation criterion. The user specifies which phase is nucleated on which substrate phase and in which phase the solutal undercooling of the nucleating phase is calculated (matrix phase). The user also determines the temperature range, the checking frequency, data for shielding subsequent nuclei, etc.

The following nucleation models are implemented in MICRESS®.

The phase number of the new grains and the reference phase must be defined. New grains can appear only where the reference phase is present. In case of concentration coupling, the driving

force for nucleation is calculated using the local composition in this phase. In solidification simulations e.g. the liquid phase is typically the reference phase.

If the "type of position" is neither "bulk" nor "region", an additional substrate phase (and an optional second substrate phase) is required for further specification of the interfaces where nucleation should occur, and for defining which of the two phases in the interface defines the curvature contribution to the nucleation undercooling .

In continuation, the nucleation model to be used for further nucleation is defined. MICRESS® uses two nucleation models, the seed density model and the seed undercooling model.

Seed density model

The seed density nucleation model implemented in MICRESS® is based on a heterogeneous nucleation model similar to the one used by Lindsay Greer.

During heat extraction from the melt, the largest particles will nucleate first at an undercooling defined by their radius (if complete wetting is assumed or an effective radius is used instead). The particles start growing and releasing latent heat, while interacting with other potential nucleation precursors. Depending on the heat extraction rate and the amount and dimensions of all other seeding particles, the temperature will drop more or less below the liquidus temperature, thus defining the amount of seeds to be activated. According to the model, the effectiveness of inoculants added for grain refinement is defined by:

- the maximum particle size
- the particle size distribution

In MICRESS®, the seed density model should be used together with latent heat or with coupling to the one-dimensional temperature field (1d_temp) in order to allow an interaction of the potential nucleation sites via release of latent heat, but sometimes it may seem appropriate to use it just as a simple way to randomly distribute a given number of nuclei in a defined region.

The model describes nucleation from the melt, triggered by small seeding particles which may be added intentionally or which may exist as impurities. Essentially, the critical undercooling for nucleation of a given phase on this seeding particle depends on the radius of the seeding particle and the surface energy of the new phase in the liquid. Consequently, if a radius-density distribution of the seeding particles is known, depending on the cooling conditions, the model can predict how many nuclei will be formed.

If the different grains of the new phase grow competitively, like in equiaxed solidification, the latent heat released by the growing particles has to be taken into account. The easiest way to do that in MICRESS ® is to specify the global volume heat extraction rate as a temperature boundary condition. Thus, the total amount of latent heat is released globally on the whole simulation.

At the beginning of the simulation, for all seed types which use the seed density model, discrete positions with discrete radius for the potential nucleation sites are determined and stored. During the simulation run, nucleation is checked only at these predefined places.

These seeding particles are not "consumed" by nucleation and cannot move. An exception is the "moving_frame" option in the section the predefined nucleation sites move with the frame, the sites which move out at the bottom of the domain are copied to the top line in order to keep the density of nucleation sites constant. The user first has to specify an integer for randomization. The random number generator has to be initialized with an arbitrary integer number. This ensures that, e.g., inserting a new nucleation type would not change the random positions of all other types.

In the seed density model, the size distribution of potential nucleation sites (seeding particles) is described in terms of classes with different radius [µm] and density [cm-3]. For each class, the number of potential nucleation sites is calculated according to the given density and the volume of the simulation domain.

Using the given density, explicit positions of the potential nucleation sites are determined. The radii (and thus the local critical undercooling for nucleation on each particle) are distributed evenly according to the radius range of each seed class. Inside each class, a random radius distribution is assumed. The radius range corresponds to the radius difference to the next specified class. The finally created numbers and radius ranges for each class can be found in the log-file.

The seed classes must be specified starting with the highest radius values. At least two classes should be specified, otherwise the automatically assumed radius range may lead to unexpected results.

Seed undercooling model

Using the seed undercooling model, a new seed is set if the local undercooling at a nucleant position exceeds a predefined critical nucleation undercooling. The local undercooling depends on the local composition and temperature.

In general, the MICRESS® nucleation models are designed for micro-scale simulations and not for the nano-scale, i.e. there is no model for the prediction of homogeneous nucleation based on thermal fluctuations for the critical seed formation.

In praxis, inoculants are often added to technical alloy melts which serve as nucleation agents during solidification. They help to achieve a smaller grain size and to suppress columnar growth. Even if no active inoculation is done, impurities, dislocations or the roughness of the interface structures can lead to nucleation phenomena in all types of technical processes. Unfortunately, apart from the "seed density model" for heterogeneous nucleation from an inoculated melt, no

physical models are available for the complex nucleation conditions in technical alloys. Homogeneous nucleation, on the other hand, will typically occur only at very high undercooling and under extremely clean conditions, like in experiments with levitated drops.

Thus, besides the physically based "seed density model" for heterogeneous nucleation, MICRESS® provides the user with a pragmatic nucleation model based on a critical undercooling which can be further specified with respect to the type of seed positioning, the temperature range, the matrix and substrate phases, the nucleation rate etc. and which allows the user to mimic the complex nucleation circumstances found in technical alloys or processes. All these parameters can be specified in the section "Data for further nucleation".

The keyword "nucleation" activates nucleation input. The option "out_nucleation" in the next line gives the result outputs for the time-step when nuclei are set or a phase disappears. Next, the number the of seeds must be specified. By using several seed types, different nucleation conditions can be independently defined for different phases on different types of positions, for different temperature intervals etc.

In contrast to the seed density model, no explicit potential nucleation sites are predefined and the number of grains which can nucleate during simulation is not limited. Therefore, the user can specify a maximum number of grains which are allowed for each seed type. If this number is exceeded, nucleation of this type stops without warning .

Next, an explicit radius for the grains of this type has to be specified. If a value higher than the spatial discretisation x is chosen, then a grain with the corresponding size and a sharp interface is created.

If a value lower than the spatial discretisation x is chosen, a „small" grain consisting of only one interface cell is created. Usually, a value of 0 will be used to start with the smallest possible fraction of 2 x phMin (see section "Other numerical parameters"). By this way, any kind of concentration imbalance is avoided (given that phMin has been chosen appropriately).

Under certain circumstances, the user may wish to specify a radius value between 0 and x. Then, a grain consisting of a single cell with a fraction of the new phase corresponding to the 3D volume will appear. Afterwards, the small grain model to be used must be specified.

The minimum undercooling specifies at which undercooling nuclei are allowed to form. This undercooling is calculated using the local composition (if concentration coupling is used), temperature and, if applicable, the local curvature of the substrate phase.

After having chosen the nucleation model to be used in the simulation, the orientation of the new grains has to be specified, if the phase of the new phase has not been set to isotropic (phase input data). A random distribution, a fix value, an orientation range or a parent relation, i.e. a relative orientation to the grain of the local substrate phase, can be chosen. The last option applies only to nucleation at interfaces or junctions. Then, the shield data have to be

specified. Shielding means that no further grain of the same phase will be nucleated during the shield time within the shield distance of a previously nucleated grain. No categorisation will be applied to this grain during the shield time (otherwise the shield properties would be lost!). The shield time is also used by the "kill_metastable" option, no killing is performed during the shield time.

After the shield distance an optional parameter for nucleation distance can be entered. This parameter determines the minimal distance between grains of the same phase that nucleate at the same time. If no nucleation distance is given it defaults to the shield distance.

In case of the seed density model, explicit shielding is not compatible with the underlying physical model. The user is requested to specify only a "shield time" which still is necessary to control the categorisation and „kill_metastable" functions.

If in section "phase data" "categorize" and "anisotropic" have been chosen for the nuclei phase, the user has to decide whether for this seed type categorisation of the orientation values to orientation categories shall be performed. This is important, if different grains shall be assigned to the same grain number during run-time, because this is only possible if all grain properties including orientations of the grains are identical. After the keyword "categorize", the number of orientation categories can be specified, default is 36 (corresponding to 10° difference between the orientation categories in 2D).

Further, MICRESS® requests a minimum and a maximum nucleation temperature for the actual seed type. A minimum and maximum temperature should be chosen around the temperature where nucleation is expected.The parameters primarily help to minimize unnecessary nucleation checks and thus to improve performance. In some cases with TQ coupling, checking nucleation too far from the temperature where the new phase gets stable can cause numerical problems. Then, proper values have to be found, depending on the system.

In a first trial, it is wise not to restrict the nucleation range. The time between checks for nucleation determines the frequency of nucleation checking. If chosen too high, insufficient seeding may occur in spite of high local undercooling. If chosen too small, an unnecessarily high numerical effort and a corresponding performance loss can be the consequence.

The noise is applied as $\Delta G\ (1+k*(random\ -0.5))*\ \Delta G$ where k is user defined noise amplitude, $0 <$ random $<\ 1$ is the value of the random number generator and ΔG is the nucleation driving force.

Input for each seed type

For each seed type, a type of positioning must be given. Seeds may be placed in the bulk (="inner" part of the grains), in regions, at interfaces, in the bulk, at triple or at quadruple junctions. Unless the additional keyword "restrictive" is used, the choice of a given keyword includes all keywords which in the options list are found right of this keyword. Thus, "bulk" or

"region" include all interfaces, triple points and higher junctions, "interface" includes all triple or quadruple junctions and so on. If "region" is requested, the coordinate ranges (mm) in micrometer must be given in the following lines.

After that, the phase number of the new grains and the reference phase must be defined. New grains can appear only where the reference phase is present. In case of concentration coupling, the driving force for nucleation is calculated using the local composition in this phase. In solidification simulations e.g. the liquid phase is typically the reference phase.

If the "type of position" is neither "bulk" nor "region", an additional substrate phase (and an optional second substrate phase) is required for further specification of the interfaces where nucleation should occur, and for defining which of the two phases in the interface defines the curvature contribution to the nucleation undercooling (for "interface" only). This curvature contribution is disregarded if the substrate phase is identical to the reference phase. In continuation, the nucleation model to be used for further nucleation is defined. MICRESS® uses two nucleation models – the seed density model and the seed undercooling model.The seed density model is designed for heterogeneous nucleation in a melt, therefore it is only available for "bulk" or "region". In all other cases, the seed undercooling model is chosen by default.Both models will be presented separately within the next sections.

Input for all seed types

After specification of all seed types, some few inputs remain to be done which apply to all seed types. First of all, if any of the seed types is using random noise, an integer number for randomization has to be given to assure reproducibility. The maximum number of simultaneous nucleations is the number of grains of all seed types allowed to be nucleated in the same time step. A list of possible seeds is created and ordered with respect to the undercooling or driving force for each nucleus. If the maximum number is exceeded, the less favourable seeds are discarded. The option may lead to unexpected results if more than one seed type is defined and therefore should be used carefully. Setting the maximum number of simultaneous nucleations to "automatic" (=0) removes this check. In some cases, "stabilised" small grains can erroneously reach a metastable state at which they stop growing, but also do not vanish because their stabilisation implies a reduced curvature. By enabling the flag "kill_metastable", the stabilisation of small grains is removed after their shield time has elapsed. This makes sure that "metastable grains" can vanish correctly. The option "kill_metastable" is also relevant in case of categorisation, because after „killing", small stabilized grains are considered as „big" and such can be assigned to a common grain number. The "kill_metastable" flag is only relevant for small grains which use the "stabilisation" model.

```
# Data for further nucleation
# ===========================
# Enable further nucleation?
# Options: nucleation  nucleation_symm  no_nucleation [verbose|no_verbose]
nucleation
```

```
# Additional output for nucleation?
# Options:    out_nucleation    no_out_nucleation
no_out_nucleation
#
# Number of types of seeds?
2
#
# Input for seed type 1:
# ----------------------
# Type of 'position' of the seeds?
# Options: bulk region interface triple quadruple [restrictive]
bulk
# Phase of new grains (integer) [unresolved]?
1
# Reference phase (integer) [min. and max. fraction (real)]?
0
# Which nucleation model shall be used?
# Options:   seed_undercooling   seed_density
seed_density
# Integer for randomization?
134
# How many classes shall be chosen for the critical radius?
17
# Specify radius [micrometers] and seed density [cm**-3] for class  1
0.45   100
# Specify radius [micrometers] and seed density [cm**-3] for class  2
0.3   200
# Specify radius [micrometers] and seed density [cm**-3] for class  3
0.25   500
# Specify radius [micrometers] and seed density [cm**-3] for class  4
0.18  1000
# Specify radius [micrometers] and seed density [cm**-3] for class  5
0.15  2000
# Specify radius [micrometers] and seed density [cm**-3] for class  6
0.12  5000
# Specify radius [micrometers] and seed density [cm**-3] for class  7
0.10  9000
# Specify radius [micrometers] and seed density [cm**-3] for class  8
0.08  14000
# Specify radius [micrometers] and seed density [cm**-3] for class  9
0.07  25000
# Specify radius [micrometers] and seed density [cm**-3] for class 10
0.06  50000
# Specify radius [micrometers] and seed density [cm**-3] for class 11
```

0.05 80000
Specify radius [micrometers] and seed density [cm**-3] for class 12
0.04 120000
Specify radius [micrometers] and seed density [cm**-3] for class 13
0.03 220000
Specify radius [micrometers] and seed density [cm**-3] for class 14
0.025 330000
Specify radius [micrometers] and seed density [cm**-3] for class 15
0.02 500000
Specify radius [micrometers] and seed density [cm**-3] for class 16
0.015 1000000
Specify radius [micrometers] and seed density [cm**-3] for class 17
0.010 30000000
Class 1: 0 seed(s), 3.7500E-01 < radii < 5.2500E-01 [micrometers]
Class 2: 0 seed(s), 2.7500E-01 < radii < 3.7500E-01 [micrometers]
Class 3: 0 seed(s), 2.1500E-01 < radii < 2.7500E-01 [micrometers]
Class 4: 0 seed(s), 1.6500E-01 < radii < 2.1500E-01 [micrometers]
Class 5: 0 seed(s), 1.3500E-01 < radii < 1.6500E-01 [micrometers]
Class 6: 0 seed(s), 1.1000E-01 < radii < 1.3500E-01 [micrometers]
Class 7: 0 seed(s), 9.0000E-02 < radii < 1.1000E-01 [micrometers]
Class 8: 0 seed(s), 7.5000E-02 < radii < 9.0000E-02 [micrometers]
Class 9: 0 seed(s), 6.5000E-02 < radii < 7.5000E-02 [micrometers]
Class 10: 0 seed(s), 5.5000E-02 < radii < 6.5000E-02 [micrometers]
Class 11: 0 seed(s), 4.5000E-02 < radii < 5.5000E-02 [micrometers]
Class 12: 0 seed(s), 3.5000E-02 < radii < 4.5000E-02 [micrometers]
Class 13: 0 seed(s), 2.7500E-02 < radii < 3.5000E-02 [micrometers]
Class 14: 1 seed(s), 2.2500E-02 < radii < 2.7500E-02 [micrometers]
Class 15: 1 seed(s), 1.7500E-02 < radii < 2.2500E-02 [micrometers]
Class 16: 1 seed(s), 1.2500E-02 < radii < 1.7500E-02 [micrometers]
Class 17: 9 seed(s), 1.0000E-08 < radii < 1.2500E-02 [micrometers]
Determination of nuclei orientations?
Options: random randomZ fix range parent_relation
random
Shield effect:
Shield time [s] ?
1.0000
Nucleation range
min. nucleation temperature for seed type 1 [K]
0.000000
max. nucleation temperature for seed type 1 [K]
1000.000
Time between checks for nucleation? [s]
1.00000E-03
Shall random noise be applied?

```
# Options:    nucleation_noise  no_nucleation_noise
no_nucleation_noise
#
# Input for seed type 2:
# ----------------------
# Type of 'position' of the seeds?
# Options: bulk region interface triple quadruple [restrictive]
interface
# Phase of new grains (integer) [unresolved]?
2
# Reference phase (integer) [min. and max. fraction (real)]?
0
# Substrat phase [2nd phase in interface]?
# (set to 0 to disable the effect of substrate curvature)
1
# maximum number of new nuclei 2?
100000
# Grain radius [micrometers]?
0.00000
# Choice of growth mode:
# Options:  stabilisation analytical_curvature
stabilisation
# min. undercooling [K] (>0)?
2.0000
# Shield effect:
# Shield time [s] ?
1.00000E-02
# Shield distance [micrometers]  [ nucleation distance [micrometers] ]?
10.000
# Nucleation range
# min. nucleation temperature for seed type 2 [K]
0.000000
# max. nucleation temperature for seed type 2 [K]
820.0000
# Time between checks for nucleation? [s]
1.00000E-02
# Shall random noise be applied?
# Options:    nucleation_noise  no_nucleation_noise
no_nucleation_noise
#
# Max. number of simultaneous nucleations?
# ---------------------------------------
# (set to 0 for automatic)
1000
```

#
Shall metastable small seeds be killed?

Options: kill_metastable no_kill_metastable
no_kill_metastable
#

Phase interaction data

In this section the user defines the phase interaction data and the grain boundary properties. Phase interactions can be defined for all pair-wise combinations of the phases which have been included in the "phase data " section.

In the standard input sequence, the user is requested to specify all phase interaction data in a fixed order, starting with the phase pair 0/1. Phase interactions which are not used are switched off using the keyword "no_phase_interaction". No further input is required in this case. The standard input sequence is recommended for less experienced users and for low numbers of phases. No further input is required in this case. The standard input sequence is recommended for less experienced users and for low number of phases. Enabling phase interactions means that one of the phases may grow or shrink on the expense of the other. On the other hand, if a phase interaction is switched off, no movement of the corresponding interfaces is possible.

This also concerns the initialisation of the interface: if such an interface is created via the initial grain setting, the interface will stay sharp even if an initialization is requested. Nevertheless, in case of concentration coupling, there can be diffusion through switched off interfaces. The partition coefficients which are necessary for diffusion through interfaces are accessed from the other phase interactions using a "constant" approximation. If e.g. interactions are defined for phases 0/1 and 0/2, a simplified description can be derived for the 1/2 interface. This description is stored for each interface cell in the moment of creation (as initial structure or from moving triple junctions) and kept constant during the further simulation steps. Switching off phase interactions can greatly reduce the complexity of a simulation, especially if many phases are included. In solidification, it is in most cases wise to discard all solid-solid interactions, if a continuation of the simulation (with heat treatment etc.) is not intended.

When the interaction of one phase with itself is enabled, solid-state interactions between grains of the same phase will be activated. In this case, no chemical driving force is included and the movement will be controlled only by curvature.

The option "phase interaction" can be followed by an optional keyword which selects apecial interaction models:

"standard" : this is a default interaction choise.

In the next line, the driving force options have to be specified. Except for the local RX model,where these options have been specified always, they have been specified only in the case of interaction between different phases. All DeltaG options have to be written in one line, consisting of concatenated pairs of a keyword and the corresponding value.

The keyword "avg" is used to define an averaging of the driving force across the interface. Averaging prevents spreading of the interface if a strong concentration gradient is causing opposite driving forces on both sides of the interface. The user can specify a value between 0 (no averaging) and 1 (maximum averaging).

The keyword "max" specifies the maximum driving force allowed (value above which the driving force will be cut-off). This value is useful to shrug off some temporary problems during initial transients or to reduce the impact of numerical fluctuations. The value should be chosen high enough in order not to limit kinetics during normal growth. If a too small value is chosen for the maximum allowed driving force, the movement of the interface can be drastically slowed down

The "smooth" keyword has only effect if averaging is specified: The gradient direction along which averaging of the driving force is performed, is randomly rotated with the specified maximum value in degrees. Depending on other circumstances, this option may help to reduce the effect of grid anisotropy on the growth morphology. A typical value is 45, default is 0.

The interface energy, which scales the effect of curvature, can be given either as a constant value (keyword "constant") or defined as "temperature_dependent". Interface energies have to be specified in J/cm^2.

One of the most important phase interaction parameter is the interface mobility which defines the interface velocity for a given driving force or curvature. The mobility may be defined as constant, temperature dependent or driving force dependent. Interface mobilities have to be specified in cm^4/Js.

```
#
# Phase interaction data
# ======================
#
# Data for phase interaction 0 / 1:
# ---------------------------------
# Simulation of interaction between phase 0 and 1?
# Options: phase_interaction  no_phase_interaction
#  [standard|particle_pinning[_temperature]|solute_drag]
#   | [redistribution_control]
phase_interaction
# 'DeltaG' options:  default
# avg ... []  max ... [J/cm**3]  smooth ... [degrees]  noise ... [J/cm**3]
```

```
avg 0.55   max 100
# I.e.:  avg +0.55  smooth +45.0  max +1.00000E+02
# Type of surface energy definition between phases LIQUID and 1?
# Options:  constant  temp_dependent
constant
# Surface energy between phases LIQUID and 1? [J/cm**2]
#    [max. value for num. interface stabilisation [J/cm**2]]
1.00000E-05
# Type of mobility definition between phases LIQUID and 1?
# Options:  constant  temp_dependent  dg_dependent
temp_dependent
# File for kinetic coefficient between phases LIQUID and 1?
C:\Users\User\Desktop\Kar\Results_30%\AlCu_Temp1d_mueVonT0_1
# Is interaction isotropic?
# Optionen: isotropic  anisotropic [harmonic_expansion]
anisotropic
# Anisotropy of interfacial stiffness? (cubic)
# 1 - delta * cos(4*phi), (delta =delta_stiffness =15*delta_energy)
# Coefficient delta (<1.) ?
0.50000
# Anisotropy of interfacial mobility? (cubic)
# 1 + delta * cos(4*phi)
# Coefficient delta (<1.) ?
0.20000
#
# Data for phase interaction 0 / 2:
# ---------------------------------
# Simulation of interaction between phase 0 and 2?
# Options: phase_interaction  no_phase_interaction  identical phases nb
#  [standard|particle_pinning[_temperature]|solute_drag]
#   | [redistribution_control]
phase_interaction
# 'DeltaG' options:  default
# avg ... []  max ... [J/cm**3]  smooth ... [degrees]  noise ... [J/cm**3]
avg 0.55   max 100
# I.e.:  avg +0.55  smooth +45.0  max +1.00000E+02
# Type of surface energy definition between phases LIQUID and 2?
# Options:  constant  temp_dependent
constant
# Surface energy between phases LIQUID and 2? [J/cm**2]
#    [max. value for num. interface stabilisation [J/cm**2]]
1.00000E-05
# Type of mobility definition between phases LIQUID and 2?
# Options:  constant  temp_dependent  dg_dependent
```

```
temp_dependent
# File for kinetic coefficient between phases LIQUID and 2?
C:\Users\User\Desktop\Kar\Results_30%\AlCu_Temp1d_mueVonT0_2
#
# Data for phase interaction 1 / 1:
# --------------------------------
# Simulation of interaction between phase 1 and 1?
# Options: phase_interaction  no_phase_interaction  identical phases nb
#  [standard|particle_pinning[_temperature]|solute_drag]
#   | [redistribution_control]
no_phase_interaction
#
# Data for phase interaction 1 / 2:
# --------------------------------
# Simulation of interaction between phase 1 and 2?
# Options: phase_interaction  no_phase_interaction  identical phases nb
#  [standard|particle_pinning[_temperature]|solute_drag]
#   | [redistribution_control]
no_phase_interaction
#
# Data for phase interaction 2 / 2:
# --------------------------------
# Simulation of interaction between phase 2 and 2?
# Options: phase_interaction  no_phase_interaction  identical phases nb
#  [standard|particle_pinning[_temperature]|solute_drag]
#   | [redistribution_control]
no_phase_interaction
#
```

Concentration data

If "concentration coupling" in the "Flags" section at the beginning of the input file has been chosen, in this section, the concentration data have to be defined. The concentration data section begins with the number of dissolved constituents.Afterwards, the user has to specify whether the concentrations units will be atom or weight percent. This definition applies as well to all concentration inputs and outputs as also for the phase diagram data.

Also part of the "Concentration data" section is the input of diffusion coefficients. Normally, data have to be specified for all contributions, i.e., for each component in each phase (looping automatically through all phases for each consecutive component). In case of many components and many phases, the number of inputs required can be very large, even if for many (e.g. intermetallic) phases no diffusion coefficients are available or need not be specified.

"diff": This keyword indicates that only the diagonal term of the diffusion matrix will be used and specified directly by the user. If "diff " is selected, the pre-exponential factor and the activation energy (which can be set to 0 for no temperature dependence) of the diffusion coefficient have to be specified.

"no_diff": No diffusion flux will be simulated for the element in the given phase.

```
...
# Concentration data
# ==================
# Number of dissolved constituents?  (int)
1
# Type of concentration?
# Options:   atom_percent  (at%)
#            weight_percent  (wt%)
weight_percent
#
# Options:  diff  no_diff  infinite  infinite_restricted
#           multi  database_global  database_local  from_file
#           [+b] for grain-boundary diffusion
# ('multi' can be followed by a string of "n", "d", "g", "l", or "f"
#  to describe each contribution: respectively no diffusion,
#  user-defined diffusion coefficient,'global' or 'local' value from
#  database, and 'from file, the default is global values from database).
# Extra line option (prefactor on time step): cushion <0-1>
# Extra line option: infinite_limit [cm**2/s]
# How shall diffusion of component 1  in phase 0  be solved?
diff
# Diff.-coefficient:
# Prefactor? (real) [cm**2/s]
2.00000E-04
# Activation energy? (real) [J/mol]
0.0000
# How shall diffusion of component 1  in phase 1  be solved?
diff
# Diff.-coefficient:
# Prefactor? (real) [cm**2/s]
1.00000E-08
# Activation energy? (real) [J/mol]
0.0000
# How shall diffusion of component 1  in phase 2  be solved?
diff
# Diff.-coefficient:
# Prefactor? (real) [cm**2/s]
```

1.00000E-08
Activation energy? (real) [J/mol]
0.0000
...

Parameters for latent heat and 1D temperature field

Latent heat describes the amount of energy released or absorbed during phase transition. In concentration coupled simulations, the latent heat option is typically applied to equiaxed growth with negligible temperature gradients. In this case, the latent heat is released averaged over the calculation domain. MICRESS® also allows the use of latent heat in connection with thermal gradients, but in such cases, rather the use of the 1d_temp option is recommended. At the top of this input section, the user has to choose between the keywords "no_lat_heat", "lat_heat" and "lat_heat_3d".

If latent heat is used, the enthalpy of each phase (including the phase 0), as well as its specific thermal capacity need to be specified. In case of TQ-coupling, the values are read automatically from the database. In case the 1d_temp option has been selected, heat conductivity input is necessary for each phase. The keyword "lat_heat_3d" switches on a correction of the amount of latent heat which may be wrongly predicted in some types of 2D simulations. An additional phase number input allows specifying a reference phase for this correction, otherwise phase 0 is assumed. If "lat_heat_3d" is chosen, the user can activate or deactivate the 2D/3D correction for each further phase by the keywords "pseudo_3D" / "no_pseudo_3D" followed by the critical fraction of the matrix phase for limiting the correction.

Actually, there is an additional source of numerical instabilities, which is not covered by the automatic time stepping criteria. If the interface mobility of a growing phase is too high and the time step is too long, the latent heat release in one time step can be so high, that the driving force created from the corresponding temperature change is also high. This would cause an even bigger (opposite) release of heat in the next time step. This behavior is difficult to predict, because it depends not only on the thermodynamics of the system, but also on the amount of interface in the calculation domain and on the diffusion coefficients. Consequently, there is no systematic way to prevent that, other than reducing the time step manually if necessary.

The use of latent heat as well as the "1d_temp" option has further implications for the definition of the boundary conditions.

...
#
Parameters for latent heat and 1D temperature field
==
Simulate release of latent heat?
Options: lat_heat lat_heat_3d [matrix phase]
lat_heat_3d 0

Type of thermal conductivity definition for phase 0 (LIQUID) ?
Options: constant temp_dependent
constant
Thermal conductivity of phase 0 (LIQUID) ? [W/cm/K]
1.3000
Type of thermal conductivity definition for phase 1 (FCC_A1) ?
Options: constant temp_dependent
constant
Thermal conductivity of phase 1 (FCC_A1) ? [W/cm/K]
1.2000
Simulation with release of pseudo-3D latent heat of phase 1 (FCC_A1)?
Options: pseudo_3d [crit. matrix fraction] no_pseudo_3d
pseudo_3D 0.75
Type of thermal conductivity definition for phase 2 (ALCU_THETA) ?
Options: constant temp_dependent
constant
Thermal conductivity of phase 2 (ALCU_THETA) ? [W/cm/K]
1.2000
Simulation with release of pseudo-3D latent heat of phase 2 (ALCU_THETA)?
Options: pseudo_3d [crit. matrix fraction] no_pseudo_3d
no_pseudo_3D
Interval for updating enthalpy data [s]
1.00000E-02
...

Boundary conditions

Two classes of boundary conditions are distinguished in MICRESS:

Thermal boundary conditions

- temperature vs. time
- net heat flow vs. time
- temperature gradient vs. time
- 1d-temperature field

Conditions for boundaries of the calculation domain

- for the phase-field parameter
- for the concentration field
- for the 1d-temperature field, the stress field, flow field etc.

This section starts with the specification of the temperature boundary condition, if neither "temperature" coupling nor "1d_temp" is chosen in section "Flags and Settings" at the top of

the input file. Three alternatives are available to describe the type of temperature trend: If the flag "linear" is chosen, the number of connecting points has to be defined. Then, first the initial temperature at the bottom of the simulation domain and the initial temperature gradient in z-direction are requested. Afterwards, for each connecting point, the time the bottom a temperature and the temperature gradient in z-direction have to be specified. The temperature and temperature gradient will be interpolated linearly between these transition points. In this way, an arbitrarily complex temperature time profile can be applied.

If the number of connection points is set to 0, only the initial temperature at the bottom, the temperature gradient in z direction and a constant cooling rate in K/s are requested. Using the flag "linear_from_file", it is also possible to read the same information from a file consisting of three columns: the time in seconds, the temperature at the bottom in Kelvin, and the gradient in Kelvin per centimetre. This allows a more compact input for complex temperature-time input data.

If the release of latent heat is enabled and "1d_temp" is not selected, specification of the thermal boundary condition is made via the input of a heat flux (in Js/cm 3) instead of a cooling rate or temperature trend ("DTA approximation"). Like in the case of the temperature trend, an input of complex heat flux-time relations is possible via connection points or by reading from a file. Of course, the option "profiles_from_file" is not available in case of using latent heat.

As next, the "moving frame" options have to be set. This feature is very useful for simulations related to directional solidification, as it allows the reduction to a smaller simulation domain which follows the movement of the solidification front. This option is not available for the use of latent heat without 1d temp because it is not compatible with the assumptions of the "DTA approximation". If the flag "moving frame" is selected, the user has to select the criterion which controls the movement of the simulation domain. Available criteria are "temperature" or "distance". In case of "temperature", a critical temperature is requested. If the temperature at the bottom falls below this value, the domain is moved in z-direction until the bottom temperature reaches the critical value. In case of a constant cooling rate, this option leads to a constant moving velocity like in a typical Bridgman furnace experiment.

The boundary conditions of the simulation domain have to be set for the phase-field variables, the concentration, temperature and displacement fields depending on the type of coupling which has been defined at the beginning. The MICRESS® boundary conditions are defined by a text string with length 4 or 6 which represent a sequence of key characters. The characters specify the type of boundary condition, their sequential order addresses the different sides of the simulation domain (west-east-bottom-top for 2D and west-east-south-north-bottom-top for 3D).

The following conditions are available:

insulation ("i"): The boundary cell (the first cell outside of the simulation domain) is assumed to have the same field value (e.g. phase-field variable) as its direct neighbour (the outermost cell

of the domain). The name of the flag reflects the fact that no gradients and, thus, no fluxes exist between the boundary cell and its neighbour inside the simulation domain.

symmetric ("s"): defines the field value of the boundary cell to be identical to its second neighbour in the simulation domain, thus implying a symmetry plane through the centre of the outermost cells of the domain. This condition is similar to an isolation condition which is shifted by half a cell.

periodic ("p"): with this condition, the field value of the boundary cell is set to the value of the outermost cell on the opposite side of the simulation domain. Thus, objects like dendrites which touch one side are continued on the other side. The periodic condition preserves the field balance.

gradient ("g"): the field value of the boundary cell is extrapolated from the first and second neighbour inside the domain. The use of this boundary condition is allowed for all fields (concentration, temperature, phase-field) but not always reasonable. The gradient condition for phase-field is very useful for grain growth. If "periodic is not suitable for any reason – the flag "g" should be the best choice for minimising the impact of the boundary condition on the grain structure.

fixed ("f"): Uses a fixed value for the boundary cell. This value is requested in an extra input line. Naturally, the "f" condition does not preserve the average of the field value. A typical application of the fixed condition for the concentration field is directional solidification with moving frame (fixed condition for top boundary).

In case of using a 1D extension of the concentration field (by selecting the "1d_far_field" option in the "Flags" section), the top boundary condition for the concentration field is automatically shifted to the top of the 1D extension.

If the option "1d_temp" has been selected at the beginning of the input file ("Flags and Settings"), at this place the boundary conditions for the 1D temperature field have to be specified. The user can select between insulation (i), symmetric (s), periodic (p), global gradient (g), fixed (f) and flux (j). While "i", "s" and "p" have already been explained above, the other conditions are either new or have further implications or a slightly different meaning.

global gradient ("g"): This condition establishes a given global temperature gradient between the actual boundary and the opposite boundary. This modified gradient condition is especially useful for coupling to external process simulation results: If temperature vs. time and the thermal gradient are known from a macroscopic process simulation (or a corresponding experiment), a time-dependent fixed "f" condition (see below) can be applied on one side of the 1D temperature field, and the "g" condition on the other side to maintain the gradient. The definition of "g" on both sides is not allowed.

fixed ("f"): The definition of this condition corresponds to that of the fixed condition for the normal simulation domain. But, not only of a fixed temperature value, but also a temperature-time profile can be read from a text file using the "from_file" option. If a constant temperature is chosen, a heat transfer coefficient is requested additionally, allowing the definition of a heat transfer condition to an external medium with fixed temperature.

flux ("j"): This condition allows the assumption of a constant or time-dependent flux [W/cm^2] as boundary condition.

After defining the boundary conditions of the 1D-temperature field, the user has to choose whether to apply constant thermo-physical data (enthalpy, heat capacity and thermal diffusivity) for this temperature field, or to specify files where these thermophysical data shall be read from as a function of temperature. All three thermodynamic quantities are read separately for the part of the 1D-temperature field which lies above and below the micro-simulation domain. This can be important if e.g. a strongly undercooled columnar dendritic front is simulated.

```
#
# Boundary conditions
# ===================
# Moving-frame system in z-direction?
# Options:    moving_frame    no_moving_frame
no_moving_frame
# Type of initial temperature profile?
# Options:   linear    from_file
linear
# Initial temperature at the bottom [K]
950.0000
# Initial temperature at the top [K]
950.0000
# Initial position of the 1D temperature field [micrometer]
# (distance between bottom of 1D temp field and bottom of simulation area, <0!)
-500.000000000000
#
# Boundary conditions for phase field in each direction
# Options: i (insulation) s (symmetric) p (periodic/wrap-around)
#        g (gradient)  f (fixed)    w (wetting)
# Sequence: W E (S N, if 3D) B T borders
ppii
#
# Boundary conditions for concentration field in each direction
# Options: i (insulation) s (symmetric) p (periodic/wrap-around) g (gradient) f (fixed)
# Sequence: W E (S N, if 3D) B T borders
```

```
ppii
#
# Boundary conditions for 1D temperature field bottom and top
# Options: i (insulation) s (symmetric) p (periodic/wrap-around) g (global grad) f (fixed) j (flux)
# Sequence: B T
fi
# How shall temperature in B-direction be read?
# # Options:  constant  from_file
constant
# Fixed value for temperature [K]
298.00
# Fixed value for heat transfer coefficient [W/cm2K]
1.50000000000000
# Please specify for the 1D temperature field, which enthalpy
# below the calculation domain should be present!
# The following options are available:
# # Options:  constant  from_file
from_file
# file name:
C:\Users\User\Desktop\Kar\Results_3%\AlCu_Temp1d_latHeatData columns 2 8
# Please specify for the 1D temperature field, which value of Cp
# below the calculation domain should be present!
# The following options are available:
# # Options:  constant  from_file
from_file
# file name:
C:\Users\User\Desktop\Kar\Results_3%\AlCu_Temp1d_latHeatData columns 2 6
# Please specify for the 1D temperature field, which value of the heat conductivity
# below the calculation domain should be present!
# The following options are available:
# # Options:  constant  from_file
from_file
# file name:
C:\Users\User\Desktop\Kar\Results_3%\AlCu_Temp1d_latHeatData columns 2 7
# Please specify for the 1D temperature field, which enthalpy
# above the calculation domain should be present!
# The following options are available:
# # Options:  constant  from_file
from_file
# file name:
C:\Users\User\Desktop\Kar\Results_3%\AlCu_Temp1d_latHeatData columns 2 8
# Please specify for the 1D temperature field, which value of Cp
# above the calculation domain should be present!
# The following options are available:
```

```
# # Options:  constant  from_file
from_file
# file name:
C:\Users\User\Desktop\Kar\Results_3%\AlCu_Temp1d_latHeatData columns 2 6
# Please specify for the 1D temperature field, which value of the heat conductivity
# above the calculation domain should be present!
# The following options are available:
# # Options:  constant  from_file
from_file
# file name:
C:\Users\User\Desktop\Kar\Results_3%\AlCu_Temp1d_latHeatData columns 2 7
# Unit-cell model symmetric with respect to the x/y diagonal plane?
# Options:  unit_cell_symm  no_unit_cell_symm
no_unit_cell_symm
#
```

Other numerical parameters

In this last section, some purely numerical parameters for the phase-field, concentration and stress solver are defined. The maximum number of concentration solving per phase-field iteration has only to be defined, if concentration coupling is used in combination with a fixed phase-field time step. An error message is given if the number is too small to be consistent with the time-step criterion of the explicit diffusion solver. This input is not required when automatic time-stepping is used.

In case of stress coupling, the convergence criteria for the iterative BiCG-stab matrix solver as well as an upper limit (maximum number) of iterations have to be defined. In the input line for the maximum number of iterations, the input of a second integer is also possible. It is set to 20 by default and specifies the maximum number of iterations allowed for achieving a good solution for quasi-static equilibrium. In most cases, the default settings are sufficient. Next, a value for the phase minimum is required. A cell with a phase or grain fraction below this value is not considered to be in the interface any more but in a bulk region (liquid or solid). In most cases, a value of 1.E-4 can be recommended.

Finally, the interface thickness (in cells) also has to be input in this section. Generally, with increasing interface thickness, the curvature evaluation of the phase-field profile is improved. On the other hand, a higher resolution is required to resolve highly curved structures, and numerical artefacts related to the finite interface thickness like "artificial solute trapping" is increased. In case of using extremely small values for the interface thickness (<≈3 cells), curvature evaluation is poor and nucleation at the interface is not working correctly anymore.

```
#
# Other numerical parameters
# ==========================
# Phase minimum?
1.00E-03
# Interface thickness (in cells)?
3.50
#
```

4. RESULTS AND DISCUSION

The solidification behavior of four binary Al:Cu alloys were studied in this work e.g.: Al-3%Cu, Al-30%Cu, Al-33%Cu (eutectic composition), Al-45%Cu as indicated on the phase diagram depicted in Fig. 4.1. According to the phase diagram these alloys consist of fcc and Al_2Cu at RT. (Figure 4.1). The input parameters used in MICRESS simulations are given in Table 4.1. All simulations were start assuming that each binary alloy was liquid, with initial composition equal to the composition of each alloy under consideration each time.

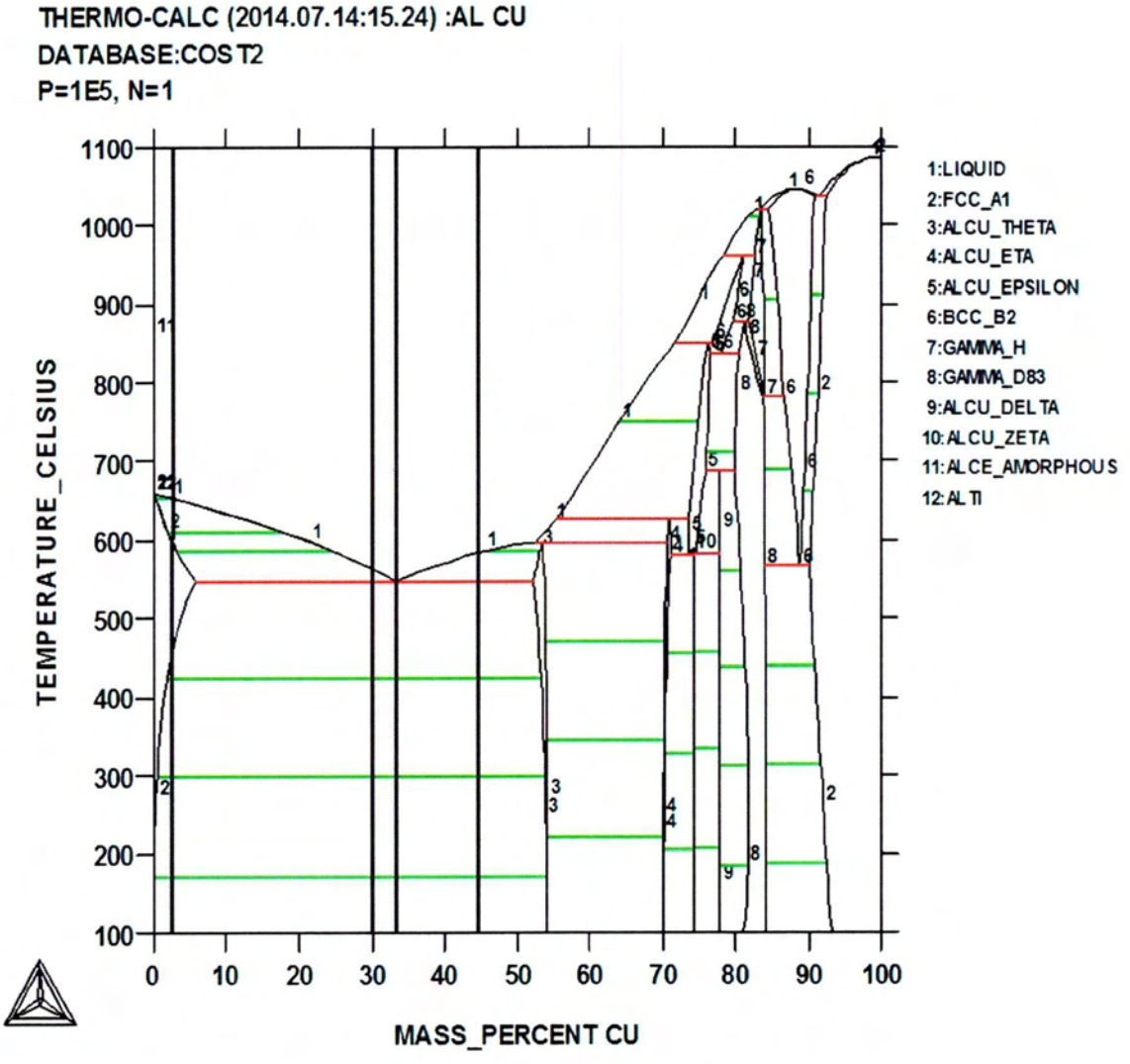

Figure 4.1: **Al:Cu Phase diagram (Calculated in ThermoCalc). The Al:Cu alloys studied are depicted.**

1D temperature field solver was used for all simulations [96]. Latent heat release was included as a function of temperature using tabulated values for the average enthalpy $H(T)$ (Fig. 4.2), heat capacity $c_P(T)$ and the local heat conductivity $\lambda(T)$. These values were introduced via the AlCu_Temp1d_latHeatData.txt file and the equation (5.1) determines the temperature change inside a volume V.

$$dT = \frac{1}{c_P}\left(\lambda \frac{d^2T}{dx^2}dt - dH + \bar{c'}_p dT'\right) \tag{4.1}$$

For the Al-3%Cu alloy a parametric study was performed at selected undercooling values and its influence on the solidification process was recorded.

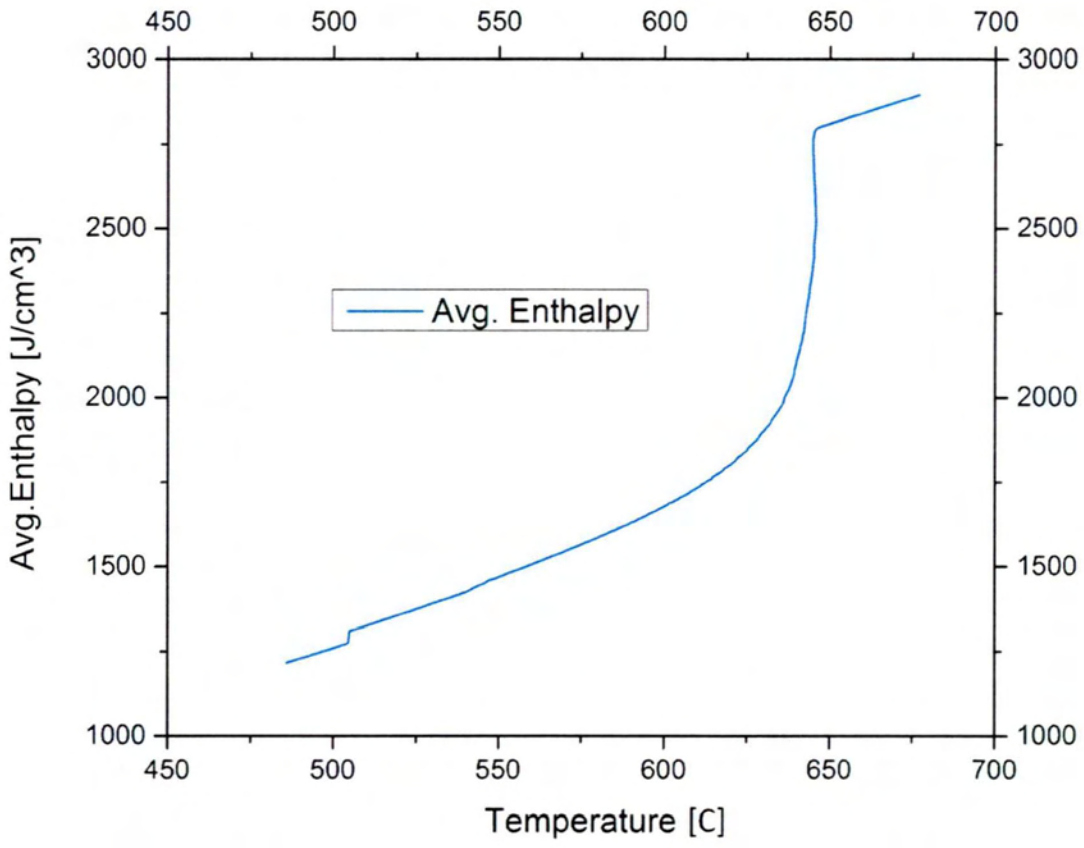

Figure 4.2: **The temperature dependent average Enthalpy of AlCu_Temp1d_latHeatData file**

Table 4.1: **Input parameters for the binary Al- Cu alloys**

		Al-3%Cu	Al-30%Cu	Al-45%Cu	Al-33%Cu
Surface energy Liquid/solid [J/cm^2]		1E-05(liquid-fcc) 1E-05(liquid-θ)			
Kinetic coefficients between phases [cm^4/(Js)]		liquid-fcc		liquid-θ	
		925 0.2 890 0.1 860 0.02 800 0.01 700 0.005		925 0.05 800 0.05 795 0.005 700 0.005	
Undercooling		2			
Surface energy solid/solid [J/cm^2]		no_phase_interaction			
Diffison coefficient:		Cu→Liquid	Cu→Fcc	Cu→Al2Cu	
		2.00E-04	1.00E-08	1.00E-08	
Initial Temperature[K]	Bottom	950			820
	Top	950			950
Boundary conditions	Phase field	ppii			ppii
	concentration	ppii			ppfi
	1D Temperature field	fi			
Thermal conductivity (W/cmK)		1.3 (liquid) 1.2 (fcc) 1.2 (θ)			

Al-3%Cu

A domain 200x200 μm was constructed in MICRESS with uniform composition and initial temperature 950°K at the onset of the simulation. The seed density model assuming 17 discrete classes of potential nucleation sites was employed.

Characteristic results from the simulations are depicted in Figure 4.3. The early stages of solidification are illustrated in Figure 4.3.a with two dendrites (orange) growing in the liquid (red) while surrounded by the interface (blue). Secondary branches were appeared during solidification (Fig. 4.3.b). In the next stages (Figs.4.3.c,d) the fcc phase was growing at the expense of the liquid phase, followed by the formation of the Al_2Cu phase (white) at the grain boundaries.

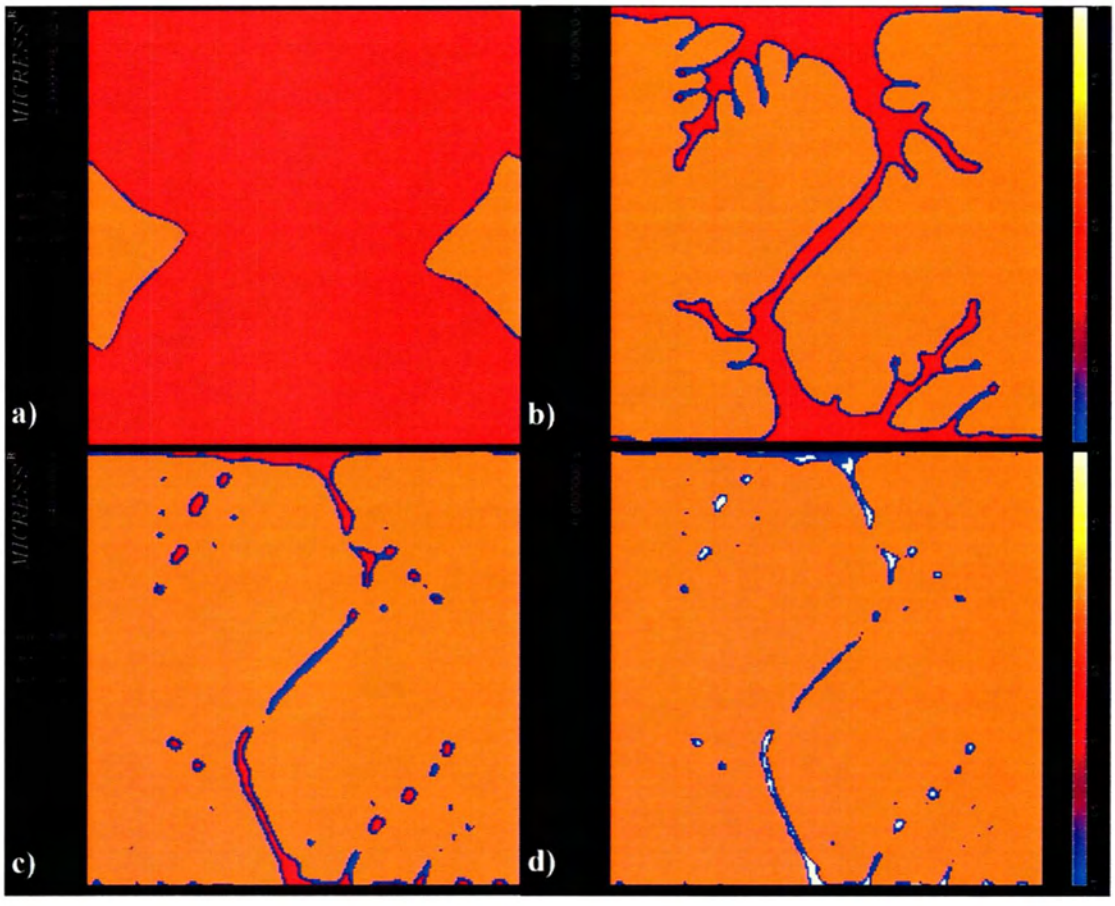

Figure 4.3: **Microstructure formation of Al-3%Cu wt. alloy, a) t=0.03 sec, b) t=0.1 sec, c) t=0.4 sec, d) t=0.8 sec.**

Cu profiles, in the liquid, fcc and Al_2Cu at selected time-steps are shown in Fig. 4.4. thes profiles were calculated from the virtual EDX module, incorporated in MICRESS. The rejection of Cu from the liquid phase is clearly observed in Figure 4.4.a, however the profile of Cu in Fcc phase differ in the center from the tip of dendrite. The same is observed in Figure 4.4.b but in this time step liquid reaches the highest value in Cu. The concentration of Cu in Al_2Cu, at the end of solidification is presented in Fig. 4.4c.

The phase-fraction of Fcc and Al_2Cu as a function of temperature under different undercooling values, chosen from the open literature, is shown in Figure 4.5 and Figure 4.6, respectively. It can be observed from the simulation results by increasing the undercooling value from 2 to 60 the fraction of the Fcc phase follow increases while the fraction of the Al_2Cu phase exhibits a declination.

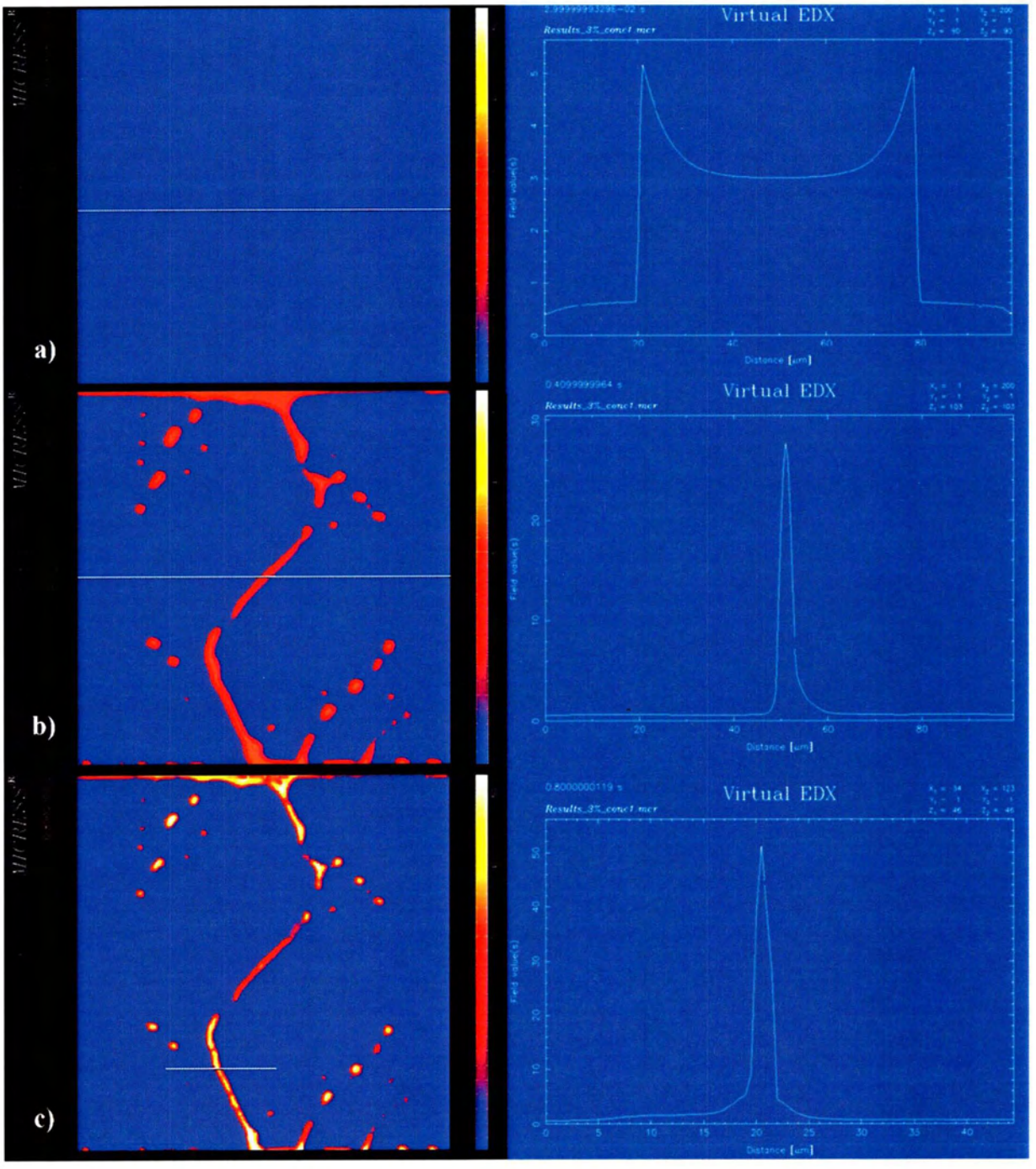

Figure 4.4: Virtual EDX for Al-3%Cu wt. alloy, a) t=0.03 sec, b) t=0.1 sec, c) t=0.8 sec.

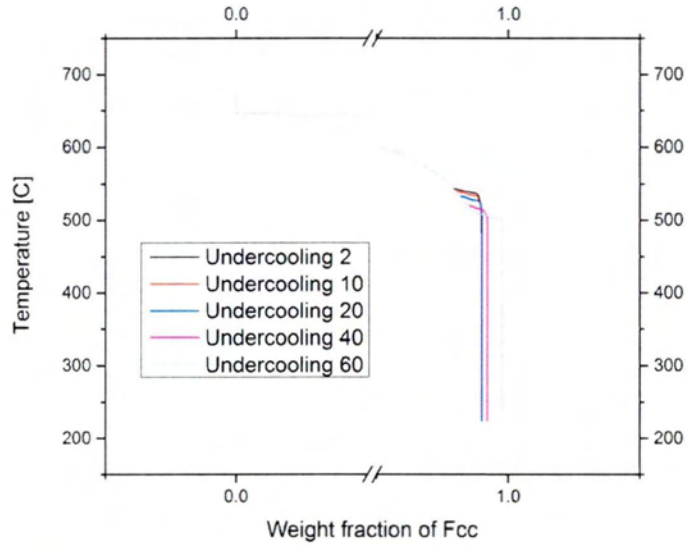

Figure 4.5: **Phase fraction of Fcc phase during different undercooling**

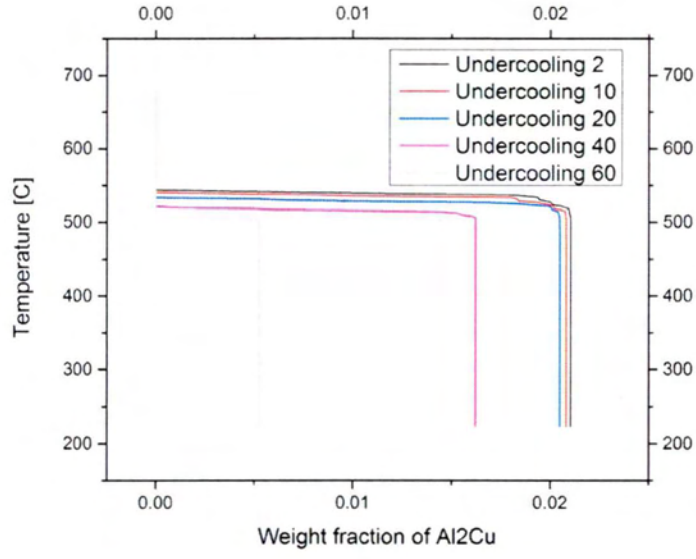

Figure 4.6: **Phase fraction of Al_2Cu phase during different undercooling**

The evolution of the phase fractions versus temperature during solidification was also compared to Equilibrioum calclulations as well as to the predictions of the Scheil solidification model. According to thediagrams of Fig. 4.7 a significant difference is observed for the solidification of Al_2Cu phase, where MICRESS predicts smaller phase fraction in comparison to the Scheil model.

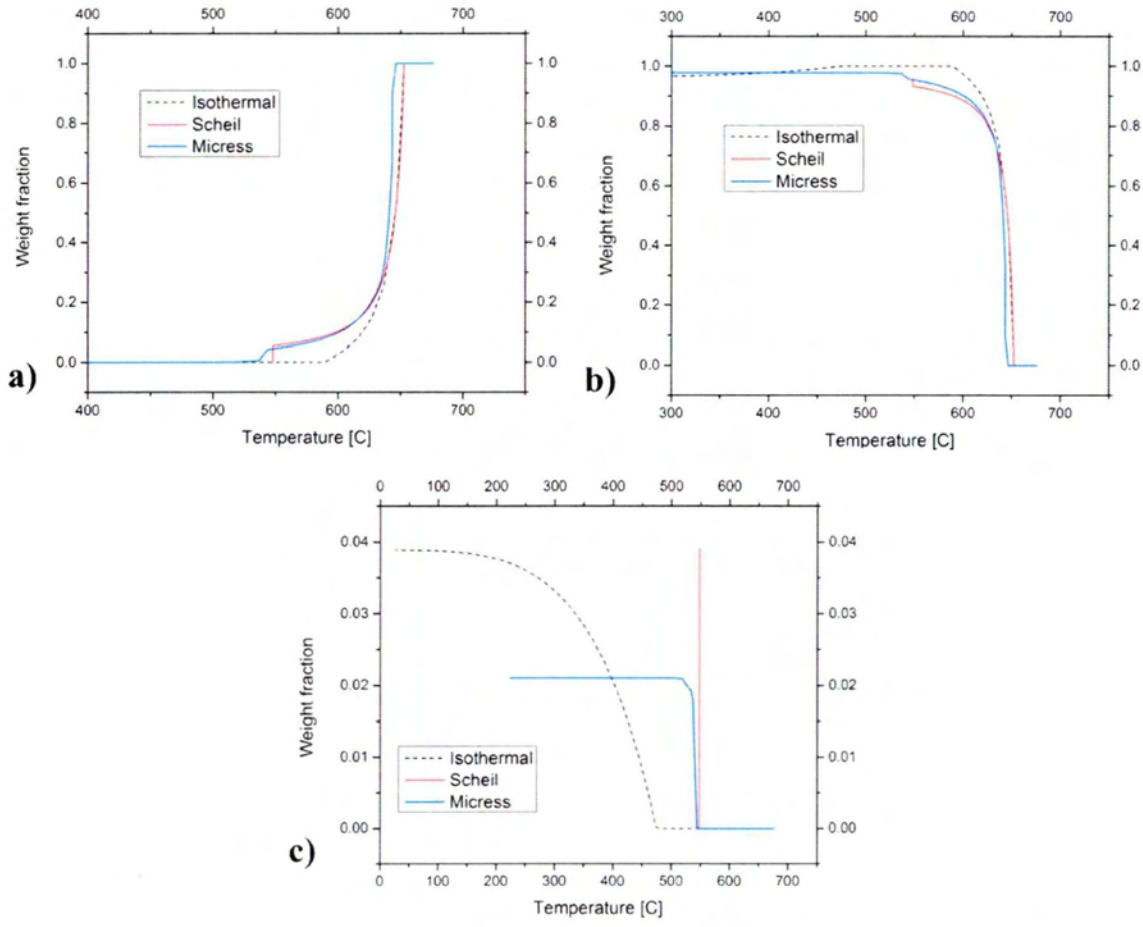

Figure 4.7: **Comparisons of phase fractions according to Phase-field, Scheil and Equilibrioum simulations of Al-3%Cu wt. alloy a) Liquid phase b) Fcc phase c) Al_2Cu phase**

Al-30%Cu

The simulation of this alloy was carried out, at the same simulation conditions as the Al-3%Cu alloy .

The evolution of microstructure is illustrated at certain time steps in Fig. 4.8. The early stages of solidification are depicted at the Figure 4.8.a. In this time step three dendrites are observed and a grain which has just nucleated. According to the Figure 4.8.b these dendrites continue to grow in the liquid. Also at 0.42 sec of simulation the formation of Al_2Cu (white) is obvious at the interface of the top-left dendrite of Fig. 4.8.b. In Fig. 4.8.c it is clear that Al_2Cu nucleated first at the boundary of the dendrite and next in the remaining liquid which remained followed an eutectic solidification. Finally at the end of Al-30%Cu solidification the fraction of the interface (blue) is prevailing amongst others, this phenomenon means that eutectic solidification took

place. This is a valid result as it is also predicted from the phase diagram of Fig. 4.1. The eutectic structure can be seen clearly from the conc1.mcr file of MICRESS, which provides the the concentration of Cu in the simulation domain as shown in Figure 4.9.

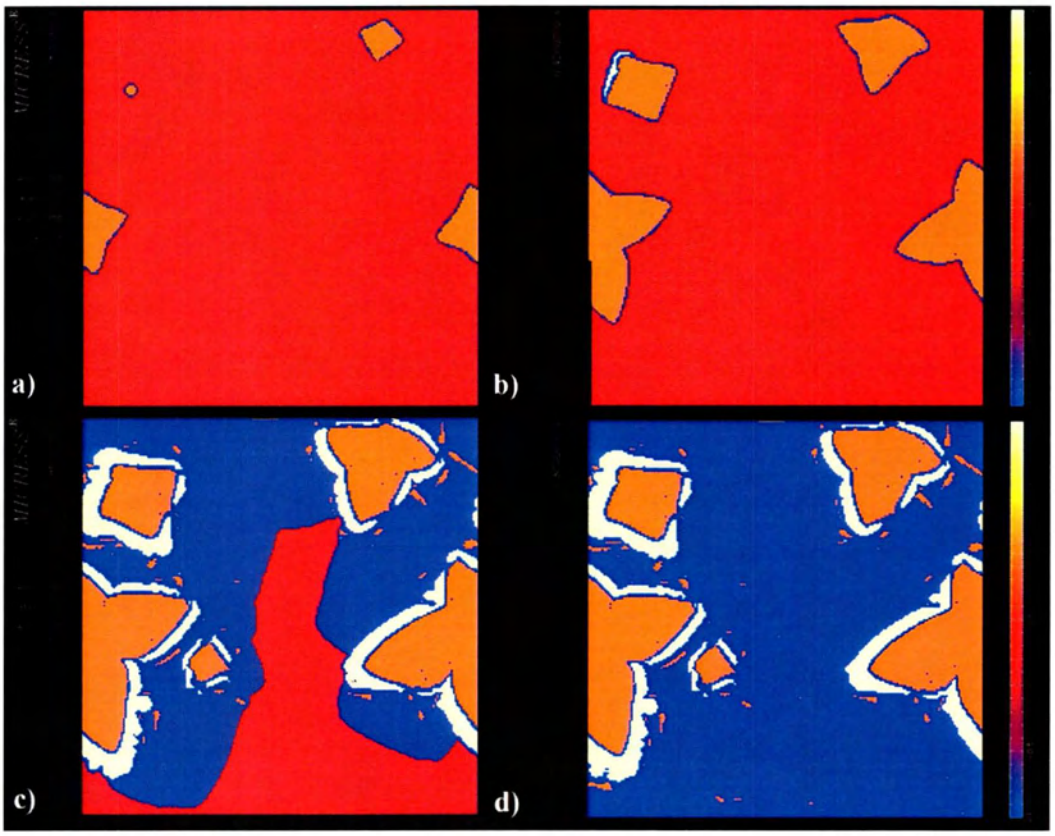

Figure 4.8: **Microstructure formation of Al-30%Cu wt. alloy, a) t=0.38 sec, b) t=0.42 sec, c) t=0.46 sec, d) t=0.8 sec.**

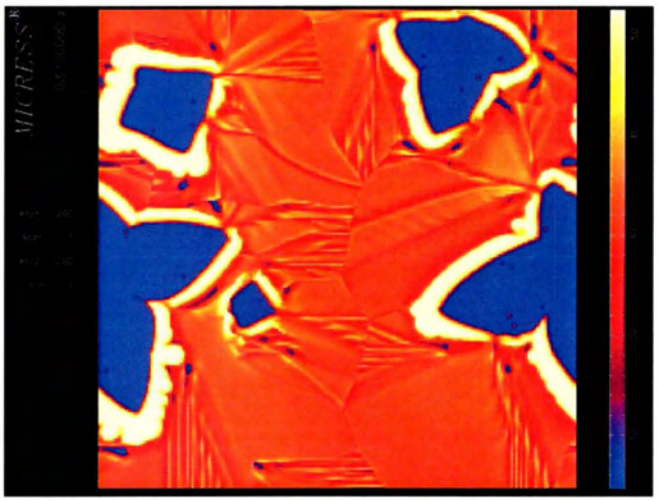

Figure 4.9: **Microstructure formation form conc1.mcr file of Al-30%Cu wt. alloy at t=0.8 sec**

The composition of Cu in the phases Fcc, Al_2Cu and the liquid at different time-steps is presented in Fig. 4.10. The rejection of the second component is clearly observed in Figure 4.10.a, however in comparison with the Al-3%Cu in this alloy the rejection of Cu to liquid follow a smoother distribution. Virtual EDX results of Cu concentration in the three phases of the system are depocted in Figure 4.10.b close to the time of Al_2Cu nucleation. Figure 4.10.c shows the concentration of Cu between of two dendrites at the end of solidification. At this graph, a fluctuating periodic trend of Cu is observed as a result of eutectic transformation.

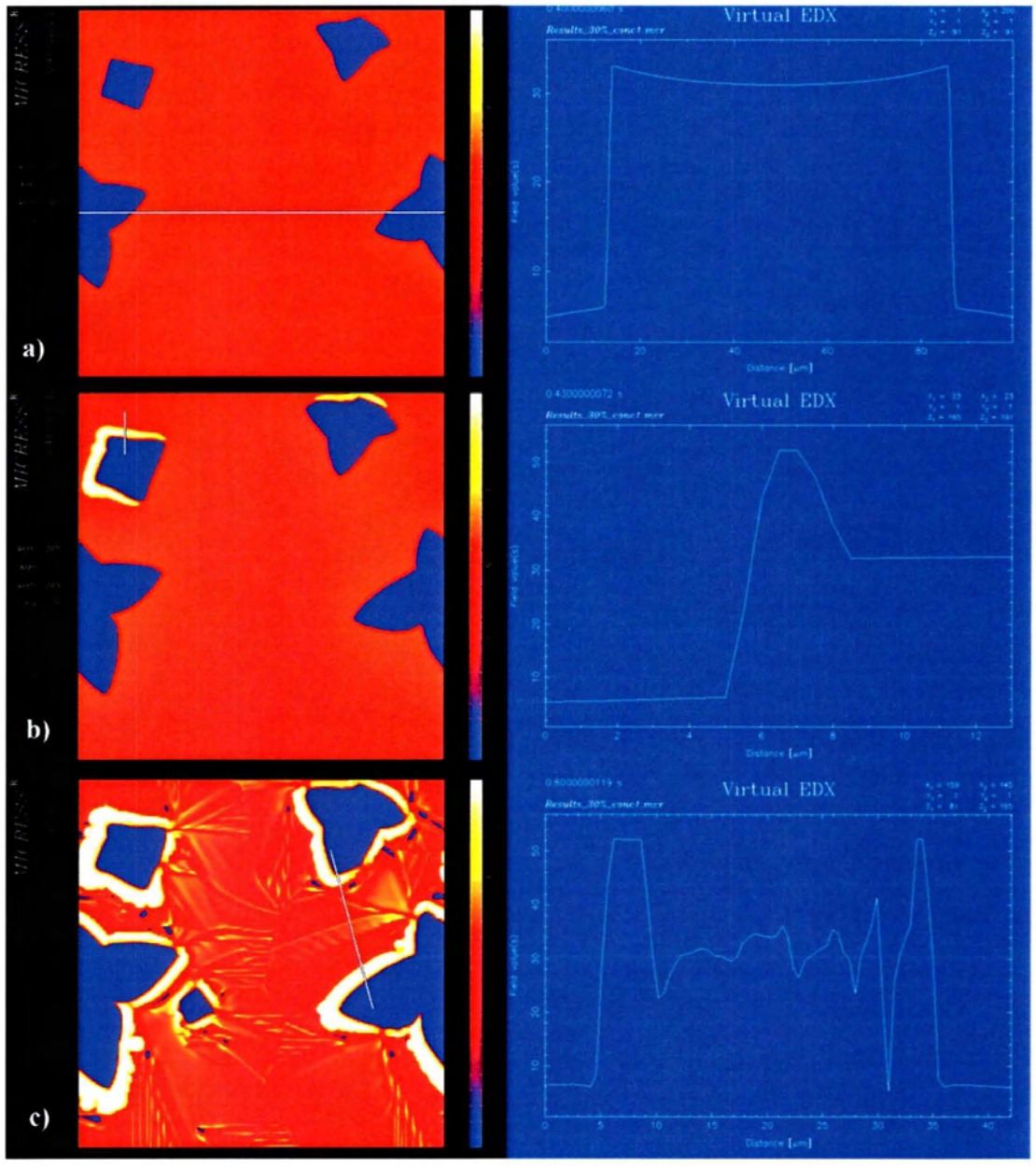

Figure 4.10: **Virtual EDX for Al-30%Cu wt. alloy, a) t=0.40 sec, b) t=0.43 sec, c) t=0.8 sec.**

Additionally the fraction of the phases versus temperature was also calculated for the Al-30%Cu alloy with MICRESS, and compared then to Equilibrioum and Scheil solidification models. According to Figures 4.11.a,b,c a difference is observed at the temperature where solidification begins. On the other hand the Scheil model predicts less Fcc phase than Phase-field and Equilibrioum model.

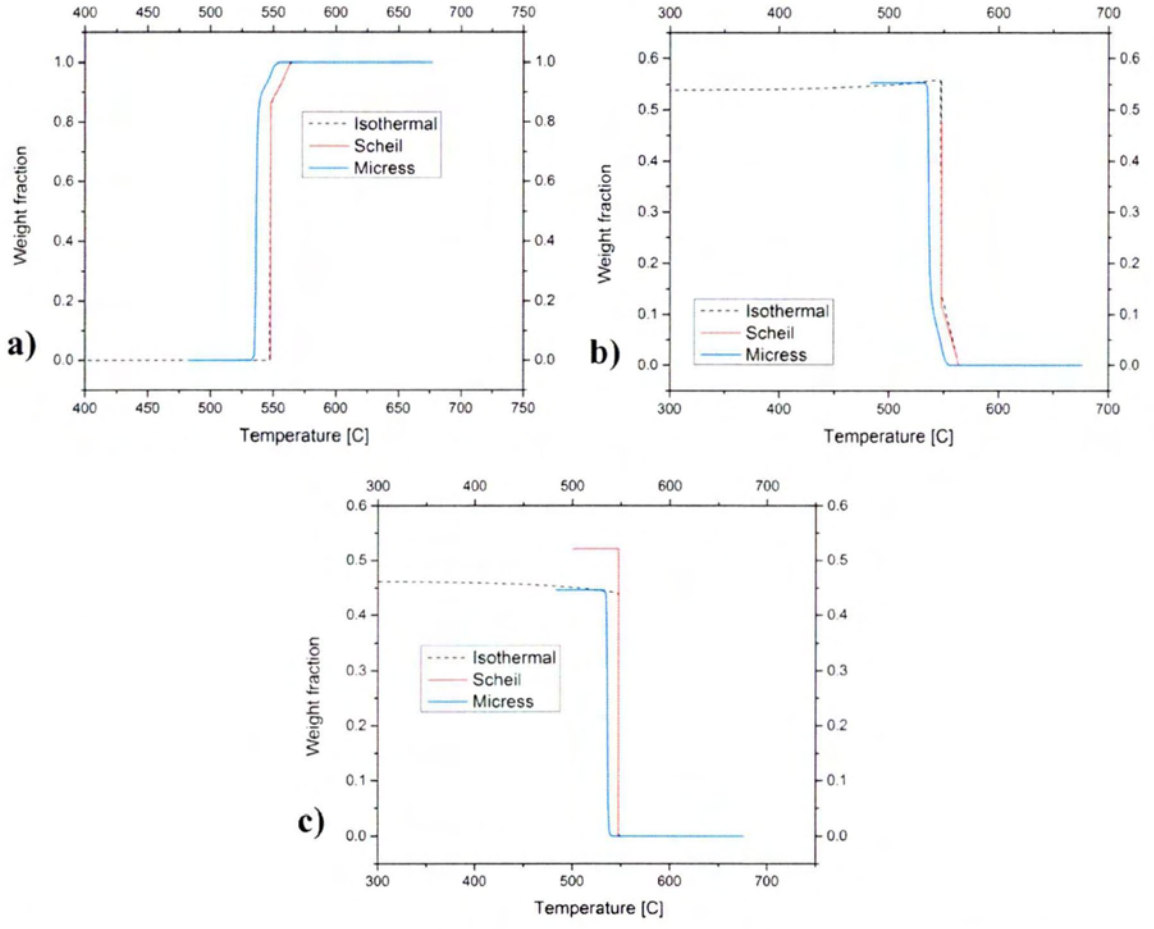

Figure 4.11: Comparisons of phase fractions according to Phase-field, Scheil and Equilibrioum simulations of Al-30%Cu wt. alloy a) Liquid phase b) Fcc phase c) Al_2Cu phase.

Al-45%Cu

Similar simulation conditions as in Al-30%Cu was adopted for the simulation of Al-45%Cu alloy. The evolution of microstructure, according to the Phase-field model is illustrated at selected stages of solidification process in the Figure 4.12. In this case of study the solidification begins with two coarse grains which develop in the liquid (Figure 4.12.a), from dendrites. As

the solidification continues and the temperature drops the interface becomes unstable creating projections (Figure 4.12.b), at the same time the appearance of Al_2Cu phase is obvious in a few areas of the domain. The co existence of the three phases Fcc, Al_2Cu and liquid it is clearly observed in Figure 4.12.c. The final microstructure is shown at the Figure 4.12.d at 0.8 sec of simulation time. In comparison to the Al-30%Cu alloy, the eutectic solidification is not clearly demontrarted in this case.

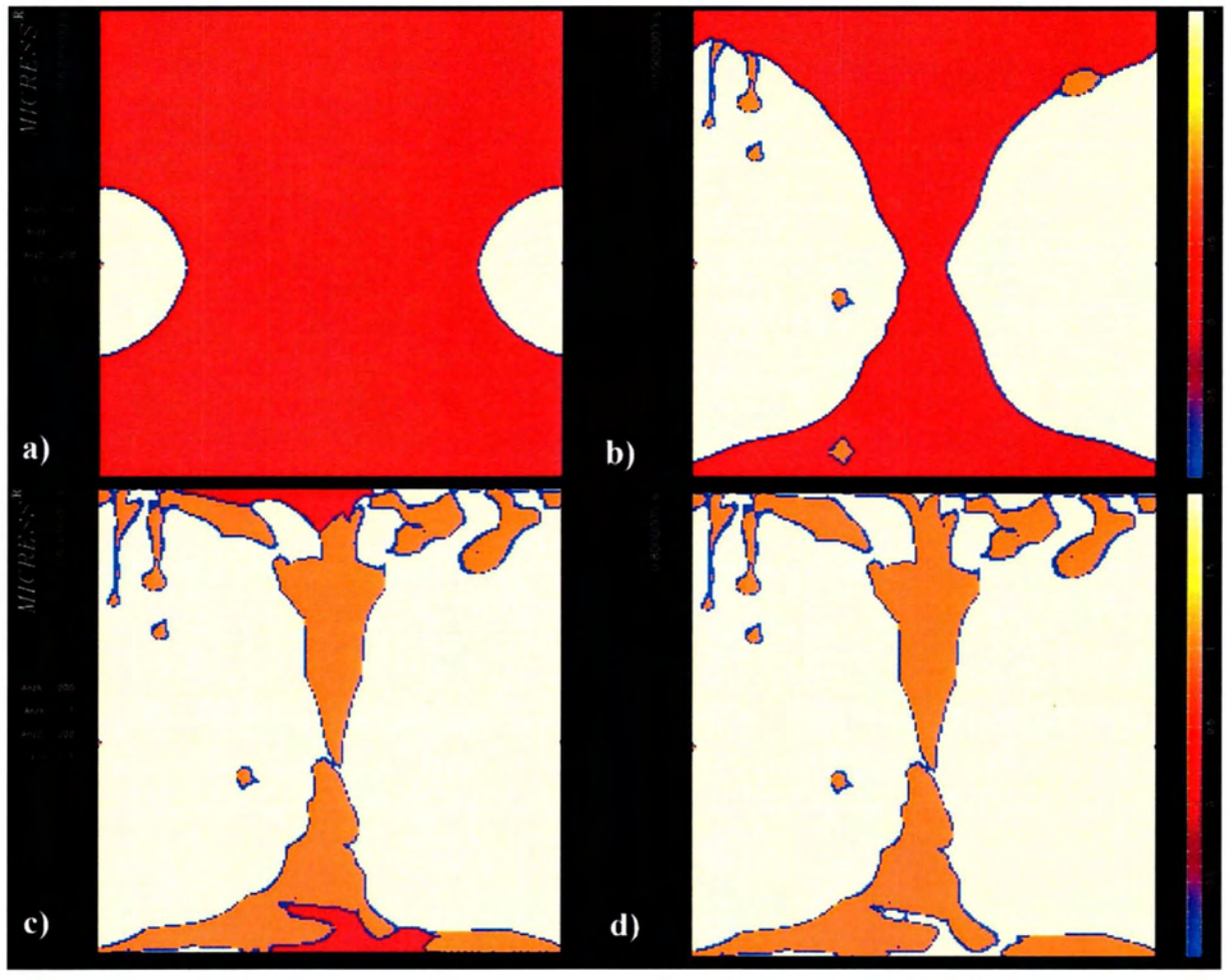

Figure 4.12: **Microstructure formation of Al-45%Cu wt. alloy, a) t=0.57 sec, b) t=0.59 sec, c) t=0.61 sec, d) t=0.8 sec.**

The composition of Cu in the phases Fcc, Al_2Cu and liquid at different time-steps is presented in Fig. 4.13. In this case there is no solute rejection from the solid to liquid, but the opposite happens i.e. for the formation of Al_2Cu phase there is absorption of Cu from the liquid phase, resulting in lower Cu concentration in the liquid.(Figure 4.13.b). The Figure 4.13.c demonstrates the concentration of Cu between of the grains when the solidification ends.

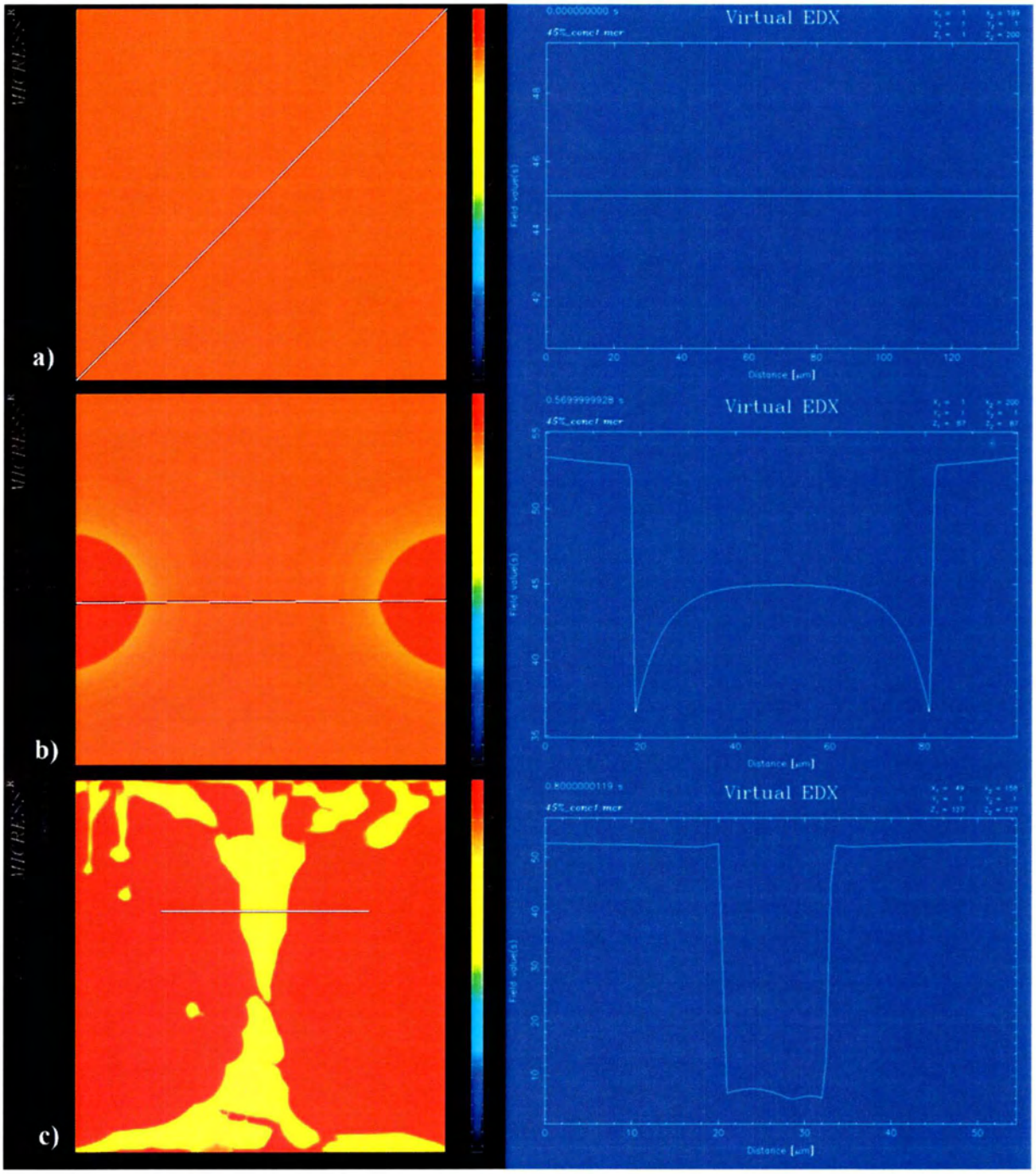

Figure 4.13: **Virtual EDX for Al-45%Cu wt. alloy, a) t=0.0 sec, b) t=0.57 sec, c) t=0.8 sec.**

The fraction of the phases versus temperature was calculated also for the Al-45%Cu alloy and the results were compared to Equilibrioum and Scheil solidification models. According to Figures 4.14.a,b,c similarly to the Al-30%Cu alloy a difference is observed at the onset of solidification, it seems like a "delay" of solidification. On the other hand the Scheil model predicts lesser Fcc phase in relation to the Phase-field and the Equilibrioum model.

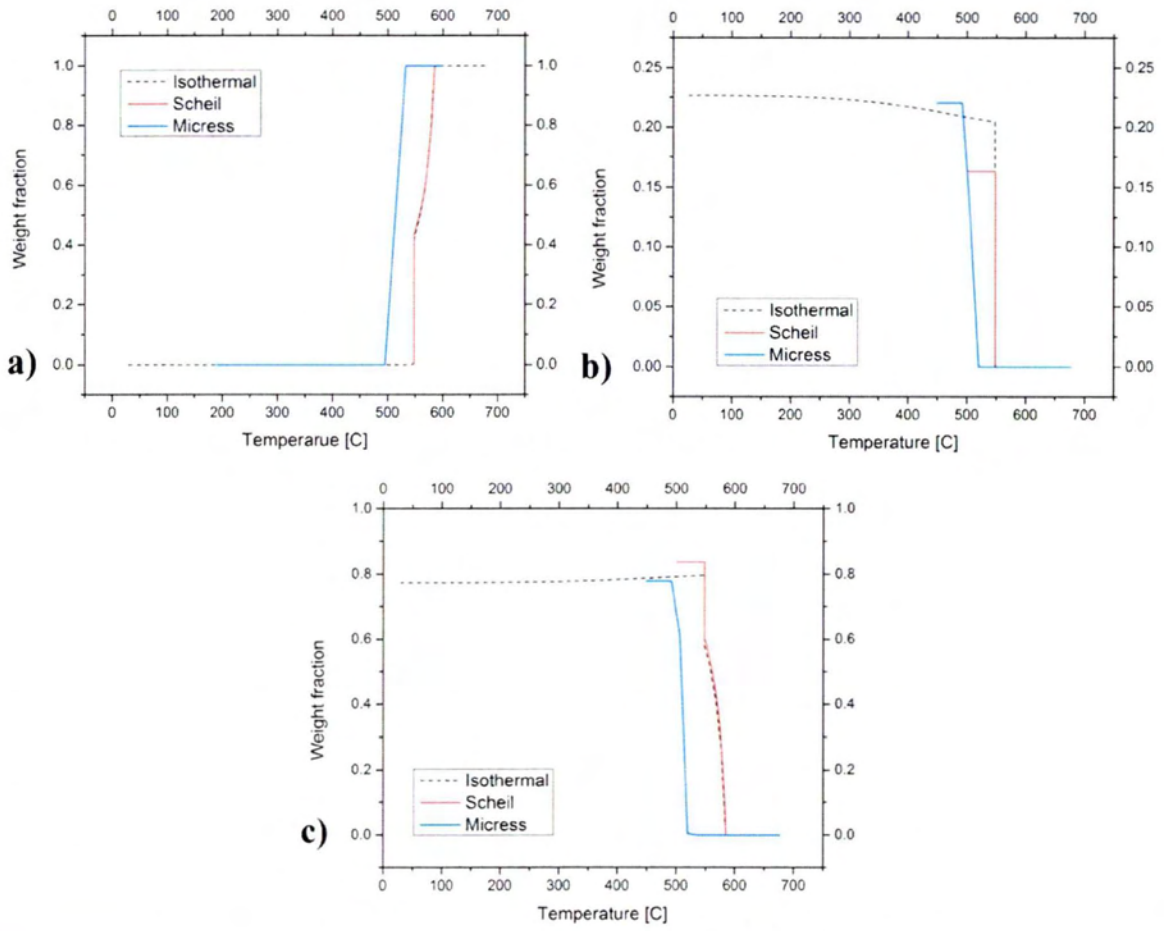

Figure 4.14: **Comparisons of phase fractions according to Phase-field, Scheil and Equilibrioum simulations of Al-45%Cu wt. alloy a) Liquid phase b) Fcc phase c) Al_2Cu phase.**

Al-33%Cu

The approach for the simulation of solidification of Al-33%Cu alloy in MICRESS was completely different from the previous alloys. According to the phase diagram this alloy solidifies as eutectic creating a lamellar pattern.

The domain in this case was selected 100x200 grid cells x and z direction. According to MIICRESS it is prefferable to start with a rather small domain size, which can be increased afterwards when the numerical parameters are properly set and the simulation is running correctly.

The key for achieving lamellar pattern was to create an initial lamellar structure by defining initial grains of alternating phases at the bottom of the domain which overlap. It is most convenient to use a quadratic shape for these grains. Additionally setting the initial

temperature at the bottom slightly below the eutectic temperature and using the moving frame option in order to track the solidification front.

The corresponding microstructure is illustrated at the Figure 4.15. The grains which defined in the input file are observed in the Figure 4.15.a at the bottom of the domain.

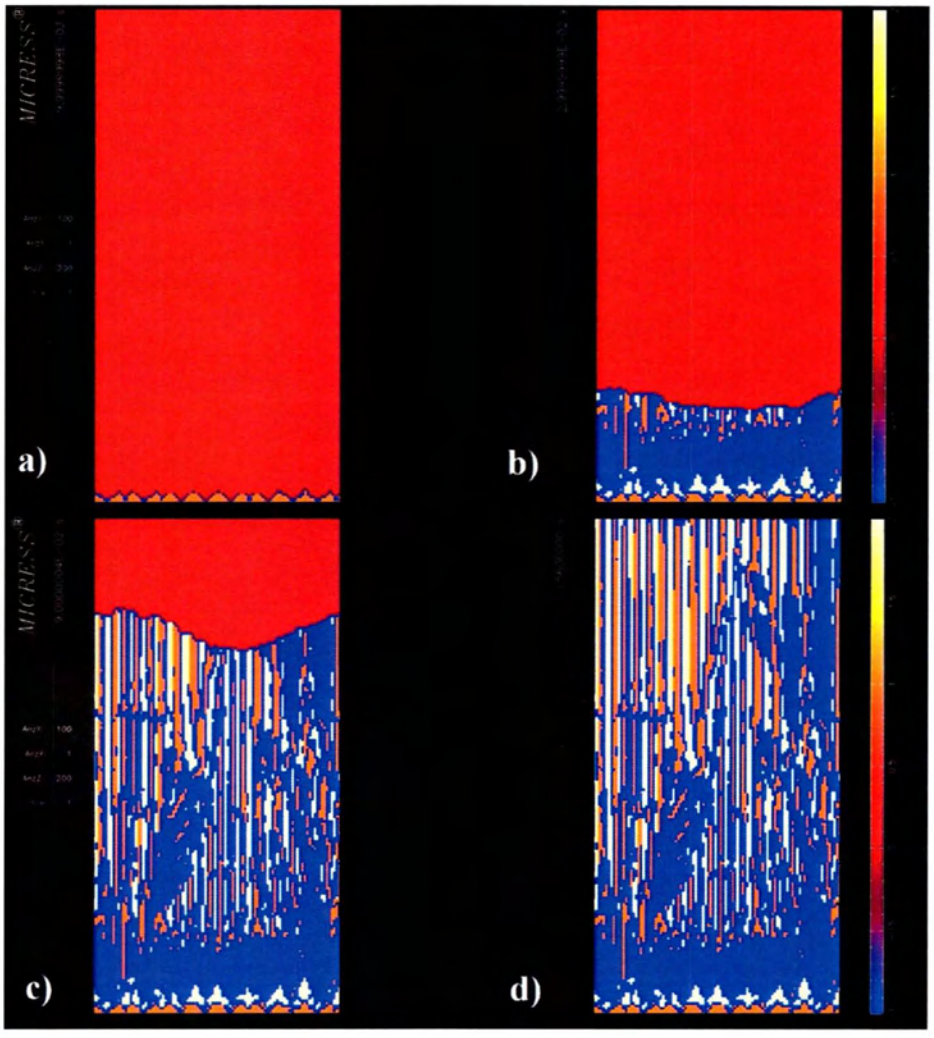

Figure 4.15: **Microstructure formation of Al-33%Cu wt. alloy, a) t=0.01 sec, b) t=0.03 sec, c) t=0.09 sec, d) t=0.56 sec.**

The solidification front is observed in the Figure 4.15.b where the lamellar formation begins. A more detailed picture of the solidification front and eutectic pattern are shown in the Figure 4.15.c. Finally at the end of the process the whole pattern of the microstructure is observed in Figure 4.15.d.

The composition of Cu in selected areas of the simulation domain and the rejection of it in the liquid at different time-steps is presented in the Figure 4.16. The rejection of Cu is clearly observed in Figure 4.16.a and Figure 4.16.b, likewise to the Al-30%Cu alloy, the rejection of Cu

to liquid in the Al-33%Cu alloy follow a smooth curve. The Figure 4.16.c shows the concentration of Cu at the top of the domain where the lamellar microstructure is developed in the proper way. From the Virtual EDX generally is observed a periodic trend of change of the microstructure which proves the existence of repetitive switching phases (eutectic microstructure).

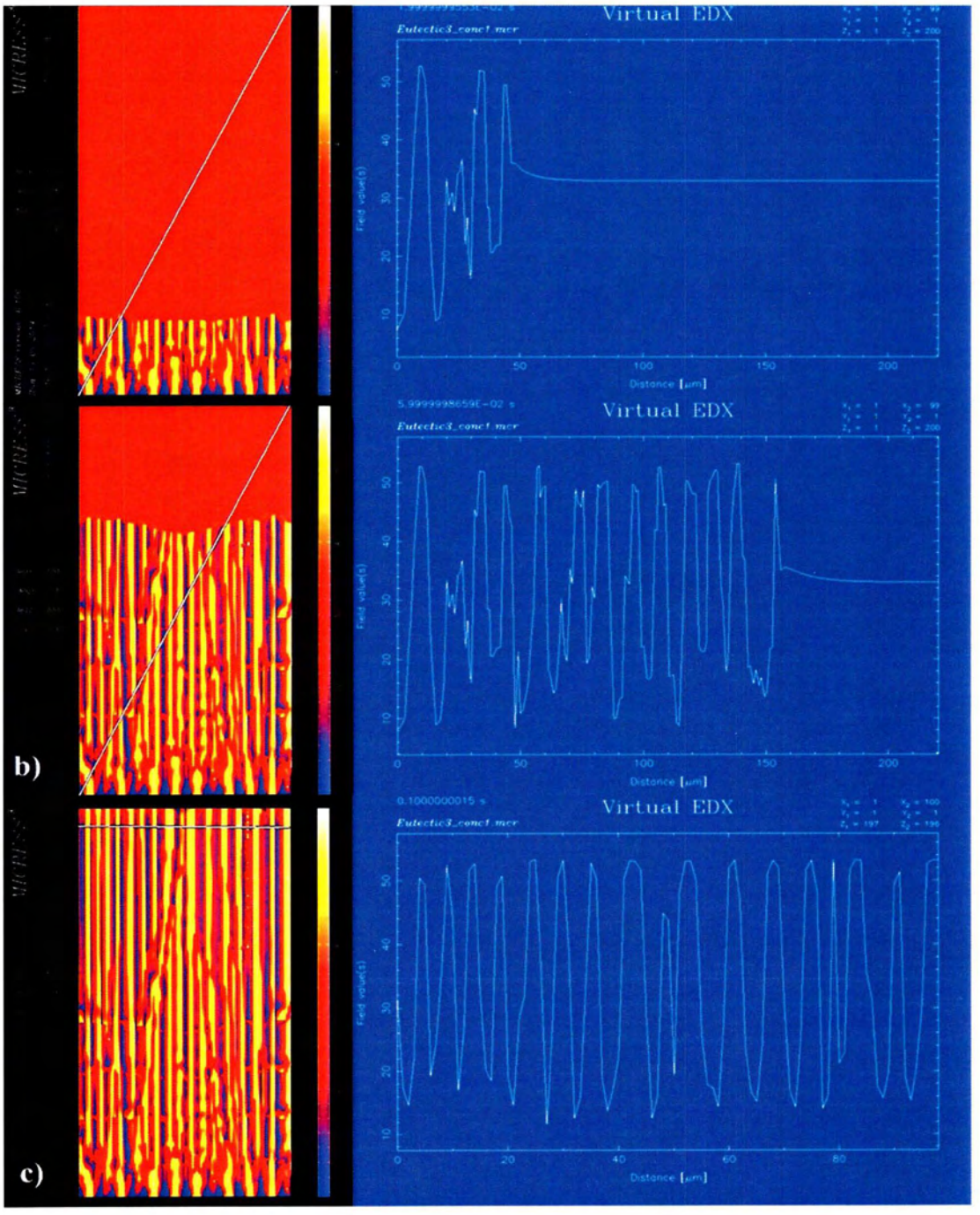

Figure 4.16: **Virtual EDX for Al-33%Cu wt. alloy, a) t=0.02 sec, b) t=0.06 sec, c) t=0.1 sec.**

Additionally the fraction of the phases versus temperature is calculated likewise for Al-33%Cu with Phase-field method, which is compared to Equilibrioum and Scheil solidification models. According to the Figures 4.17.a,b,c there is a difference at the temperature where solidification begins. On the other hand the Scheil model predicts less Fcc and more Al_2Cu phase than Phase-field and Equilibrioum model.

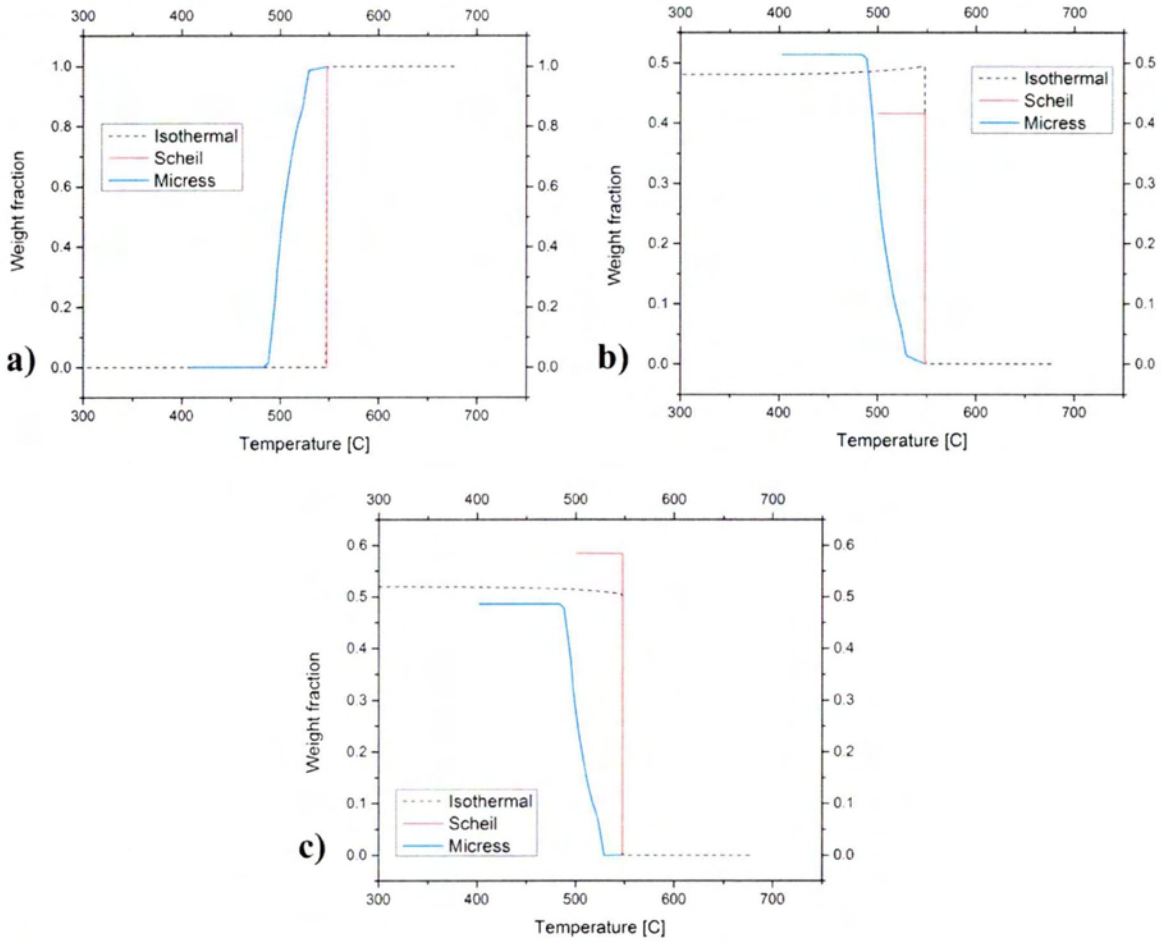

Figure 4.17: Comparisons of phase fractions according to Phase-field, Scheil and Equilibrioum simulations of Al-33%Cu wt. alloy a) Liquid phase b) Fcc phase c) Al_2Cu phase.

5. CONCLUSIONS

From the results presented in the previous sections the following conclusions can be drawn.

- The phase field method is an efficient method to simulate microstructure evolution in time and space during solidification. Basic prerequirement for reliable results is an accurate set of input parameters describing the alloy system and proper boundary conditions.
- The main results of this study include the visualization of the microstructure evolution during solidification, the concentration of the second component in each phase at certain solidification time-steps, and the resulting phase fractions which were compared with Equilibrioum and Scheil models incorporated in ThermoCalc. An additional simulation has been done for Al-3%Cu alloy in several undercooling values .
- The presence of temperature gradient is observed from the Figure 4.2, which shows the average enthalpy of the bulk in each temperature. Also the formation of dendrites during solidification in Figures 4.3, 4.8 and 4.12 indicates the temperature gradient. The same can be drawn about the solidification of the Al-33%Cu in Figure 4.15, due to the tracking of the solidification front resulting to lamellar microstructure.
- The effect of different undercooling during solidification is demonstrated in Figs. 4.5 and 4.6. The prediction of less Al_2Cu phase at higher undercooling result in the presence of solute trapping to the system during solidification, that means that the Fcc phase is richer in second component when undercooling is bigger.

6. PROPOSED FUTURE WORK

The Phase field method can be used in the future for solidification modeling in welding, by setting accurate input parameters.

From the above described aspects related to solidification in Al:Cu alloys, it emerges as challenging to question what would be the effect of undercooling to the other alloy systems as well as to the velocity of dendrite tip.

Simulation of Al Cu alloys with higher Cu concentration in order to be able to predict the formation of the intermetallic phases in space and time.

REFERENCES

[1] http://www.micress.de/

[2] Steinbach I., *Phase-field models in materials science*, Mater. Sci. Eng. 17, 2009, 31

[3] Caginalp G., *Efficient Computation of a Sharp Interface by Spreading via Phase Field Methods*, Phys Rev A 39, 1989, 5887.

[4] Kobayashi R., *Modeling and numerical simulations of dendritic crystal growth*, Physica D. 63, 1993, 410.

[5] Wheeler A.A., Murray B.T., Schaefer R. J., *Computation of dendrites using a phase field model*, Physica D. 66, 1993, 243.

[6] N. Provatas, N. Goldenfeld, J. Dantzig, *Efficient computation of dendritic microstructures using adaptive mesh refinement*, Phys. Rev. Lett. 80 15, 1998, 3308-3311

[7] Karma A, Rappel W-J. *Quantitative phase-field modeling of dendritic growth in two and three dimensions*, Phys Rev E 57, 1997,R3017.

[8] Chen Y, Kang XH, Li DZ. Acta Phys Sin 2009;58:390.

[9] Wheeler A.A., Boettinger W.J., McFadden G.B., *Phase-field model for isothermal phase transitions in binary alloys*, Phys Rev A 45, 1992, 7424.

[10] Wheeler A.A., Boettinger W.J., McFadden G.B., *Phase-field model of solute trapping during solidification*, Phys Rev E 47,1993, 1893.

[11] Warren JA, Boettinger WJ., *Prediction of dendritic growth and microsegregation patterns in a binary alloy using the Phase-field method*, Acta Metall. Mater.,43, 1995, 689.

[12] A. Karma, *Phase field formulation for quantitative modelling of alloy solidification*, Phys.Rev.Lett 8711 ,11, 2001, 115701.

[13] B. Echebarria, R. Folch , A. Karma , M. Plapp, *Quantitative phase-field model of alloy solidification*, Phys. Rev. E 70 6, 2004, 061604.

[14] Kim S.G., Kim W.T., Suzuki T., *Phase-field model for binary alloys*, Phys. Rev. E 60, 1999, 7186.

[15] Loginova I, Amberg G, Argen J., *Phase-field simulations of non-isothermal binary alloy solidification*, Acta Mater. 49, 2001, 573.

[16] Lan C.W., Chang Y.C., Shih C.J., *Adaptive phase field simulation of non-isothermal free dendritic growth of a binary alloy*, Acta Mater. 51, 2003, 1857.

[17] Ohno M, Matsuura K., *Quantitative phase-field modeling for dilute alloy solidification involving diffusion in the solid*, Phys Rev E 79, 2009, 031603.

[18] L. Gránásy, T. Pusztai, T. Börzsönyi, J.A. Warren, and J.F. Douglas, *A general mechanism of polycrystalline growth,* Nature Materials 3, 2004, 645.

[19] Warren J.A., Kobayashi R., Lobkovsky A.E., Carter W.C., *Extending phase field models of solidification to polycrystalline materials*, Acta Mater. 51, 2003, 6035.

[20] Pusztai T, Tegze G, Tóth GI, Koernyei L, Bansel G, Fan Z, L. Gránásy, *Phase-field approach to polycrystalline solidification including heterogeneous and homogeneous nucleation*, J. Phys. Condens. Matter. 20, 2008, 404205.

[21] Karma A., *Phase-field model of eutectic growth*, Phys Rev E 49, 1994, 2245.

[22] Yang YJ, Wang JC, Yang GC, Zhu YC. Acta Metall Sin 2006;42:914.

[23] B. Sudman, B. Jonsson, J.O. Andersson, *The Thermo-Calc Databank System*, CALPHAD, 9, 1985, 153

[24] J.Agren, I.S.I.J. Inter., 1992, vol.32, p.291.

[25] A. Engstrom, I. Hoglud, and J. Agren, *Computer Simulation of Diffusion in Multiphase Systems*, Metall. Mater. Trans., 25A, 1994, 1127–1134.

[26] A.G.Georgakou, Diploma thesis, June 2013, Department of Mechanical Engineering, University of Thessaly.

[27] M.Flemmings, *Solidification Processing*, McGraw-Hill, 1974.

[28] Scheil E., *Z. Metallkunde,* 1942, 34- 70

[29] Mullins W. W., Sekerka R. F., *Morphological stability of a particle growing by diffusion or heat flow*. J. Appl. Phys. 34, 1963, 323–329.

[30] Kurz W, Fisher D. J., *Dendrite growth at the limit of stability: Tip radius and spacing*. Acta Metall. 29, 1981, 11–20.

[31] Jackson K. A., Hunt J. D. *Lamellar and rod eutectic growth*. *Trans.* Metall. Soc. AIME 236, 1966, 1129–1142.

[32] Boettinger W. J., Coriell S. R., Greer A. L., Karma A., Kurz W., Rappaz M., Trivedi R., *Solidification microstructures: Recent developments, future directions*. Acta Mater. 48, 2000, 43–70.

[33] Phanikumarg G. and Chattopadhyay K., *Solidification microstructure development*. Sadhana 26, 2001, 25-34.

[34] I. Steinbach, F. Pezzolla, B. Nestler, M. Seeßelberg, R. Prieler, G. J. Schmitz, J. L. L. Rezende, *A phase field concept for multiphase systems*, Physica D 94, 1996, p.135-147.

[35] I. Steinbach, B. Böttger, J. Eiken, N. Warnken, S.G. Fries, *CALPHAD and Phase-Field Modeling: A Succesful Liaison*, Journal of Phase Equilibria and Diffusion 28 1, 2007, 101.

[36] T. Kitashima: *Coupling of the phase-field and CALPHAD methods for predicting multicomponent, solid-state phase transformations*, Philosophical Magazine Vol. 88, No.11, 11 April 2008, 1615–1637.

[37] S.G.Fries, B.Böttger, J.Eiken, I. Steinbach, *Upgrading CALPHAD to microstructure simulation: the phase-field method*, Int.J.Mat.Res. 100, 2009, 2.

[38] I. Steinbach, *Phase-field models in Materials Science –Topical Review*, Modelling Simul. Mater. Sci. Eng. 17, 2009, 073001.

[39] H. Emmerich, *Advances of and by phase-field modelling in condensed-matter physics*, Advances in Physics 57, 2008, 1.

[40] U. Hecht et. al., *Advances of and by phase-field modelling in condensed-matter physics*, vol. 57, pg 1, 2008 Advances in Physics 59, 3, 2010, 257.

[41] H.J. Diepers, Diploma thesis, Access, RWTH Aachen 1997.

[42] C. Beckermann, H.J. Diepers, I. Steinbach, A. Karma, X. Tong, *Modeling Melt Convection in Phase-Field Simulations of Solidification*, Journal of Computational Physics 154, 1999, 468.

[43] I. Steinbach, F. Pezzolla, B. Nestler, M. Seeßelberg, R. Prieler, G. J. Schmitz, J. L. L. Rezende, *A phase field concept for multiphase systems,* Physica D. 94, 1996, 135-147.

[44] Qin, R.S., Wallach, E.R., Thomson, R.C., *A phase-field model for the solidification of multicomponent and multiphase alloys*, J. Cryst. Growth 279 (1–2), 2005,163.

[45] Kovacevic, I., *Simulation of spheroidisation of elongated Si particle in Al-Si alloys by the phase-field model*, Mater. Sci. Eng. A 496 (1–2), 2008, 345.

[46] Wang J.S., Lee P.D., *Quantitative simulation of Fe-rich intermetallics in Al-Si-Cu-Fe alloys during solidification*. In: Proceedings of 138th TMS Annual Meeting and Exhibition, San Francisco, Materials Processing and Properties, 1, 2009.

[47] Eiken, J., Boettger, B., Steinbach, I., *Multiphase-field approach for multicomponent alloys with extrapolation scheme for numerical application*, Phys. Rev. E 73, 2006, 066122.

[48] Boettger, B., Carre´, A., Schmitz, G.J., Eiken, J., Apel, M., *Simulation of the microstructure formation in technical aluminum alloys using the multi-phase-field method*, Trans. Indian Inst. Met. 62 (4–5), 2009, 299.

[49] Zimmermann, G., Sturz, L., Walterfang, M., Dagner, J., *Effect of melt flow on dendritic growth in $AlSi_7$-based alloys during directional solidification*. Int. J. Cast Met. Res. 22 (1–4), 2009, 335.

[50] Nomoto, S., Minamoto, S., Nakajima, K., *Numerical simulation for grain refinement of aluminum alloy by multi-phase-field model coupled with CALPHAD*, ISIJ Int. 49 (7), 2009, 1019.

[51] Buenck, M., Warnken, N., Buehrig-Polaczek, A., *Microstructure evolution of rheo-cast A356 aluminium alloy in consideration of different cooling conditions by means of the cooling channel process*,J. Mater. Process. Technol. 210 (4), 2010, 624.

[52] Carre´, A., Boettger, B., Apel, M., *Phase-field modelling of gas porosity formation during the solidification of aluminium*, Int. J. Mater. Res. 2010/04, 510–514.

[53] Boettger, B., Eiken, J., Ohno, M., Klaus, G., Fehlbier, M., Schmid-Fetzer, R., Steinbach, I., Buehrig-Polaczek, A., *Controlling microstructure in magnesium alloys: a combined thermodynamic, experimental and simulation approach*, Adv. Eng. Mater. 8 (4), 2006, 241.

[54] Eiken, J., *Phase-field simulation of microstructure formation in technical magnesium alloys*, Int. J. Mater. Res. 2010/04, 503–509

[55] Eiken, J., *A phase-field model for technical alloy solidification*, PhD thesis, Access RWTH Aachen, 2010.

[56] Eiken, J., Boettger, B., Steinbach, I., *Simulation of microstructure evolution during solidification of magnesium-based alloys*, Trans. Indian Inst. Met. 60 (2–3), 2007, 179–184.

[57] Eiken, J., *Dendritic growth texture evolution in Mg-based alloys investigated by phase-field simulation*, Int. J. Cast Met. Res.22 (1–4), 2009, 86–89.

[58] Eiken, J., *Phase-field simulations of dendritic orientation selection in Mg-alloys with hexagonal anisotropy*, Mater. Sci. Forum 649, 2010, 199–204.

[59] Khan, S.S., Hort, N., Eiken, J., Steinbach, I., Schmauder, S.,*Numerical determination of heat distribution and castability simulations of as cast Mg-Al alloys*, Adv. Eng. Mater. 11 (3), 2009, 162.

[60] Tiaden, J., *Phase field simulations of the peritectic solidification of Fe-C*, J. Cryst. Growth 198/199, 1999,1275–1280.

[61] Boettger, B., Apel, M., Eiken, J., Schaffnit, P., Steinbach, I.,*Phase-field simulation of solidification and solid-state transformations in multicomponent steels,* Steel Res. Int. 79 (8) ,2008, 608.

[62] Boettger, B., Stratemeier, S., Subasic, E., Goehler, K., Steinbach,I., Senk, D.:, *Modeling of hot ductility during solidification of steel grades in continuous casting-part II*, Adv. Eng. Mater.12 (4), 2010, 101.

[63] Pariser, G., Schaffnit, P., Steinbach, I., Bleck, W., *Simulation of the gamma-alpha-transformation using the phase-field method*, Steel Res. 72 (9), 2001, 354–360.

[64] Mecozzi, M.G., Sietsma, J., van der Zwaag, S., Apel, M., Schaffnit, P., Steinbach, I., *Analysis of the gamma-alpha transition in C-Mn steels by dilatometry, Laser confocal scanning microscopy and phase-field modelling*, In: Proceedings MS&T, 2003, 353ff.

[65] Mecozzi, M.G., Sietsma, J., van der Zwaag, S., Apel, M., Schaffnit, P., Steinbach, I., *Analysis of the gamma-alpha transformation in C-Mn steel by phase-field modelling*, Metall. Mater. Trans. A 36A (9), 2005, 2327.

[66] Mecozzi, M.G., *Phase field modelling of the austenite to ferrite transformation in steels*, PhD thesis, TU Delft, 2007.

[67] Thiessen, R.G., *Physically-based modelling of material response to welding*. PhD thesis, TU Delft, 2006.

[68] Militzer, M., Mecozzi, M.G., Sietsma, J., van der Zwaag, S., *Three-dimensional phase field modelling of the austenite-to ferrite transformation*, Acta Mater. 54(15), 2006, 3961–3972.

[69] Apel, M., Benke, S., Steinbach, I., *Virtual dilatometer curves and effective Young's modulus of a 3D multiphase structure calculated by the phase-field method*, Comput. Mater. Sci. 45, 2009, 589.

[70] Savran, V.I. *Austenite formation in C-Mn steel*, PhD thesis, TUDelft, 2009.

[71] Azizi-Alizamini, H., Militzer, M., *Phase field modelling of austenite formation from ultrafine ferrite–carbide aggregates in Fe–C*, Int. J. Mater. Res. 2010/04, 534–541.

[72] Rudnizki, J., Bo¨ttger, B., Prahl U., Bleck, W., *Phase-field modelling of austenite formation from a ferrite plus pearlite microstructure during annealing of cold-rolled dual-phase steel*, Metall. Mater. Trans. A (in press).

[73] Nakajima, K., Apel, M., Steinbach, I., *The role of carbon diffusion in ferrite on the kinetics of cooperative growth of pearlite: a multi-phase-field study*. Acta Mater. 54, 2006, 3665–3672.

[74] Hillert, M., *The role of interfacial energy during solid state phase transformations*. Jerekont Ann. 147, 1957, 757.

[75] Zener, C., *Kinetics of the Decomposition of Austenite*. Wiley, New York, 1947.

[76] Steinbach, I., Apel, M., *The influence of lattice strain on pearlite formation in Fe–C*, Acta Mater. 55, 2007, 4817.

[77] Thiessen, R.G., Sietsma, J., Palmer, T.A., Elmer, J.W., Richardson, I.M., *Phase-field modelling and synchrotron validation of phase transformations in martensitic dual-phase steel*, Acta Mater. 55, 2007, 601–614.

[78] Schaffnit, P., Apel, M., Steinbach, I., *Simulation of ideal grain growth using the multi-phase-field model*, Mater. Sci. Forum 558–559, 2007, 1177.

[79] Apel, M., Boettger, B., Rudnizki, J., Schaffnit, P., Steinbach, I., *Grain growth simulations including particle pinning using the multi-phase-field concept*,ISIJ Int. 49 (7), 2009, 1024.

[80] Rudnizki, J., Zeislmair, B., Prahl, U., Bleck, W., *Prediction of abnormal grain growth during high temperature treatment*, Comput. Mater. Sci. 49 (2), 2010, 209.

[81] Rudnizki, J., Zeislmair, B., Prahl, U., Bleck, W., *Thermodynamical simulation of carbon profiles and precipitation evolution during high temperature case hardening*. Steel Res. Int. 81 (6), 2010, 472.

[82] Toloui, M., Militzer, M., *Phase field simulation of austenite grain growth in the HAZ of microalloyed linepipe steel*, Int. J. Mater. Res. 2010/04, 542–548.

[83] Sommerfeld, A., Boettger, B., Tonn, B., *Graphite nucleation in cast iron melts based on solidification experiments and microstructure simulation*, J. Mater. Sci. Technol. 24 (3), 2008, 321–324.

[84] Warnken, N., *Simulation of microstructure formation during solidification and solution heat treatment of a novel single crystal superalloy*, PhD thesis, Access RWTH Aachen, 2007.

[85] Boettger, B., Grafe, U., Ma, D., Fries, S.G., *Simulation of microsegregation and microstructural evolution in directionally solidified superalloys*, Mater. Sci. Technol. 16, 2000, 1425.

[86] Warnken, N., Ma, D., Mathes, M., Steinbach, I., *Investigation of eutectic island formation in SX superalloys*, Mater. Sci. Eng. A 413 (12), 2005, 267–271.

[87] Warnken, N., Ma, D., Drevermann, A., Reed, R.C., Fries, S.G., Steinbach, I., *Phase-field modelling of as-cast microstructure evolution in nickel-based superalloys*, Acta Mater. 57, 2009, 5862.

[88] Schmitz, G.J., Zhou, B., Boe ttger, B., Villain, J., Klima, S., *Phase-field modeling and experimental observations of microstructures in solidifying Sn-Ag-Cu solders*, Paper presented at the COST531 meeting in Bochum, to be submitted to Journal of Electronic Materials, 2009.

[89] Eiken, J., Apel, M., Witusiewicz, V.T., Zollinger, J., *Hecht, U., Interplay between a(Ti) nucleation and growth during peritectic solidification investigated by phase-field simulations*, J. Phys. Condens. Matter 21, 2009, 464104.

[90] Kim, S.G., Kim, W.T., Suzuki, T., Ode, M., *Phase field modeling of eutectic solidification*, J. Cryst. Growth 261 (1), 2004, 135.

[91] Tiaden, J., Nestler, B., Diepers, H.-J., Steinbach, I., *The multiphase-field model with an integrated concept for modeling solute diffusion*, Physica D 115, 1998, 73–86.

[92] Ramirez, J.C., Beckermann, C., Karma, A., Diepers, H.-J.: Phase-field modeling of binary alloy solidification with coupled heat and solute diffusion. Phys. Rev. E 69, 2004, 051607.

[93] Steinbach, I.: Pattern formation in constrained dendritic growth with solutal buoyancy. Acta Mater. 57, 2009, 2640–2645.

[94]. Boettger, B., Eiken, J., Apel, M., *Phase-field simulation of microstructure formation in technical castings—a self-consistent homoenthalpic approach to the micro–macro problem*, J. Comput.Phys. 228, 2009, 6784–6795.

APPENDICES

Appendix 1- Input file for Al-3%Cu, Al-30%Cu, Al-45%Cu

```
# Automatic 'Driving File' written out by MICRESS.
# Type of input?
# ==============
shell input
#
# MICRESS binary
# ==============
# version number: 6.100 (Windows)
# compiled: 06/25/2013
# compiler version: Intel 1210 20120821
# Thermo-Calc coupling: enabled (version S/7)
# OpenMP: disabled
# ('double precision' binary)
# permanent license
#
# Language settings
# =================
#  Please select a language: 'English', 'Deutsch' or 'Francais'
English
#
# Flags and settings
# ==================
#
# Geometry
# --------
# Grid size?
# (for 2D calculations: AnzY=1, for 1D calculations: AnzX=1, AnzY=1)
# AnzX:
200
# AnzY:
1
# AnzZ:
200
# Cell dimension (grid spacing in micrometers):
# (optionally followed by rescaling factor for the output in the form of '3/4')
0.50000
#
# Flags
# -----
# Type of coupling?
# Options: phase concentration temperature temp_cyl_coord
#        [stress] [stress_coupled] [flow] [dislocation]
concentration
# Type of potential?
```

```
# Options: double_obstacle multi_obstacle [fd_correction]
double_obstacle
# Enable one dimensional far field approximation for diffusion?
# Options:   1d_far_field   no_1d_far_field
no_1d_far_field
# Shall an additional 1D field be defined in z direction
# for temperature coupling?
# Options: no_1d_temp 1d_temp 1d_temp_cylinder 1d_temp_polar [kin. Coeff]
# kin. Coeff: Kinetics of latent heat release (default is 0.01)
1d_temp
# Number of cells?
500
# cell width (micrometer):
100.000000000000
#
# Phase field data structure
# -------------------------
# Coefficient for initial dimension of field iFace
#  [minimum usage] [target usage]
0.1
# Coefficient for initial dimension of field nTupel
#  [minimum usage] [target usage]
0.1
#
# Restart options
# ===============
# Restart using old results?
# Options:   new     restart [reset_time]
new
#
# Name of output files
# ====================
# Name of result files?
C:\Users\User\Desktop\Kar\Results_3%
# Overwrite files with the same name?
# Options:   overwrite    write_protected    append
#          [zipped|not_zipped|vtk]
#          [unix|windows|non_native]
overwrite
#
# Selection of the outputs
# ========================
# [legacy|verbose|terse]
# Restart data output?                    ('rest')
# Options:   out_restart    no_out_restart      [wallclock time, h.]
out_restart
# Grain number output?                     ('korn')
# Options:   out_grains     no_out_grains
```

```
out_grains
# Phase number output?                    ('phas')
# Options:   out_phases     no_out_phases      [no_interfaces]
out_phases
# Fraction output?                        ('frac')
# Options:   out_fraction   no_out_fraction    [phase number]
out_fraction
# Average fraction table?                 ('TabF')
# Options:   tab_fractions  no_tab_fractions   [front_temp] [TabL_steps]
tab_fractions
# Interface output?                       ('intf')
# Options:   out_interface  no_out_interface   [sharp]
out_interface
# Driving-force output?                   ('driv')
# Options:   out_driv_force  no_out_driv_force
out_driv_force
# Number of relinearisation output?       ('numR')
# Options:   out_relin   no_out_relin
out_relin
# Interface mobility output?              ('mueS')
# Options:   out_mobility   no_out_mobility
out_mobility
# Curvature output?                       ('krum')
# Options:   out_curvature   no_out_curvature
out_curvature
# Interface velocity output?              ('vel')
# Options:   out_velocity   no_out_velocity
out_velocity
# Should the grain-time file be written out?      ('TabK')
# Options:   tab_grains     no_tab_grains      [extra|standard]
tab_grains
# Should the 'von Neumann Mullins' output be written out?     ('TabN')
# Options:  tab_vnm   no_tab_vnm
no_tab_vnm
# Should the 'grain data output' be written out?     ('TabGD')
# Options:  tab_grain_data   no_tab_grain_data
no_tab_grain_data
# Temperature output?                     ('temp')
# Options:   out_temp       no_out_temp
no_out_temp
# Concentration output?                   ('conc')
# Options: out_conc  no_out_conc  [component numbers]  [element_extensions]
out_conc
# Concentration of reference phase output?        ('cPha')
# Options: out_conc_phase  no_out_conc_phase
#   phase 0 [component numbers (default = all)] | ...
#   ... | phase n [component numbers] [element_extensions]
out_conc_phase 0
```

```
# Output for phase: 0  Concentrations: All
# Average concentration per phase (and extrema)?      ('TabC')
# Options:    tab_conc      no_tab_conc
tab_conc
# Recrystallisation energy output?                    ('rex')
# Options:    out_recrystall   no_out_recrystall
no_out_recrystall
# Recrystallised fraction output?                     ('TabR')
# Options:    tab_recrystall   no_tab_recrystall
no_tab_recrystall
# Dislocation density output?                         ('rhoD')
# Options:    out_disloc      no_out_disloc
no_out_disloc
# Miller-Indices output?                              ('mill')
# Options:    out_miller      no_out_miller
no_out_miller
# Orientation output?                                 ('orie')
# Options:    out_orientation  no_out_orientation
out_orientation
# Should the orientation-time file be written?        ('TabO')
# Options:  tab_orientation  no_tab_orientation   [rotmat]
tab_orientation
# Linearisation output?    ('TabLin')
# Options:   tab_lin  no_tab_lin
tab_lin
# Should monitoring outputs be written out?           ('TabL')
# Options:    tab_log [simulation time, s] [wallclock time, min]  no_tab_log
tab_log 0.001
#
# Time input data
# ===============
# Finish input of output times (in seconds) with 'end_of_simulation'
# 'regularly-spaced' outputs can be set with 'linear_step'
# or 'logarithmic_step' and then specifying the increment
# and end value
#  'first'              : additional output for first time-step
#  'end_at_temperature'    : additional output and end of simulation
#                        at given temperature
linear_step 0.01 0.8
end_of_simulation
# Time-step?
# Options:  (real)   automatic [0<factor_1<=1] [0<=factor_2] [max.] [min.]
# (Fix time steps: just input the value)
automatic 0.9 0.9 1.E-2 1.E-6
# Number of steps to adjust profiles of initially sharp interfaces [exclude_inactive]?
0
# Phase data
# ==========
```

```
# Number of distinct solid phases?
2
#
# Data for phase 1:
# ----------------
# Simulation of recrystallisation in phase 1?
# Options: recrystall no_recrystall [verbose|no_verbose]
no_recrystall
# Is phase 1 anisotrop?
# Options: isotropic anisotropic faceted antifaceted
anisotropic
# Crystal symmetry of the phase?
# Options: none cubic hexagonal tetragonal orthorhombic
cubic
# Should grains of phase 1 be reduced to categories?
# Options: categorize no_categorize
no_categorize
#
# Data for phase 2:
# ----------------
# [identical phase number]
# Simulation of recrystallisation in phase 2?
# Options: recrystall no_recrystall [verbose|no_verbose]
no_recrystall
# Is phase 2 anisotrop?
# Options: isotropic anisotropic faceted antifaceted
isotropic
# Should grains of phase 2 be reduced to categories?
# Options: categorize no_categorize
categorize
#
# Orientation
# ----------
# How shall grain orientations be defined?
# Options: angle_2d euler_zxz angle_axis miller_indices quaternion
angle_2d
#
# Grain input
# ===========
# Type of grain positioning?
# Options: deterministic random from_file
deterministic
# NB: the origin of coordinate system is the bottom left-hand corner,
#    all points within the simulation domain having positive coordinates.
# Number of grains at the beginning?
0
#
# Data for further nucleation
```

```
# ============================
# Enable further nucleation?
# Options: nucleation nucleation_symm no_nucleation [verbose|no_verbose]
nucleation
# Additional output for nucleation?
# Options: out_nucleation no_out_nucleation
no_out_nucleation
#
# Number of types of seeds?
2
#
# Input for seed type 1:
# ----------------------
# Type of 'position' of the seeds?
# Options: bulk region interface triple quadruple [restrictive]
bulk
# Phase of new grains (integer) [unresolved]?
1
# Reference phase (integer) [min. and max. fraction (real)]?
0
# Which nucleation model shall be used?
# Options: seed_undercooling seed_density
seed_density
# Integer for randomization?
134
# How many classes shall be chosen for the critical radius?
17
# Specify radius [micrometers] and seed density [cm**-3] for class 1
0.45 100
# Specify radius [micrometers] and seed density [cm**-3] for class 2
0.3 200
# Specify radius [micrometers] and seed density [cm**-3] for class 3
0.25 500
# Specify radius [micrometers] and seed density [cm**-3] for class 4
0.18 1000
# Specify radius [micrometers] and seed density [cm**-3] for class 5
0.15 2000
# Specify radius [micrometers] and seed density [cm**-3] for class 6
0.12 5000
# Specify radius [micrometers] and seed density [cm**-3] for class 7
0.10 9000
# Specify radius [micrometers] and seed density [cm**-3] for class 8
0.08 14000
# Specify radius [micrometers] and seed density [cm**-3] for class 9
0.07 25000
# Specify radius [micrometers] and seed density [cm**-3] for class 10
0.06 50000
# Specify radius [micrometers] and seed density [cm**-3] for class 11
```

```
0.05  80000
# Specify radius [micrometers] and seed density [cm**-3] for class 12
0.04  120000
# Specify radius [micrometers] and seed density [cm**-3] for class 13
0.03  220000
# Specify radius [micrometers] and seed density [cm**-3] for class 14
0.025 330000
# Specify radius [micrometers] and seed density [cm**-3] for class 15
0.02  500000
# Specify radius [micrometers] and seed density [cm**-3] for class 16
0.015 1000000
# Specify radius [micrometers] and seed density [cm**-3] for class 17
0.010 30000000
# Class  1:   0 seed(s), 3.7500E-01 < radii < 5.2500E-01 [micrometers]
# Class  2:   0 seed(s), 2.7500E-01 < radii < 3.7500E-01 [micrometers]
# Class  3:   0 seed(s), 2.1500E-01 < radii < 2.7500E-01 [micrometers]
# Class  4:   0 seed(s), 1.6500E-01 < radii < 2.1500E-01 [micrometers]
# Class  5:   0 seed(s), 1.3500E-01 < radii < 1.6500E-01 [micrometers]
# Class  6:   0 seed(s), 1.1000E-01 < radii < 1.3500E-01 [micrometers]
# Class  7:   0 seed(s), 9.0000E-02 < radii < 1.1000E-01 [micrometers]
# Class  8:   0 seed(s), 7.5000E-02 < radii < 9.0000E-02 [micrometers]
# Class  9:   0 seed(s), 6.5000E-02 < radii < 7.5000E-02 [micrometers]
# Class  10:   0 seed(s), 5.5000E-02 < radii < 6.5000E-02 [micrometers]
# Class  11:   0 seed(s), 4.5000E-02 < radii < 5.5000E-02 [micrometers]
# Class  12:   0 seed(s), 3.5000E-02 < radii < 4.5000E-02 [micrometers]
# Class  13:   0 seed(s), 2.7500E-02 < radii < 3.5000E-02 [micrometers]
# Class  14:   1 seed(s), 2.2500E-02 < radii < 2.7500E-02 [micrometers]
# Class  15:   1 seed(s), 1.7500E-02 < radii < 2.2500E-02 [micrometers]
# Class  16:   1 seed(s), 1.2500E-02 < radii < 1.7500E-02 [micrometers]
# Class  17:   9 seed(s), 1.0000E-08 < radii < 1.2500E-02 [micrometers]
# Determination of nuclei orientations?
# Options:  random   randomZ  fix   range   parent_relation
random
# Shield effect:
# Shield time [s] ?
1.0000
# Nucleation range
# min. nucleation temperature for seed type 1 [K]
0.000000
# max. nucleation temperature for seed type 1 [K]
1000.000
# Time between checks for nucleation? [s]
1.00000E-03
# Shall random noise be applied?
# Options:    nucleation_noise   no_nucleation_noise
no_nucleation_noise
#
# Input for seed type 2:
```

```
# ----------------------
# Type of 'position' of the seeds?
# Options: bulk region interface triple quadruple [restrictive]
interface
# Phase of new grains (integer) [unresolved]?
2
# Reference phase (integer) [min. and max. fraction (real)]?
0
# Substrat phase [2nd phase in interface]?
# (set to 0 to disable the effect of substrate curvature)
1
# maximum number of new nuclei 2?
100000
# Grain radius [micrometers]?
0.00000
# Choice of growth mode:
# Options:  stabilisation analytical_curvature
stabilisation
# min. undercooling [K] (>0)?
2.0000
# Shield effect:
# Shield time [s] ?
1.00000E-02
# Shield distance [micrometers]  [ nucleation distance [micrometers] ]?
10.000
# Nucleation range
# min. nucleation temperature for seed type 2 [K]
0.000000
# max. nucleation temperature for seed type 2 [K]
820.0000
# Time between checks for nucleation? [s]
1.00000E-02
# Shall random noise be applied?
# Options:   nucleation_noise  no_nucleation_noise
no_nucleation_noise
#
# Max. number of simultaneous nucleations?
# ----------------------------------------
# (set to 0 for automatic)
1000
#
# Shall metastable small seeds be killed?
# ---------------------------------------
# Options:   kill_metastable    no_kill_metastable
no_kill_metastable
#
# Phase interaction data
# ======================
```

```
#
# Data for phase interaction 0 / 1:
# ---------------------------------
# Simulation of interaction between phase 0 and 1?
# Options: phase_interaction  no_phase_interaction
#  [standard|particle_pinning[_temperature]|solute_drag]
#   | [redistribution_control]
phase_interaction
# 'DeltaG' options:  default
# avg ... []  max ... [J/cm**3]  smooth ... [degrees]  noise ... [J/cm**3]
avg 0.55   max 100
# I.e.:  avg +0.55  smooth +45.0  max +1.00000E+02
# Type of surface energy definition between phases LIQUID and 1?
# Options:  constant  temp_dependent
constant
# Surface energy between phases LIQUID and 1? [J/cm**2]
#    [max. value for num. interface stabilisation [J/cm**2]]
1.00000E-05
# Type of mobility definition between phases LIQUID and 1?
# Options:  constant  temp_dependent  dg_dependent
temp_dependent
# File for kinetic coefficient between phases LIQUID and 1?
C:\Users\User\Desktop\Kar\Results_3%\AlCu_Temp1d_mueVonT0_1
# Is interaction isotropic?
# Optionen: isotropic  anisotropic [harmonic_expansion]
anisotropic
# Anisotropy of interfacial stiffness? (cubic)
# 1 - delta * cos(4*phi), (delta =delta_stiffness =15*delta_energy)
# Coefficient delta (<1.) ?
0.50000
# Anisotropy of interfacial mobility? (cubic)
# 1 + delta * cos(4*phi)
# Coefficient delta (<1.) ?
0.20000
#
# Data for phase interaction 0 / 2:
# ---------------------------------
# Simulation of interaction between phase 0 and 2?
# Options: phase_interaction  no_phase_interaction  identical phases nb
#  [standard|particle_pinning[_temperature]|solute_drag]
#   | [redistribution_control]
phase_interaction
# 'DeltaG' options:  default
# avg ... []  max ... [J/cm**3]  smooth ... [degrees]  noise ... [J/cm**3]
avg 0.55   max 100
# I.e.:  avg +0.55  smooth +45.0  max +1.00000E+02
# Type of surface energy definition between phases LIQUID and 2?
# Options:  constant  temp_dependent
```

```
constant
# Surface energy between phases LIQUID and 2? [J/cm**2]
#    [max. value for num. interface stabilisation [J/cm**2]]
1.00000E-05
# Type of mobility definition between phases LIQUID and 2?
# Options: constant temp_dependent dg_dependent
temp_dependent
# File for kinetic coefficient between phases LIQUID and 2?
C:\Users\User\Desktop\Kar\Results_3%\AlCu_Temp1d_mueVonT0_2
#
# Data for phase interaction 1 / 1:
# ---------------------------------
# Simulation of interaction between phase 1 and 1?
# Options: phase_interaction  no_phase_interaction  identical phases nb
#  [standard|particle_pinning[_temperature]|solute_drag]
#   | [redistribution_control]
no_phase_interaction
#
# Data for phase interaction 1 / 2:
# ---------------------------------
# Simulation of interaction between phase 1 and 2?
# Options: phase_interaction  no_phase_interaction  identical phases nb
#  [standard|particle_pinning[_temperature]|solute_drag]
#   | [redistribution_control]
no_phase_interaction
#
# Data for phase interaction 2 / 2:
# ---------------------------------
# Simulation of interaction between phase 2 and 2?
# Options: phase_interaction  no_phase_interaction  identical phases nb
#  [standard|particle_pinning[_temperature]|solute_drag]
#   | [redistribution_control]
no_phase_interaction
#
# Concentration data
# ==================
# Number of dissolved constituents?  (int)
1
# Type of concentration?
# Options:    atom_percent   (at%)
#             weight_percent  (wt%)
weight_percent
#
# Options:  diff   no_diff   infinite   infinite_restricted
#           multi   database_global   database_local   from_file
#           [+b] for grain-boundary diffusion
# ('multi' can be followed by a string of "n", "d", "g", "l", or "f"
#  to describe each contribution: respectively no diffusion,
```

```
#  user-defined diffusion coefficient,'global' or 'local' value from
#  database, and 'from file, the default is global values from database).
# Extra line option (prefactor on time step): cushion <0-1>
# Extra line option: infinite_limit [cm**2/s]
# How shall diffusion of component 1  in phase 0  be solved?
diff
# Diff.-coefficient:
# Prefactor? (real) [cm**2/s]
2.00000E-04
# Activation energy? (real) [J/mol]
0.0000
# How shall diffusion of component 1  in phase 1  be solved?
diff
# Diff.-coefficient:
# Prefactor? (real) [cm**2/s]
1.00000E-08
# Activation energy? (real) [J/mol]
0.0000
# How shall diffusion of component 1  in phase 2  be solved?
diff
# Diff.-coefficient:
# Prefactor? (real) [cm**2/s]
1.00000E-08
# Activation energy? (real) [J/mol]
0.0000
#
# Phase diagram - input data
# ==========================
#
# List of phases and components which are stoichiometric:
#  phase and component(s) numbers
# List of concentration limits (at%):
#  <Limits>, phase number and component number
# List for ternary extrapolation (2 elements + main comp.):
#  <interaction>, component 1, component 2
# Switches: <stoich_enhanced_{on|off}> <solubility_{on|off}>
# End with 'no_more_stoichio' or 'no_stoichio'
2 1
no_stoichio
# In phase 2 component 1 is defined stoichiometric.
#
# Is a thermodynamic database to be used?
# Options: database   database_verbose   no_database
database
#
# Name of Thermo-Calc *.GES5 file without extension?
C:\Users\User\Desktop\Kar\Results_3%\3_phases(theta)
# Interval for updating thermodynamic data [s] =
```

```
1.00000E-02
# Input of the phase diagram of phase 0 and phase 1:
# ------------------------------------------------
# Which phase diagram is to be used?
# Options: database [local|global][start_value_{1|2}] linear linearTQ
database
# Maximal allowed local temperature deviation [K] [Interval [s] ]
-1.00000000
# Input of the phase diagram of phase 0 and phase 2:
# ------------------------------------------------
# Which phase diagram is to be used?
# Options: database [local|global][start_value_{1|2}] linear linearTQ
database
# Maximal allowed local temperature deviation [K] [Interval [s] ]
-1.00000000
# Reading GES5 workspace ...
# Index relations between TC and MICRESS
# --------------------------------------
# The database contains the following components:
# 1: AL
# 2: CU
# Specify relation between component indices Micress -> TC!
# The main component has in MICRESS the index 0
# Thermo-Calc index of (MICRESS) component 0?
1
# Thermo-Calc index of (MICRESS) component 1?
2
# 0 -> AL
# 1 -> CU
# The database contains 3 phases:
# 1: LIQUID
# 2: ALCU_THETA
# 3: FCC_A1
# Specify relation between phase indices Micress -> TC!
# The matrix phase has in MICRESS the index 0
# Thermo-Calc index of the (MICRESS) phase 0?
1
# Thermo-Calc index of the (MICRESS) phase 1?
3
# Thermo-Calc index of the (MICRESS) phase 2?
2
# 0 -> LIQUID
# 1 -> FCC_A1
# 2 -> ALCU_THETA
#
# Molar volume of (MICRESS) phase 0 (LIQUID)? [cm**3/mol]
10.000
# Molar volume of (MICRESS) phase 1 (FCC_A1)? [cm**3/mol]
```

```
10.000
# Molar volume of (MICRESS) phase 2 (ALCU_THETA)? [cm**3/mol]
10.000
# Temperature at which the initial equilibrium
# will be calculated? [K]
925.0000
#
# Initial concentrations
# ======================
# How shall initial concentrations be set?
# Options:  input  equilibrium  from_file    [phase number]
equilibrium
# Initial concentration of component 1 (CU) in phase 0 (LIQUID) ?wt%]
3.0000 /or 30.00 for Al-30%Cu/or 45.00 for Al-45%Cu
#
#
# Parameters for latent heat and 1D temperature field
# ===================================================
# Simulate release of latent heat?
# Options:      lat_heat    lat_heat_3d [matrix phase]
lat_heat_3d 0
# Type of thermal conductivity definition for phase  0 (LIQUID) ?
# Options:   constant    temp_dependent
constant
# Thermal conductivity of phase  0 (LIQUID) ?  [W/cm/K]
1.3000
# Type of thermal conductivity definition for phase  1 (FCC_A1) ?
# Options:   constant    temp_dependent
constant
# Thermal conductivity of phase  1 (FCC_A1) ?  [W/cm/K]
1.2000
# Simulation with release of pseudo-3D latent heat of phase 1 (FCC_A1)?
# Options:      pseudo_3d [crit. matrix fraction]    no_pseudo_3d
pseudo_3D 0.75
# Type of thermal conductivity definition for phase  2 (ALCU_THETA) ?
# Options:   constant    temp_dependent
constant
# Thermal conductivity of phase  2 (ALCU_THETA) ?  [W/cm/K]
1.2000
# Simulation with release of pseudo-3D latent heat of phase 2 (ALCU_THETA)?
# Options:      pseudo_3d [crit. matrix fraction]    no_pseudo_3d
no_pseudo_3D
# Interval for updating enthalpy data [s]
1.00000E-02
#
# Boundary conditions
# ===================
# Moving-frame system in z-direction?
```

```
# Options:    moving_frame    no_moving_frame
no_moving_frame
# Type of initial temperature profile?
# Options:   linear    from_file
linear
# Initial temperature at the bottom [K]
950.0000
# Initial temperature at the top [K]
950.0000
# Initial position of the 1D temperature field [micrometer]
# (distance between bottom of 1D temp field and bottom of simulation area, <0!)
-500.000000000000
#
# Boundary conditions for phase field in each direction
# Options: i (insulation) s (symmetric) p (periodic/wrap-around)
#        g (gradient)   f (fixed)    w (wetting)
# Sequence: W E (S N, if 3D) B T borders
ppii
#
# Boundary conditions for concentration field in each direction
# Options: i (insulation) s (symmetric) p (periodic/wrap-around) g (gradient) f (fixed)
# Sequence: W E (S N, if 3D) B T borders
ppii
#
# Boundary conditions for 1D temperature field bottom and top
# Options: i (insulation) s (symmetric) p (periodic/wrap-around) g (global grad) f (fixed) j (flux)
# Sequence: B T
fi
# How shall temperature in B-direction be read?
# # Options:   constant    from_file
constant
# Fixed value for temperature [K]
298.00
# Fixed value for heat transfer coefficient [W/cm2K]
1.50000000000000
# Please specify for the 1D temperature field, which enthalpy
# below the calculation domain should be present!
# The following options are available:
# # Options:   constant    from_file
from_file
# file name:
C:\Users\User\Desktop\Kar\Results_3%\AlCu_Temp1d_latHeatData columns 2 8
# Please specify for the 1D temperature field, which value of Cp
# below the calculation domain should be present!
# The following options are available:
# # Options:   constant    from_file
from_file
# file name:
```

C:\Users\User\Desktop\Kar\Results_3%\AlCu_Temp1d_latHeatData columns 2 6
Please specify for the 1D temperature field, which value of the heat conductivity
below the calculation domain should be present!
The following options are available:
Options: constant from_file
from_file
file name:
C:\Users\User\Desktop\Kar\Results_3%\AlCu_Temp1d_latHeatData columns 2 7
Please specify for the 1D temperature field, which enthalpy
above the calculation domain should be present!
The following options are available:
Options: constant from_file
from_file
file name:
C:\Users\User\Desktop\Kar\Results_3%\AlCu_Temp1d_latHeatData columns 2 8
Please specify for the 1D temperature field, which value of Cp
above the calculation domain should be present!
The following options are available:
Options: constant from_file
from_file
file name:
C:\Users\User\Desktop\Kar\Results_3%\AlCu_Temp1d_latHeatData columns 2 6
Please specify for the 1D temperature field, which value of the heat conductivity
above the calculation domain should be present!
The following options are available:
Options: constant from_file
from_file
file name:
C:\Users\User\Desktop\Kar\Results_3%\AlCu_Temp1d_latHeatData columns 2 7
Unit-cell model symmetric with respect to the x/y diagonal plane?
Options: unit_cell_symm no_unit_cell_symm
no_unit_cell_symm
#
Other numerical parameters
==========================
Phase minimum?
1.00E-03
Interface thickness (in cells)?
3.50
#

Appendix 2- Input file for Al-33%Cu

```
# Automatic 'Driving File' written out by MICRESS.
#
# Type of input?
# ==============
shell input
#
# MICRESS binary
# ==============
# version number: 6.100 (Windows)
# compiled: 06/25/2013
# compiler version: Intel 1210 20120821
# Thermo-Calc coupling: enabled (version S/7)
# OpenMP: disabled
# ('double precision' binary)
# permanent license
#
# Language settings
# =================
#  Please select a language: 'English', 'Deutsch' or 'Francais'
English
#
# Flags and settings
# ==================
#
# Geometry
# --------
# Grid size?
# (for 2D calculations: AnzY=1, for 1D calculations: AnzX=1, AnzY=1)
# AnzX:
100
# AnzY:
1
# AnzZ:
200
# Cell dimension (grid spacing in micrometers):
# (optionally followed by rescaling factor for the output in the form of '3/4')
1.0000000
#
# Flags
# -----
# Type of coupling?
# Options: phase concentration temperature temp_cyl_coord
#        [stress] [stress_coupled] [flow] [dislocation]
concentration
# Type of potential?
# Options: double_obstacle multi_obstacle  [fd_correction]
```

```
double_obstacle
# Enable one dimensional far field approximation for diffusion?
# Options:    1d_far_field    no_1d_far_field
no_1d_far_field
# Shall an additional 1D field be defined in z direction
# for temperature coupling?
# Options:  no_1d_temp  1d_temp  1d_temp_cylinder  1d_temp_polar [kin. Coeff]
# kin. Coeff: Kinetics of latent heat release (default is 0.01)
1d_temp
# Number of cells?
500
# cell width (micrometer):
20.0000000000000
#
# Phase field data structure
# --------------------------
# Coefficient for initial dimension of field iFace
#  [minimum usage] [target usage]
0.1
# Coefficient for initial dimension of field nTupel
#  [minimum usage] [target usage]
0.1
#
# Restart options
# ===============
# Restart using old results?
# Options:    new      restart [reset_time]
new
#
# Name of output files
# ====================
# Name of result files?
C:\Users\User\Desktop\Kar\Eutectic5\
# Overwrite files with the same name?
# Options:    overwrite     write_protected     append
#          [zipped|not_zipped|vtk]
#          [unix|windows|non_native]
overwrite
#
# Selection of the outputs
# ========================
# [legacy|verbose|terse]
# Restart data output?                          ('rest')
# Options:    out_restart     no_out_restart       [wallclock time, h.]
out_restart
# Grain number output?                           ('korn')
# Options:    out_grains      no_out_grains
out_grains
```

```
# Phase number output?                    ('phas')
# Options:   out_phases     no_out_phases      [no_interfaces]
out_phases
# Fraction output?                        ('frac')
# Options:   out_fraction   no_out_fraction    [phase number]
out_fraction
# Average fraction table?                 ('TabF')
# Options:   tab_fractions  no_tab_fractions   [front_temp] [TabL_steps]
tab_fractions
# Interface output?                       ('intf')
# Options:   out_interface  no_out_interface   [sharp]
out_interface
# Driving-force output?                   ('driv')
# Options:   out_driv_force  no_out_driv_force
out_driv_force
# Number of relinearisation output?       ('numR')
# Options:   out_relin   no_out_relin
no_out_relin
# Interface mobility output?              ('mueS')
# Options:   out_mobility   no_out_mobility
out_mobility
# Curvature output?                       ('krum')
# Options:   out_curvature   no_out_curvature
out_curvature
# Interface velocity output?              ('vel')
# Options:   out_velocity   no_out_velocity
out_velocity
# Should the grain-time file be written out?      ('TabK')
# Options:   tab_grains     no_tab_grains      [extra|standard]
tab_grains
# Should the 'von Neumann Mullins' output be written out?     ('TabN')
# Options:  tab_vnm   no_tab_vnm
no_tab_vnm
# Should the 'grain data output' be written out?     ('TabGD')
# Options:  tab_grain_data   no_tab_grain_data
no_tab_grain_data
# Temperature output?                     ('temp')
# Options:   out_temp       no_out_temp
no_out_temp
# Concentration output?                   ('conc')
# Options: out_conc  no_out_conc  [component numbers]  [element_extensions]
out_conc
# Concentration of reference phase output?        ('cPha')
# Options: out_conc_phase  no_out_conc_phase
#   phase 0 [component numbers (default = all)] | ...
#   ... | phase n [component numbers] [element_extensions]
out_conc_phase 0
# Output for phase: 0  Concentrations: All
```

```
# Average concentration per phase (and extrema)?      ('TabC')
# Options:    tab_conc      no_tab_conc
tab_conc
# Recrystallisation energy output?                    ('rex')
# Options:    out_recrystall   no_out_recrystall
no_out_recrystall
# Recrystallised fraction output?                     ('TabR')
# Options:    tab_recrystall   no_tab_recrystall
no_tab_recrystall
# Dislocation density output?                         ('rhoD')
# Options:    out_disloc      no_out_disloc
no_out_disloc
# Miller-Indices output?                              ('mill')
# Options:    out_miller      no_out_miller
no_out_miller
# Orientation output?                                 ('orie')
# Options:    out_orientation  no_out_orientation
out_orientation
# Should the orientation-time file be written?        ('TabO')
# Options:  tab_orientation  no_tab_orientation   [rotmat]
tab_orientation
# Linearisation output?    ('TabLin')
# Options:   tab_lin  no_tab_lin
no_tab_lin
# Should monitoring outputs be written out?           ('TabL')
# Options:    tab_log [simulation time, s] [wallclock time, min]  no_tab_log
tab_log 0.002
#
# Time input data
# ===============
# Finish input of output times (in seconds) with 'end_of_simulation'
# 'regularly-spaced' outputs can be set with 'linear_step'
# or 'logarithmic_step' and then specifying the increment
# and end value
#  'first'              : additional output for first time-step
#  'end_at_temperature'    : additional output and end of simulation
#                        at given temperature
linear_step 0.01 0.8
end_of_simulation
# Time-step?
# Options:  (real)   automatic [0<factor_1<=1] [0<=factor_2] [max.] [min.]
# (Fix time steps: just input the value)
automatic 0.9 0.9 1.E-2 1.E-6
# Number of steps to adjust profiles of initially sharp interfaces [exclude_inactive]?
0
# Phase data
# ==========
# Number of distinct solid phases?
```

```
2
#
# Data for phase 1:
# -----------------
# Simulation of recrystallisation in phase 1?
# Options: recrystall no_recrystall [verbose|no_verbose]
no_recrystall
# Is phase 1 anisotrop?
# Options: isotropic anisotropic faceted antifaceted
anisotropic
# Crystal symmetry of the phase?
# Options: none cubic hexagonal tetragonal orthorhombic
cubic
# Should grains of phase 1 be reduced to categories?
# Options: categorize no_categorize
categorize
#
# Data for phase 2:
# -----------------
# [identical phase number]
# Simulation of recrystallisation in phase 2?
# Options: recrystall no_recrystall [verbose|no_verbose]
no_recrystall
# Is phase 2 anisotrop?
# Options: isotropic anisotropic faceted antifaceted
isotropic
# Should grains of phase 2 be reduced to categories?
# Options: categorize no_categorize
categorize
#
# Orientation
# -----------
# How shall grain orientations be defined?
# Options: angle_2d euler_zxz angle_axis miller_indices quaternion
angle_2d
#
# Grain input
# ===========
# Type of grain positioning?
# Options: deterministic random from_file
deterministic
# NB: the origin of coordinate system is the bottom left-hand corner,
#    all points within the simulation domain having positive coordinates.
# Number of grains at the beginning?
22
# Input data for grain number 1:
# Geometry?
# Options: round rectangular elliptic
```

```
rectangular
# Center x,z coordinates [micrometers], grain number 1?
0.00000
0.00000
# Length along x-axis [micrometers]
1.00000
# Length along z-axis [micrometers]
10.0000
# Should the Voronoi criterion?
# Options:   voronoi    no_voronoi
voronoi
# Phase number?  (integer)
1
# Rotation angle? [Degree]
10.0000000000000
# Input data for grain number 2:
# Geometry?
# Options: round    rectangular   elliptic
rectangular
# Center x,z coordinates [micrometers], grain number 2?
5.00000
0.00000
# Length along x-axis [micrometers]
1.00000
# Length along z-axis [micrometers]
10.0000
# Should the Voronoi criterion?
# Options:   voronoi    no_voronoi
voronoi
# Phase number?  (integer)
2
# Input data for grain number 3:
# Geometry?
# Options: round    rectangular   elliptic
rectangular
# Center x,z coordinates [micrometers], grain number 3?
10.0000
0.00000
# Length along x-axis [micrometers]
1.00000
# Length along z-axis [micrometers]
10.0000
# Should the Voronoi criterion?
# Options:   voronoi    no_voronoi
voronoi
# Phase number?  (integer)
1
# Rotation angle? [Degree]
```

0.000000000000000E+000
Input data for grain number 4:
Geometry?
Options: round rectangular elliptic
rectangular
Center x,z coordinates [micrometers], grain number 4?
15.0000
0.00000
Length along x-axis [micrometers]
1.00000
Length along z-axis [micrometers]
10.0000
Should the Voronoi criterion?
Options: voronoi no_voronoi
voronoi
Phase number? (integer)
2
Input data for grain number 5:
Geometry?
Options: round rectangular elliptic
rectangular
Center x,z coordinates [micrometers], grain number 5?
15.0000
0.00000
Length along x-axis [micrometers]
1.00000
Length along z-axis [micrometers]
10.0000
Should the Voronoi criterion?
Options: voronoi no_voronoi
voronoi
Phase number? (integer)
1
Rotation angle? [Degree]
15.0000000000000
Input data for grain number 6:
Geometry?
Options: round rectangular elliptic
rectangular
Center x,z coordinates [micrometers], grain number 6?
20.0000
0.00000
Length along x-axis [micrometers]
1.00000
Length along z-axis [micrometers]
10.0000
Should the Voronoi criterion?
Options: voronoi no_voronoi

voronoi
Phase number? (integer)
2
Input data for grain number 7:
Geometry?
Options: round rectangular elliptic
rectangular
Center x,z coordinates [micrometers], grain number 7?
25.0000
0.00000
Length along x-axis [micrometers]
1.00000
Length along z-axis [micrometers]
10.0000
Should the Voronoi criterion?
Options: voronoi no_voronoi
voronoi
Phase number? (integer)
1
Rotation angle? [Degree]
5.00000000000000
Input data for grain number 8:
Geometry?
Options: round rectangular elliptic
rectangular
Center x,z coordinates [micrometers], grain number 8?
30.0000
0.00000
Length along x-axis [micrometers]
1.00000
Length along z-axis [micrometers]
10.0000
Should the Voronoi criterion?
Options: voronoi no_voronoi
voronoi
Phase number? (integer)
1
Rotation angle? [Degree]
40.0000000000000
Input data for grain number 9:
Geometry?
Options: round rectangular elliptic
rectangular
Center x,z coordinates [micrometers], grain number 9?
35.0000
0.00000
Length along x-axis [micrometers]
1.00000

```
# Length along z-axis [micrometers]
10.0000
# Should the Voronoi criterion?
# Options:   voronoi    no_voronoi
voronoi
# Phase number?  (integer)
2
# Input data for grain number 10:
# Geometry?
# Options: round    rectangular    elliptic
rectangular
# Center x,z coordinates [micrometers], grain number 10?
40.0000
0.00000
# Length along x-axis [micrometers]
1.00000
# Length along z-axis [micrometers]
10.0000
# Should the Voronoi criterion?
# Options:   voronoi    no_voronoi
voronoi
# Phase number?  (integer)
1
# Rotation angle? [Degree]
40.0000000000000
# Input data for grain number 11:
# Geometry?
# Options: round    rectangular    elliptic
rectangular
# Center x,z coordinates [micrometers], grain number 11?
45.0000
0.00000
# Length along x-axis [micrometers]
1.00000
# Length along z-axis [micrometers]
10.0000
# Should the Voronoi criterion?
# Options:   voronoi    no_voronoi
voronoi
# Phase number?  (integer)
2
# Input data for grain number 12:
# Geometry?
# Options: round    rectangular    elliptic
rectangular
# Center x,z coordinates [micrometers], grain number 12?
50.0000
0.00000
```

Length along x-axis [micrometers]
1.00000
Length along z-axis [micrometers]
10.0000
Should the Voronoi criterion?
Options: voronoi no_voronoi
voronoi
Phase number? (integer)
1
Rotation angle? [Degree]
45.0000000000000
Input data for grain number 13:
Geometry?
Options: round rectangular elliptic
rectangular
Center x,z coordinates [micrometers], grain number 13?
55.0000
0.00000
Length along x-axis [micrometers]
1.00000
Length along z-axis [micrometers]
10.0000
Should the Voronoi criterion?
Options: voronoi no_voronoi
voronoi
Phase number? (integer)
2
Input data for grain number 14:
Geometry?
Options: round rectangular elliptic
rectangular
Center x,z coordinates [micrometers], grain number 14?
60.0000
0.00000
Length along x-axis [micrometers]
1.00000
Length along z-axis [micrometers]
10.0000
Should the Voronoi criterion?
Options: voronoi no_voronoi
voronoi
Phase number? (integer)
1
Rotation angle? [Degree]
50.0000000000000
Input data for grain number 15:
Geometry?
Options: round rectangular elliptic

```
rectangular
# Center x,z coordinates [micrometers], grain number 15?
65.0000
0.00000
# Length along x-axis [micrometers]
1.00000
# Length along z-axis [micrometers]
10.0000
# Should the Voronoi criterion?
# Options:  voronoi  no_voronoi
voronoi
# Phase number?  (integer)
1
# Rotation angle? [Degree]
130.000000000000
# Input data for grain number 16:
# Geometry?
# Options: round  rectangular  elliptic
rectangular
# Center x,z coordinates [micrometers], grain number 16?
70.0000
0.00000
# Length along x-axis [micrometers]
1.00000
# Length along z-axis [micrometers]
10.0000
# Should the Voronoi criterion?
# Options:  voronoi  no_voronoi
voronoi
# Phase number?  (integer)
2
# Input data for grain number 17:
# Geometry?
# Options: round  rectangular  elliptic
rectangular
# Center x,z coordinates [micrometers], grain number 17?
75.0000
0.00000
# Length along x-axis [micrometers]
1.00000
# Length along z-axis [micrometers]
10.0000
# Should the Voronoi criterion?
# Options:  voronoi  no_voronoi
voronoi
# Phase number?  (integer)
1
# Rotation angle? [Degree]
```

150.000000000000
Input data for grain number 18:
Geometry?
Options: round rectangular elliptic
rectangular
Center x,z coordinates [micrometers], grain number 18?
80.0000
0.00000
Length along x-axis [micrometers]
1.00000
Length along z-axis [micrometers]
10.0000
Should the Voronoi criterion?
Options: voronoi no_voronoi
voronoi
Phase number? (integer)
2
Input data for grain number 19:
Geometry?
Options: round rectangular elliptic
rectangular
Center x,z coordinates [micrometers], grain number 19?
85.0000
0.00000
Length along x-axis [micrometers]
1.00000
Length along z-axis [micrometers]
10.0000
Should the Voronoi criterion?
Options: voronoi no_voronoi
voronoi
Phase number? (integer)
1
Rotation angle? [Degree]
180.000000000000
Input data for grain number 20:
Geometry?
Options: round rectangular elliptic
rectangular
Center x,z coordinates [micrometers], grain number 20?
90.0000
0.00000
Length along x-axis [micrometers]
1.00000
Length along z-axis [micrometers]
10.0000
Should the Voronoi criterion?
Options: voronoi no_voronoi

```
voronoi
# Phase number?  (integer)
2
# Input data for grain number 21:
# Geometry?
# Options: round   rectangular   elliptic
rectangular
# Center x,z coordinates [micrometers], grain number 21?
95.0000
0.00000
# Length along x-axis [micrometers]
1.00000
# Length along z-axis [micrometers]
10.0000
# Should the Voronoi criterion?
# Options:   voronoi   no_voronoi
voronoi
# Phase number?  (integer)
1
# Rotation angle? [Degree]
190.000000000000
# Input data for grain number 22:
# Geometry?
# Options: round   rectangular   elliptic
rectangular
# Center x,z coordinates [micrometers], grain number 22?
100.000
0.00000
# Length along x-axis [micrometers]
1.00000
# Length along z-axis [micrometers]
10.0000
# Should the Voronoi criterion?
# Options:   voronoi   no_voronoi
voronoi
# Phase number?  (integer)
1
# Rotation angle? [Degree]
30.0000000000000
#
#
# Data for further nucleation
# ===========================
# Enable further nucleation?
# Options: nucleation  nucleation_symm  no_nucleation  [verbose|no_verbose]
nucleation
# Additional output for nucleation?
# Options:   out_nucleation   no_out_nucleation
```

```
no_out_nucleation
#
# Number of types of seeds?
1
#
# Input for seed type 1:
# ----------------------
# Type of 'position' of the seeds?
# Options: bulk region interface triple quadruple [restrictive]
interface
# Phase of new grains (integer) [unresolved]?
2
# Reference phase (integer) [min. and max. fraction (real)]?
0
# Substrat phase [2nd phase in interface]?
# (set to 0 to disable the effect of substrate curvature)
1
# maximum number of new nuclei 1?
200
# Grain radius [micrometers]?
0.00000
# Choice of growth mode:
# Options:  stabilisation analytical_curvature
stabilisation
# min. undercooling [K] (>0)?
1.0000
# Shield effect:
# Shield time [s] ?
0.50000
# Shield distance [micrometers]  [ nucleation distance [micrometers] ]?
1.2000
# Nucleation range
# min. nucleation temperature for seed type 1 [K]
0.000000
# max. nucleation temperature for seed type 1 [K]
1000.000
# Time between checks for nucleation? [s]
1.00000E-02
# Shall random noise be applied?
# Options:   nucleation_noise  no_nucleation_noise
no_nucleation_noise
#
# Max. number of simultaneous nucleations?
# ---------------------------------------
# (set to 0 for automatic)
1000
#
# Shall metastable small seeds be killed?
```

```
# ----------------------------------------
# Options:    kill_metastable     no_kill_metastable
no_kill_metastable
#
# Phase interaction data
# ======================
#
# Data for phase interaction 0 / 1:
# ---------------------------------
# Simulation of interaction between phase 0 and 1?
# Options: phase_interaction  no_phase_interaction
#  [standard|particle_pinning[_temperature]|solute_drag]
#   | [redistribution_control]
phase_interaction
# 'DeltaG' options:  default
# avg ... []  max ... [J/cm**3]  smooth ... [degrees]  noise ... [J/cm**3]
avg 0.55   max 100
# I.e.:  avg +0.55  smooth +45.0  max +1.00000E+02
# Type of surface energy definition between phases LIQUID and 1?
# Options:  constant  temp_dependent
constant
# Surface energy between phases LIQUID and 1? [J/cm**2]
#    [max. value for num. interface stabilisation [J/cm**2]]
1.00000E-05
# Type of mobility definition between phases LIQUID and 1?
# Options:  constant  temp_dependent  dg_dependent
temp_dependent
# File for kinetic coefficient between phases LIQUID and 1?
C:\Users\User\Desktop\Kar\Eutectic3\AlCu_Temp1d_mueVonT0_1
# Is interaction isotropic?
# Optionen: isotropic  anisotropic [harmonic_expansion]
anisotropic
# Anisotropy of interfacial stiffness? (cubic)
# 1 - delta * cos(4*phi), (delta =delta_stiffness =15*delta_energy)
# Coefficient delta (<1.) ?
0.50000
# Anisotropy of interfacial mobility? (cubic)
# 1 + delta * cos(4*phi)
# Coefficient delta (<1.) ?
0.20000
#
# Data for phase interaction 0 / 2:
# ---------------------------------
# Simulation of interaction between phase 0 and 2?
# Options: phase_interaction  no_phase_interaction  identical phases nb
#  [standard|particle_pinning[_temperature]|solute_drag]
#   | [redistribution_control]
phase_interaction
```

```
# 'DeltaG' options:  default
# avg ... []  max ... [J/cm**3]  smooth ... [degrees]  noise ... [J/cm**3]
avg 0.55   max 100
# I.e.:  avg +0.55  smooth +45.0  max +1.00000E+02
# Type of surface energy definition between phases LIQUID and 2?
# Options:  constant  temp_dependent
constant
# Surface energy between phases LIQUID and 2? [J/cm**2]
#    [max. value for num. interface stabilisation [J/cm**2]]
1.00000E-05
# Type of mobility definition between phases LIQUID and 2?
# Options:  constant  temp_dependent  dg_dependent
temp_dependent
# File for kinetic coefficient between phases LIQUID and 2?
C:\Users\User\Desktop\Kar\Eutectic3\AlCu_Temp1d_mueVonT0_2
#
# Data for phase interaction 1 / 1:
# ---------------------------------
# Simulation of interaction between phase 1 and 1?
# Options: phase_interaction  no_phase_interaction  identical phases nb
#  [standard|particle_pinning[_temperature]|solute_drag]
#   | [redistribution_control]
no_phase_interaction
#
# Data for phase interaction 1 / 2:
# ---------------------------------
# Simulation of interaction between phase 1 and 2?
# Options: phase_interaction  no_phase_interaction  identical phases nb
#  [standard|particle_pinning[_temperature]|solute_drag]
#   | [redistribution_control]
no_phase_interaction
#
# Data for phase interaction 2 / 2:
# ---------------------------------
# Simulation of interaction between phase 2 and 2?
# Options: phase_interaction  no_phase_interaction  identical phases nb
#  [standard|particle_pinning[_temperature]|solute_drag]
#   | [redistribution_control]
no_phase_interaction
#
#
# Concentration data
# ==================
# Number of dissolved constituents?   (int)
1
# Type of concentration?
# Options:    atom_percent   (at%)
#             weight_percent  (wt%)
```

```
weight_percent
#
# Options:  diff   no_diff   infinite   infinite_restricted
#        multi   database_global   database_local   from_file
#          [+b] for grain-boundary diffusion
# ('multi' can be followed by a string of "n", "d", "g", "l", or "f"
#  to describe each contribution: respectively no diffusion,
#  user-defined diffusion coefficient,'global' or 'local' value from
#  database, and 'from file, the default is global values from database).
# Extra line option (prefactor on time step): cushion <0-1>
# Extra line option: infinite_limit [cm**2/s]
# How shall diffusion of component 1  in phase 0  be solved?
diff
# Diff.-coefficient:
# Prefactor? (real) [cm**2/s]
2.00000E-04
# Activation energy? (real) [J/mol]
0.0000
# How shall diffusion of component 1  in phase 1  be solved?
diff
# Diff.-coefficient:
# Prefactor? (real) [cm**2/s]
1.00000E-08
# Activation energy? (real) [J/mol]
0.0000
# How shall diffusion of component 1  in phase 2  be solved?
diff
# Diff.-coefficient:
# Prefactor? (real) [cm**2/s]
1.00000E-08
# Activation energy? (real) [J/mol]
0.0000
#
#
# Phase diagram - input data
# ==========================
#
# List of phases and components which are stoichiometric:
#  phase and component(s) numbers
# List of concentration limits (at%):
#  <Limits>, phase number and component number
# List for ternary extrapolation (2 elements + main comp.):
#  <interaction>, component 1, component 2
# Switches: <stoich_enhanced_{on|off}> <solubility_{on|off}>
# End with 'no_more_stoichio' or 'no_stoichio'
2 1
no_stoichio
# In phase 2 component 1 is defined stoichiometric.
```

```
#
# Is a thermodynamic database to be used?
# Options: database  database_verbose  no_database
database
#
# Name of Thermo-Calc *.GES5 file without extension?
C:\Users\User\Desktop\Kar\Eutectic3\3_phases(theta)
# Interval for updating thermodynamic data [s] =
1.00000E-02
# Input of the phase diagram of phase 0 and phase 1:
# ------------------------------------------------
# Which phase diagram is to be used?
# Options:  database [local|global][start_value_{1|2}]  linear  linearTQ
database
# Maximal allowed local temperature deviation [K]  [Interval [s] ]
-1.00000000
# Input of the phase diagram of phase 0 and phase 2:
# ------------------------------------------------
# Which phase diagram is to be used?
# Options:  database [local|global][start_value_{1|2}]  linear  linearTQ
database
# Maximal allowed local temperature deviation [K]  [Interval [s] ]
-1.00000000
# Reading GES5 workspace ...
# Index relations between TC and MICRESS
# --------------------------------------
# The database contains the following components:
# 1: AL
# 2: CU
# Specify relation between component indices Micress -> TC!
# The main component has in MICRESS the index 0
# Thermo-Calc index of (MICRESS) component 0?
1
# Thermo-Calc index of (MICRESS) component 1?
2
# 0 -> AL
# 1 -> CU
# The database contains 3 phases:
# 1: LIQUID
# 2: ALCU_THETA
# 3: FCC_A1
# Specify relation between phase indices Micress -> TC!
# The matrix phase has in MICRESS the index 0
# Thermo-Calc index of the (MICRESS) phase 0?
1
# Thermo-Calc index of the (MICRESS) phase 1?
3
# Thermo-Calc index of the (MICRESS) phase 2?
```

```
2
# 0 -> LIQUID
# 1 -> FCC_A1
# 2 -> ALCU_THETA
#
# Molar volume of (MICRESS) phase 0 (LIQUID)? [cm**3/mol]
10.000
# Molar volume of (MICRESS) phase 1 (FCC_A1)? [cm**3/mol]
10.000
# Molar volume of (MICRESS) phase 2 (ALCU_THETA)? [cm**3/mol]
10.000
# Temperature at which the initial equilibrium
# will be calculated? [K]
925.0000
#
# Initial concentrations
# ======================
# How shall initial concentrations be set?
# Options:  input  equilibrium  from_file    [phase number]
equilibrium
# Initial concentration of component 1 (CU) in phase 0 (LIQUID) ?wt%]
33.000
#
# Parameters for latent heat and 1D temperature field
# ===================================================
# Simulate release of latent heat?
# Options:     lat_heat    lat_heat_3d [matrix phase]
lat_heat_3d 0
# Type of thermal conductivity definition for phase  0 (LIQUID) ?
# Options:   constant    temp_dependent
constant
# Thermal conductivity of phase  0 (LIQUID) ?  [W/cm/K]
1.3000
# Type of thermal conductivity definition for phase  1 (FCC_A1) ?
# Options:   constant    temp_dependent
constant
# Thermal conductivity of phase  1 (FCC_A1) ?  [W/cm/K]
1.2000
# Simulation with release of pseudo-3D latent heat of phase 1 (FCC_A1)?
# Options:     pseudo_3d [crit. matrix fraction]    no_pseudo_3d
pseudo_3D 0.75
# Type of thermal conductivity definition for phase  2 (ALCU_THETA) ?
# Options:   constant    temp_dependent
constant
# Thermal conductivity of phase  2 (ALCU_THETA) ?  [W/cm/K]
1.2000
# Simulation with release of pseudo-3D latent heat of phase 2 (ALCU_THETA)?
# Options:     pseudo_3d [crit. matrix fraction]    no_pseudo_3d
```

```
no_pseudo_3D
# Interval for updating enthalpy data [s]
1.00000E-02
#
# Boundary conditions
# ==================
# Moving-frame system in z-direction?
# Options:    moving_frame    no_moving_frame
moving_frame
# Should the distance or the bottom temperature be
# used as criterion for moving frame?
# Options:  distance [matrix phase (negative: special phase)] temperature
distance
# At which distance from the upper boundary should the frame
# be moved?  (real)  [micrometers]
-100.0000
#
# Store data shifted out of moving-frame system?
# Options:    out_moving_frame    no_out_moving_frame
out_moving_frame
# Type of initial temperature profile?
# Options:   linear    from_file
linear
# Initial temperature at the bottom [K]
820.0000
# Initial temperature at the top [K]
950.0000
# Initial position of the 1D temperature field [micrometer]
# (distance between bottom of 1D temp field and bottom of simulation area, <0!)
-50.0000000000000
#
# Boundary conditions for phase field in each direction
# Options: i (insulation) s (symmetric) p (periodic/wrap-around)
#       g (gradient)   f (fixed)    w (wetting)
# Sequence: W E (S N, if 3D) B T borders
ppii
#
# Boundary conditions for concentration field in each direction
# Options: i (insulation) s (symmetric) p (periodic/wrap-around) g (gradient) f (fixed)
# Sequence: W E (S N, if 3D) B T borders
ppfi
# Fixed value for concentration field for component 1 in B-direction
33.000
#
# Boundary conditions for 1D temperature field bottom and top
# Options: i (insulation) s (symmetric) p (periodic/wrap-around) g (global grad) f (fixed) j (flux)
# Sequence: B T
fi
```

How shall temperature in B-direction be read?
Options: constant from_file
constant
Fixed value for temperature [K]
298.00
Fixed value for heat transfer coefficient [W/cm2K]
1.50000000000000
Please specify for the 1D temperature field, which enthalpy
below the calculation domain should be present!
The following options are available:
Options: constant from_file
from_file
file name:
C:\Users\User\Desktop\Kar\Eutectic3\AlCu_Temp1d_latHeatData columns 2 8
Please specify for the 1D temperature field, which value of Cp
below the calculation domain should be present!
The following options are available:
Options: constant from_file
from_file
file name:
C:\Users\User\Desktop\Kar\Eutectic3\AlCu_Temp1d_latHeatData columns 2 6
Please specify for the 1D temperature field, which value of the heat conductivity
below the calculation domain should be present!
The following options are available:
Options: constant from_file
from_file
file name:
C:\Users\User\Desktop\Kar\Eutectic3\AlCu_Temp1d_latHeatData columns 2 7
Please specify for the 1D temperature field, which enthalpy
above the calculation domain should be present!
The following options are available:
Options: constant from_file
from_file
file name:
C:\Users\User\Desktop\Kar\Eutectic3\AlCu_Temp1d_latHeatData columns 2 8
Please specify for the 1D temperature field, which value of Cp
above the calculation domain should be present!
The following options are available:
Options: constant from_file
from_file
file name:
C:\Users\User\Desktop\Kar\Eutectic3\AlCu_Temp1d_latHeatData columns 2 6
Please specify for the 1D temperature field, which value of the heat conductivity
above the calculation domain should be present!
The following options are available:
Options: constant from_file
from_file
file name:

C:\Users\User\Desktop\Kar\Eutectic3\AlCu_Temp1d_latHeatData columns 2 7
Unit-cell model symmetric with respect to the x/y diagonal plane?
Options: unit_cell_symm no_unit_cell_symm
no_unit_cell_symm
#
#
Other numerical parameters
==========
Phase minimum?
1.00E-03
Interface thickness (in cells)?
3.50